Aus dem Institut für Veterinär-Physiologie

des Fachbereichs Veterinärmedizin

der Freien Universität Berlin

Xenopus laevis oocyte cell model for barrier research of tight junction proteins

Inaugural Dissertation

zur Erlangung des Grades eines

PhD in Biomedical Sciences

an der

Freien Universität Berlin

vorgelegt von

Nora Brunner

Tierärztin aus Berlin

Berlin 2022

Journal Nr.: 4373

Gedruckt mit Genehmigung

des Fachbereichs Veterinärmedizin

an der Freien Universität Berlin

Dekan: Univ.-Prof. Dr. Uwe Rösler

Erster Gutachter: Univ.-Prof. Dr. Salah Amasheh

Zweiter Gutachter: Univ.-Prof. Dr. Christa Thöne-Reineke

Dritter Gutachter: Univ.-Prof. Dr. Ard Nijhof

Descriptoren (nach CAB Thesaurus): xenopus laevis, transmembrane proteins, immunohistochemistry, immunoblotting, electron microscopy, oocytes, blood brain barrier, claudins

Tag der Promotion: 21.10.2022

Table of contents

List of abbreviations

TJ	Tight junction
AJ	Adherens junction
Tjp1, ZO-1	Tight junction protein 1, Zonula occludens 1
kDa	Non-SI-unit of atomic mass, kilodalton, 1 Da =0.001 kDa
ECL	Extracellular loop
PDZ domain	Postsynaptic density protein domain
aa	Aminoacids
C	One letter code for aa, cysteine
V-Y-X-K	One letter code for aa, valine-tyrosine-any aa-lysine
HEK cells	Human embryonic kidney 293 cells
MDCK II cells	Madin-Darby canine kidney II cells
nN	Non-SI-unit of force; nano-newton; $1nN = 1 \times 10^{-9}$ N
TEER	Transepithelial electrical resistance
JAM	Junctional adhesion molecule
RhoA	Ras homolog gene family, member A, a protein with GTPase activity
MAGUK	Membrane-associated guanylate kinases, a superfamily of proteins
SH3 domain	SRC Homology 3 Domain, conserved sequence in MAGUK
GUK domain	Structurally similar to guanylate kinase but enzymatically inactive
3R	Concept of animal welfare: replace, reduce, refine
cRNA	Complimentary ribonucleic acid suitable for microinjection
PCR	Polymerase chain reaction
NF stage	Developmental stages of *Xenopus laevis* (Nieuwkoop and Faber 1994)

List of figures

1. Introduction

Tight junctions (TJs) determine the properties of epithelial barriers and therefore constitute crucial components for physiological cell processes and transport mechanisms. The epithelial barrier allows compartmentalization of the body and protects the organism against undesirable physical, chemical, and biological threats. Claudin proteins represent the largest family of tetraspan TJ proteins, and a mosaic expression of claudins determines organ-specific or tissue-specific epithelial barrier properties.

Methods for the analysis of multiple claudin interactions are limited, and therefore, this thesis focuses on the main aspects of suitable analysis protocols in close relationship with the establishment of a new barrier model for the analysis of claudins:

General suitability of *Xenopus laevis* oocytes for heterologous expression of human claudins

African clawed frog (*Xenopus laevis*) oocytes are a *widely* used classic model for the functional analysis of transporter mutants and electrophysical transport mechanisms (Wagner et al. 2000). The oocytes possess a broad translational and posttranslational apparatus and allow a reliable localization of heterologously expressed proteins in accordance with injected cRNAs, including carrier proteins and channels. To date, *Xenopus laevis* oocytes have not been utilized as a heterologous expression system for the analysis of TJ barrier proteins. The establishment of novel protocols and methods for TJ claudin protein analysis in *Xenopus* oocytes is now reported in this thesis.

In addition, an organ-specific application of the oocyte barrier model, namely a blood-brain barrier-specific combination of claudins, has been examined. Claudin-5 is a classic sealing protein of TJs of the blood-brain barrier. Its function is impaired in neurodegenerative and neuroinflammatory disorders (Greene et al. 2019). The contribution of claudin-5 to trans-claudin-claudin interactions in the oocyte junction seal has therefore been investigated and compared with that of the widely expressed claudin-3.

An investigation of the interaction between endogenous tight junction protein 1 (tjp1, ZO-1) and heterologously expressed claudins is of great relevance for the characterization and validation of the barrier model for further applications. The oocyte scaffold needs to allow undisturbed trafficking of claudins into the oocyte membrane. Thus, unfertilized oocytes expressing human claudin-1 to -5 have been scanned for endogenous tjp1 expression in protein, and mRNA analyses have been undertaken.

2. Literature review

2.1. Structure and function of an epithelial barrier

The epithelium is a cellular layer covering the outer or inner surfaces of the body (Madara et al. 1990). A tight connection between adjacent epithelial cells allows the formation of a barrier between two compartments, e.g., the inside and outside of an organ. Epithelial cells join and form a functional layer by the setting-up of cell-cell contacts or cell junctions. These cell contacts can be grouped into various categories (Figure 1). One common categorization emphasizes functional discrimination and divides cell junctions into three distinct groups (Bruce Alberts 2002):

1. **Occluding junctions** have a sealing function and prevent an undirected exchange of particles. In invertebrates, the main type of occluding junction is the septate junction (Banerjee et al. 2006), whereas in vertebrates, occluding junctions are formed by tight junctions (TJs) or zonula occludens. The main function of the epithelium, namely to serve as a selectively permeable membrane, can only be accomplished by the formation of occluding junctions.

2. **Anchoring junctions** provide mechanical attachment to neighboring cells. They connect the cytoskeleton of the cell to adjacent cells and to the extracellular matrix and provide resistance to mechanical forces (Lalan et al. 2011). Anchoring junctions are further classified into adherens junctions, desmosomes, and hemidesmosomes. Adherens junctions (AJs) consist of cadherin-catenin complexes and associated proteins that form adhesive clusters found between various cell types from loosely attached cells to strongly related cell colonies (Adams and Nelson 1998). The α-catenin of adherens junctions binds to tjp1 (Patel et al. 2003) and therefore mediates a junction between membrane integral cadherins and the actin-based cytoskeleton. An AJ is a belt-like junction edging the apical cell compartment and thereby connects a contractile bundle of actin filaments. Desmosomes or maculae adherentes are button-like adhesive junctions that are commonly found in epithelial tissue anchoring intermediate filaments to the membrane at membrane-associated plaques (Green and Gaudry 2000). As in AJs, the core components of desmosomes are cadherins. The third class of anchoring junctions, the hemidesmosomes, attach epithelial cells to the basement membrane in complex epithelia of the epidermis, the cornea, parts of the gastrointestinal and respiratory tract, and the amnion (Borradori and Sonnenberg 1999). The transmembrane adhesion proteins of hemidesmosomes, the integrins, form a core complex provided by α6β4 integrin and P1a, a cytoskeletal linker protein that is specifically associated with hemidesmosomes. The extracellular domains of the integrin molecule bind to components of the extracellular matrix, especially to laminin-332 (Walko et al. 2015).
3. **Communicating junctions** facilitate the movement of chemical or electrical signals from one cell to its neighbor and therefore play a role in signal transduction. Communicating or gap junctions are formed by transmembrane proteins called connexins that build a pore through which ions and other small polar substances up to 1 kDa can pass. The channel pore, the connexon, allows the direct coupling of the cytoplasm of adjacent cells and therefore functions as a metabolic or electrical transmitter (Nielsen et al. 2012). Gap junctions are expressed in cardiac muscle cells, smooth muscle cells and ovarian tissue (Brink 1998; Nielsen et al. 2012; Landschaft 2020) and also occur in many organs and tissues that contain vestigial innervation e.g., liver (Beyer and Berthoud 2017).

The differentiation of the inner body and outer compartments is a fundamental requirement for the organization and sustainability of an organism. The maintenance of a multicellular organism with multiple compartments, each having district functions, is enabled by the presence of a regulated diffusion barrier. However, such a barrier calls for specialized transport mechanisms between the compartments.
Two main mechanisms of transport across epithelia have been found: the paracellular pathway and the transcellular pathway are schematically depicted in Figure 1. The structural and functional key determinant for the permeability of the paracellular pathway is the tight junction (TJ), the most apical intercellular junction of the cell (Balda and Matter 1998). The TJ protects the epithelial and endothelial cells from the external environment (Förster 2008) and is arranged in a belt-like structure bordering the frontier between the apical and basolateral membrane domains (Furuse 2010).
In addition to their main function of limiting paracellular permeability (gate function), TJs maintain cellular polarity by inhibiting the intramembranous diffusion of membrane proteins (fence function). The organization and separation of the cell membrane into a basolateral and apical compartment is also a requirement for a functional epithelium (Anderson and Van Itallie 2009; Zihni et al. 2016). For instance, the cell polarity of intestinal or brain endothelial cells allows the directional uptake of desired nutrients such as glucose because of the genesis of gradients (Worzfeld and Schwaninger 2016; Schneeberger et al. 2018).
A continuous cell layer also protects the inner compartments against physical, chemical, and biological threats, and an impairment of the barrier can lead to multiple imbalances and diseases because of the loss of epithelial integrity (Vermette et al. 2018).
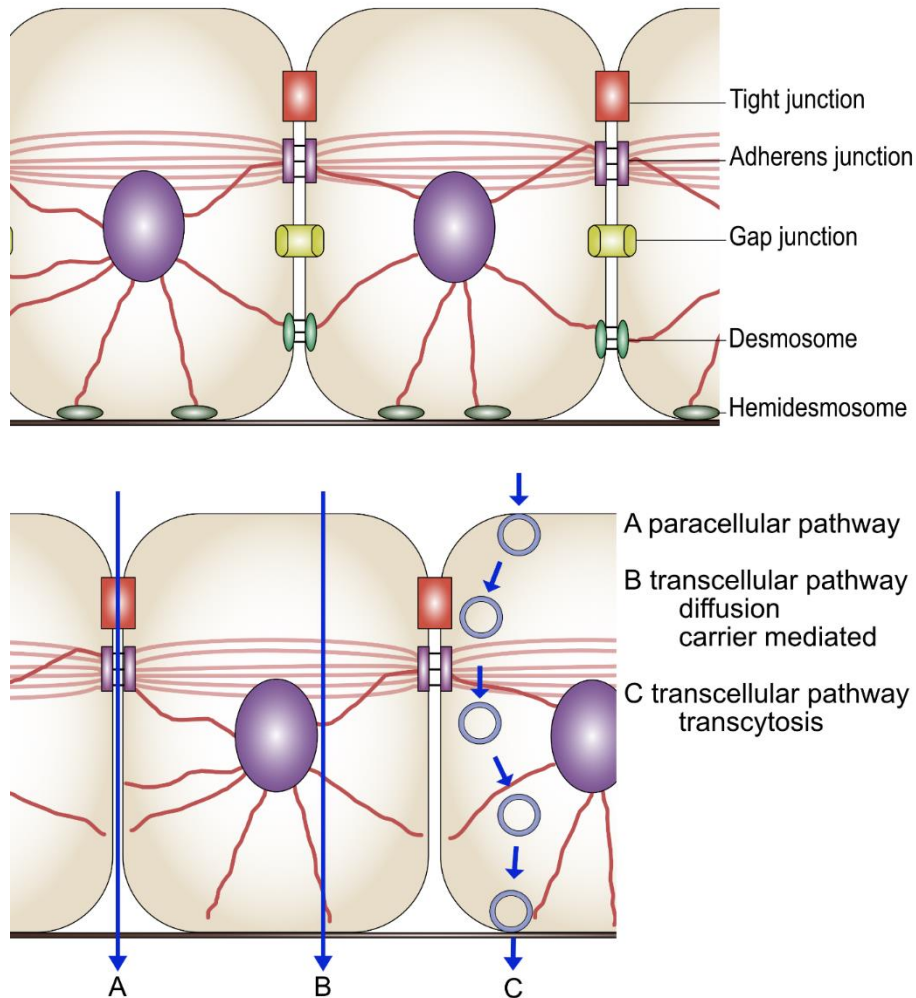
Figure 1 Cell junctions and transport mechanisms across an epithelium. Tight junctions form the most apical occluding junctions and therefore seal the paracellular space. Anchoring junctions are illustrated by adherens junctions, desmosomes, and hemidesmosomes. They function as protective complexes against mechanical forces. Gap junctions represent cell-cell contacts that function as a way of a communicative system between adjacent cells.

Transport mechanisms of substances across an epithelium. (A) Paracellular pathway. Substances are crossing the epithelium through the intercellular space between adjacent cells. The characteristics of the paracellular pathway are particularly affected by the composition of the TJ. **(B) and (C) Transcellular pathway.** Substances are transported through the cells. This can be achieved through **(B)** passive diffusion and carrier mediated (active) processes or **(C)** transcytosis. Depending on the localization and function of the epithelium, the direction of transport can be either apical-basolateral or basolateral-apical.

Claudin backbone of the TJ

Claudins were first identified in 1998 by Furuse and Tsukita et al. (Furuse et al. 1998a) as a new protein family located to the TJ. Claudins are regarded as the main structural component of the TJ with 27 mammalian claudin family members from claudin-1 to -27 (Mineta et al. 2011; Günzel and Yu 2013; Tsukita et al. 2019). The general structure of a claudin protein is depicted in Figure 2.

Claudins range from 20 to 27 kDa and have a sequence homology of four transmembrane domains in a helical structure, two extracellular loops ECL1 and ECL2, a short (2-6 aa) N-terminal sequence, and a more variable longer cytoplasmic C-terminal tail (Morita et al. 1999).

The C-terminus contains a PDZ-binding motif V-Y-X-K for binding to cytoplasmic scaffolding proteins (Itoh et al. 1999a).

The ECLs are thought to provide interactions between neighboring cell membranes. They probably determine paracellular permeability because mutations in ECL1 and ECL2 affect cell-cell contacts (Colegio et al. 2002). ECL1 contains five β-strands that form an antiparallel β sheet and an extracellular helix structure. ECL2 is shorter and consists of a helix-turn-helix motif (Krause et al. 2009; Suzuki et al. 2014). Both ECLs are described as being involved in TJ strand formation. ECL1 is critical for the determination of paracellular tightness and/or ion permeability, while EL2 is thought to narrow the paracellular gap (Krause et al. 2009).
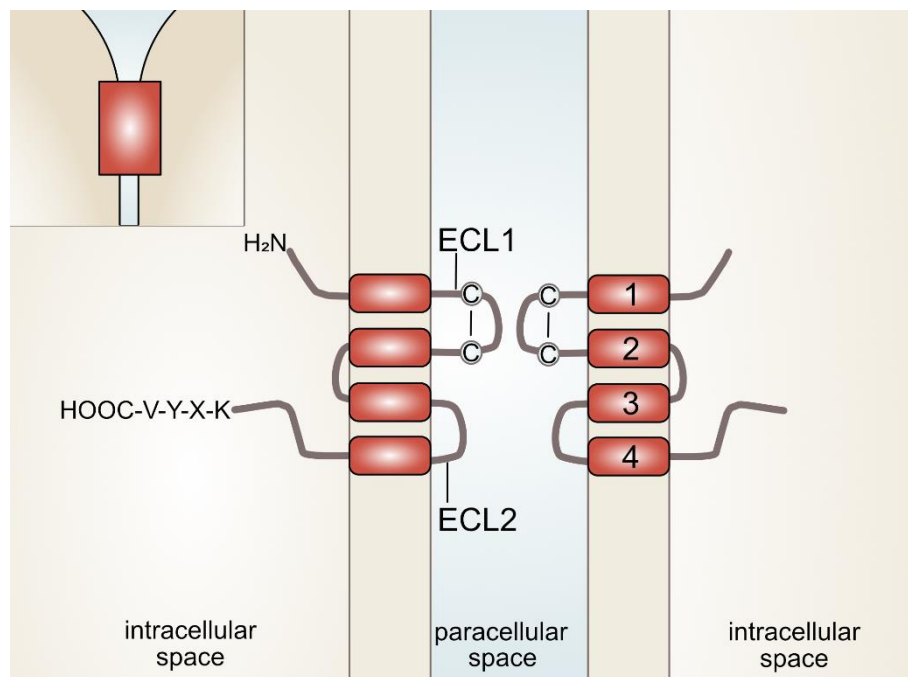

Figure 2 Schematic claudin structure at neighboring cells. A claudin monomer consists of four transmembrane domains (red), a short N-terminus, and a longer C-terminal tail with a PDZ binding motif (V-Y-X-K). The ECL1 has two preserved cysteine residues building a disulfide bridge. Two claudin monomers oppose each other at neighboring cells and therefore can form *trans*-interactions.

Because of the different functions that the various claudin family members play in epithelial barriers, claudins can be divided into functional groups of sealing or barrier-forming claudins, e.g., claudin-1, claudin-3, claudin-5, and pore- or channel-forming claudins, e.g., claudin-2, -10, or -16 (Amasheh et al. 2009). However, some recent studies on the ambivalent function of claudin-4 (Van Itallie et al. 2001; Moellic et al. 2005) and claudin-19 suggest that this classification is not rigid (Miyamoto et al. 2005; Hou et al. 2008).

Claudins have two feasible interaction sites. The first one allows the adhesion of a claudin monomer to a location on the opposing lateral cell membrane at which another claudin monomer is embedded into the cell membrane. This quality of interaction is described as **_trans_-interaction**. In ECL1, two preserved cysteine residues are crucial for the ability to build a tight paracellular seal between cells. In a claudin-5 monomer, for instance, the two cysteines are located at residues 54 and 64. Mutations in these residues have been shown to increase the paracellular flux of monosaccharides in Madin-Darby canine kidney II cells (MDCKII cells) (Wen et al. 2004).

As a second feasible interaction, claudins might polymerize side-by-side within the same cell membrane. This interaction is referred to as **_cis_-interaction**. TJ strands are described as forming a broad diversity of *cis*-interactions (Zhao et al. 2018). The *cis*-interaction is reported to be mediated by the transmembrane regions of the molecule and ECL1 (Hou et al. 2008).

The *trans-* and *cis-*interactions of claudin monomers can be either homo- or heterophilic, viz. between two molecules of the same claudin or between two molecules of different claudin family members (Furuse et al. 1999). Various claudin pairing combinations are illustrated in Figure 3.

Studies on homophilic claudin-5 interaction in claudin-5 transfected human embryonic kidney 293 cells (HEK cells) have revealed that ECL2 mutations do not primarily affect claudin-5 *cis-*interaction (Piontek et al. 2008), although *cis-*interactions are probably formed between ECL2 and an extracellular helical structure of ECL1 (Piontek et al. 2020).

Several experiments have previously been conducted to determine the strengths of *trans-* and *cis-*interactions. In 2008, Lim et. al. used atomic force microscopy to analyze the adhesive strength of homophilic claudin-2 *trans-*interactions (Lim et al. 2008). Vendula et. al. employed a micropipette aspiration technique to characterize the forces of claudin *trans-*interactions in transfected L-fibroblasts. In their experimental set-up, separating forces of 2.3 to 2.8 nN were required for the disruption of *trans-*interactions of claudin-1 and claudin-2 transfected cells (Vedula et al. 2009).
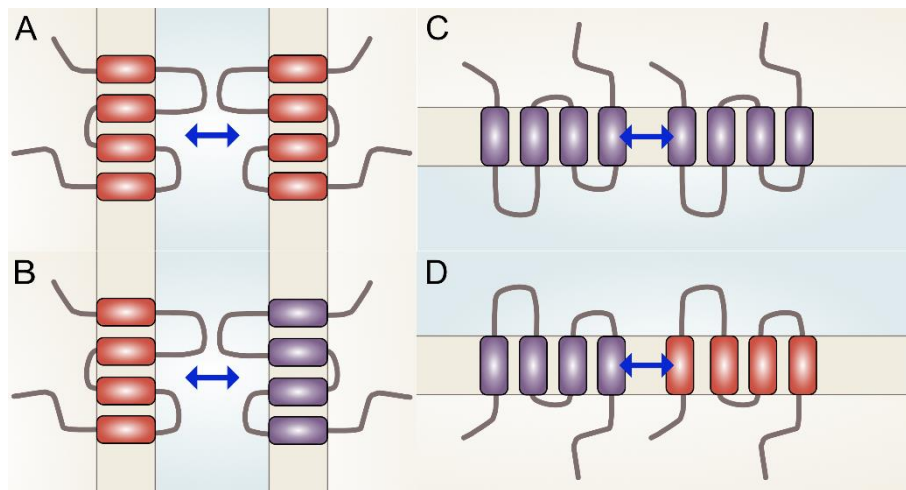

Figure 3 Schematic claudin *cis-* and *trans-*interactions. (A) homophilic *trans-*interaction **(B)** heterophilic *trans-*interaction **(C)** homophilic *cis-*interaction **(D)** heterophilic *cis-*interaction

The strand structure of TJs has been known since the 1960s (Farquhar and Palade 1963). Claudins are considered the backbone of the TJ because they can form TJ strands in the absence of other TJ proteins (Furuse et al. 1998b). The establishment of a TJ strand is described as a two-step assembly process. First, claudin monomers start assembling via *cis-*interactions. Second, the *trans-*interaction is established (Van Itallie and Anderson 2013), and hence, TJ strands or fibrils are formed. A comparison of the transepithelial electrical resistance (TEER), which is a parameter of paracellular permeability, revealed a positive logarithmic correlation between TJ fibril number and TEER (Claude and Goodenough 1973), although TJ strand morphology shows clear variations depending on the interacting claudin subtypes (Irudayanathan et al. 2018). For instance, claudin-4 has a dense, strongly fused, mesh-like strand architecture, whereas claudin-2 forms more curved patterns with non-fused particles in MDCK II cells (Colegio et al. 2002).

Claudins are ubiquitously expressed and show a distinct tissue- and organ-specific distribution, which is consistent with the distinct function of the epithelium (Mitic et al. 2000; Amasheh et al. 2011). The combination of different claudin subtypes in various tissues determines the properties of the epithelium and is frequently altered in various diseases and tumorigenesis (Swisshelm et al. 2005; Hewitt et al. 2006). The expression patterns of various organs and tissues demonstrate that claudins specifically colocalize with other claudins. Markov et al. describe this, in their review, as an indication of cluster formation with a fixed stoichiometry (Markov et al. 2015)., A segment-specific expression of claudins and associated segment-

specific barrier properties has been reported in the murine gastrointestinal tract (Markov et al. 2010).

Visualization of TJ strands can be achieved by the application of freeze fracturing and freeze fracture electron microscopy. Freeze fracture replicas are well suited for the study of membrane structures including the TJ. Images are achieved by splitting the phospholipid bilayer into an E-face, the outer membrane layer closer to the extracellular space, and a P-face, the inner layer of the cell membrane viewed from the outer surface of the cell (Carson 2014). Many studies of the last few decades have included information gained from freeze fracture replicas and depict the unique and mesmerizing structure of the TJ (Furuse 2010).

Other TJ proteins

Until now, the thesis has focused on the structural backbone of the TJ, the claudins. However, TJs exhibit a complex structure with interactions of cytoplasmic adaptor proteins and integral linker proteins. Other TJ proteins are briefly introduced here for a better understanding of the complexity of the TJ.

1. **Occludin** is a tetraspan integral membrane protein of 65 kDa identified in 1993 by the Furuse group (Furuse et al. 1993). It contributes to TJ stabilization and optimal barrier function through ECLs and at least one transmembrane domain (Balda et al. 2000). Additionally, the copolymerization of occluding and claudin has confirmed its role in TJ stabilization (Furuse et al. 1998b). In occluding-knockout experiments, murine TJ integrity was poor and characterized by chronic inflammation, although TJs were morphologically sound (Saitou et al. 2000).

2. **Junctional adhesion molecules (JAMs)** are glycosylated proteins that are characterized by two immunoglobulin folds. Additional to their expression within the TJ, they can be expressed in leukocytes and blood platelets. Recently, many authors have decided to simplify the nomenclature of JAMs and to refer to the JAM proteins as JAM-A, JAM-B, and JAM-C, ignoring the original designation of the protein members (Bazzoni 2003). In murine and human epithelia, JAM-A is described to localize in the close vicinity of TJ strands (Martìn-Padura et al. 1998; Liu et al. 2000). Similar to claudin *trans*-interactions, JAM proteins can form homophilic interactions and hence stabilize the intercellular junction (Bazzoni et al. 2000; Liang et al. 2000).

3. **Cingulin** was first described by Citi et al. in 1988 as a peripheral component of the TJ with a molecular mass of 140 kDa. Cingulin has a globular head and an α helical rod-like region that forms a parallel twisted dimer with another cingulin molecule. Cingulin can interact with scaffolding proteins from the zonula occludens family and with F-actin (Citi et al. 1988; D'atri and Citi 2001). Furthermore, cingulin functions as a scaffold for RhoA, a GTPase protein with a regulatory function on the cytoskeleton. Cingulin-depleted cells show increased RhoA activation and cell proliferation (Guillemot and Citi 2006).

4. **Tricellulin (marvelD2) and angulin-1.** Tricellulin is a membrane protein that is expressed in particular in tricellular TJs at the anastomosing contact area of three adjacent cells. Here, the 63 kDa four-transmembrane protein tricellulin is highly expressed and has a sealing effect on the epithelium (Ikenouchi et al. 2005; Krug et al. 2013). Mutations in human tricellulin lead to profound deafness because of cochlear hair cell degeneration (Riazuddin et al. 2006; Higashi et al. 2015). Angulin-1 is a single-pass transmembrane protein with the N-terminal domain targeted to the extracellular lumen and a cytosolic C-terminal domain (Higashi et al. 2013). Recent studies have revealed that angulin-1 seals tricellular TJs independently of tricellulin and claudins (Sugawara et al. 2021). This is supported by the observation that angulin-1-deficient mice exhibit embryonic death (Sohet et al. 2015) and other severe disorders such as intrahepatic cholestasis and renal dysfunction in association with angulin downregulation (Gong et al. 2017; Uehara et al. 2020).

5. **Zonula occludens (ZO)** proteins are cytoplasmic proteins showing close association with the TJ. They are classified as MAGUK (*m*embrane-*a*ssociated *g*uanylate *k*inase homologs) proteins with structurally conserved PDZ, SH3, and GUK domains. A detailed structure of tjp1 (ZO-1) is depicted in Figure 4. Tjp1 was identified in 1986 as a 225 kDa protein organized within the TJ (Stevenson et al. 1986). Even in non-epithelial cells without TJs, ZO proteins are expressed and concentrated at AJs (Itoh et al. 1993). In epithelial cells, tjp1 is coupled to the TJ through its first PDZ domain to the PDZ-binding motif at the C-terminal of the claudins (Itoh et al. 1999b). Furthermore, tjp1 can bind to JAM proteins, tjp2, and tjp3 through its second and third PDZ domains (Wittchen et al. 1999; Ebnet et al. 2000). The SH3 motif is a non-catalytic protein domain through which tjp1 can interact with transcription promotors, e.g., ZONAB, suggesting a modulating effect of tjp1 on cell differentiation and growth (Balda and Matter 2000). The GUK domain is described as a binding module for occludin rather than having enzymatic activity (Fanning et al. 1998). Finally, the carboxyl terminal region of tjp1 binds to the actin cytoskeleton (Fanning et al. 1998; Wittchen et al. 1999) and therefore acts as an adaptor between integral membrane proteins of the TJ and the cytoskeletal filaments of the cell.
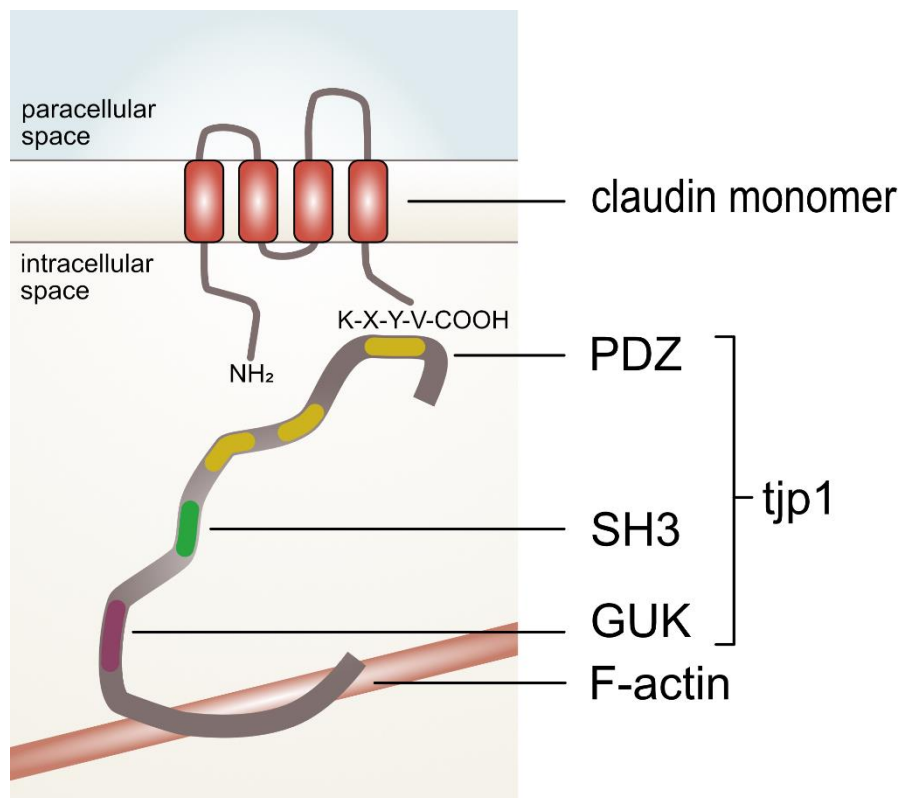

Figure 4 Schematic tjp1 structure. Tjp1 belongs to the MAGUK protein family and has structurally conserved PDZ, SH3, and GUK domains. It can bind to the carboxyl terminal PDZ binding motif of most of the claudins through its first PDZ domain. The carboxyl terminal region of tjp1 binds to F-actin. Proteins are not to scale (claudins: 20-27 kDa, tjp1: 225 kDa, F-actin: microfilament of variable size).

2.2. *Xenopus laevis* as a model organism

The South African clawed frog *Xenopus laevis* is an entirely aquatic amphibious species with a tetraploid genome because of a fertile hybridization of two ancestral species around 34 million years ago (Session et al. 2016). Notwithstanding the tetraploid set of chromosomes, approximately 90% of human disease genes can be found in homologs of *Xenopus laevis* with high sequence preservation (Blum and Ott 2018). The two sub-genomes can be differentiated by their length, by referring either to a long chromosome "L" or to a short chromosome "S" that

experienced more gene loss, deletion, and reduced gene expression. The whole genome of *Xenopus laevis* was successfully sequenced in 2016 (Session et al. 2016). This animal model is particularly appealing because of the easy accessibility of its oocytes, eggs, and embryos, the low price of housing facilities, and its low maintenance costs (Wheeler and Brandli 2009). When housed in a static water facility, oocytes of female African clawed frogs can be harvested by a surgical approach with sparsely seasonal variability (Delpire et al. 2011).

Furthermore, *Xenopus laevis* oocytes and embryos have been a stalwart model system for cell polarity and embryonic development for the last few decades (reviewed by Philpott et al in 2008 (Philpott and Yew 2008) and De Robertis in 2020 (De Robertis et al. 2000)).

From the 1970s onward, cell physiologists and molecular biologists have utilized these amphibian oocytes for microinjection experiments and to determine the heterologous expression of proteins as they are a valuable tool for protein analysis (Gurdon et al. 1971; Mertz and Gurdon 1977). Additionally, because of the large size of the single cells and the extensive availability of large cell quantities, *Xenopus* oocytes have been used as a model system for fundamental cellular processes, transport mechanisms, and many other research approaches.

Xenopus laevis oocytes

A mature female African clawed frog contains ovaries with thousands of oocytes in asynchronous stages of oogenesis (Sato and Tokmakov 2020). The oocytes are surrounded by multiple cell layers forming ovarian lobes (about 24 per ovary), which are attached to each other via connective tissue. The layers surrounding the oocytes comprise the ovarian inner epithelium, blood vessels, theca layer, and follicle cells and the vitelline envelope. The thecal layer is an extracellular matrix containing oocytes at the beginning of oogenesis (Rasar and Hammes 2006). At the beginning of oogenesis, oocytes are directly surrounded by the flat cell layer of follicle cells. During the development, the follicle cell layer becomes separated from the oocytes by the emergence of the vitelline envelope or vitelline membrane, which is an acellular layer of mucopolysaccharides. During fertilization, the vitelline envelope undertakes fundamental functions including sperm binding and polyspermy block (Olson and Chandler 1999). The vitelline envelope is of particular relevance for our studies. In many of the experiments described in this thesis, the vitelline envelope was manually removed by forceps to allow direct contact between two germ cells.

James Dumont first described oogenesis in *Xenopus laevis* as being a six-stage process from stage I to VI based on morphology and size (Dumont 1972). Oocytes at stages I to III are uniformly whitish and non-polar. Beginning with late stage III, a distinct partition becomes apparent giving a darker animal hemisphere and a whitish to yellow vegetal hemisphere. The darker brown shading of the former is attributable to the accumulation of pigment, which is less intense in the latter. Additionally, yolk platelets become distributed asymmetrically toward the vegetal hemisphere in the later phases of oogenesis. The yolk constitutes 80% of the total oocyte protein mass and is densely packed into platelets (Danilchik and Gerhart 1987). Platelets localized in the vegetal hemisphere are larger and of a higher density compared with the platelets of the animal pole (Danilchik and Gerhart 1987). This results in the localization of the geminal vesicle, the large nucleus of the oocyte, toward the animal hemisphere (Mowry 2020).

Whereas oocyte stages III-IV exhibit an intermediate state of cytoskeletal organization, oocytes that have further matured display the final radial symmetry of the microtubule network and cortical actin (Carotenuto and Tussellino 2018). Oocytes at stages V and VI are suitable for cRNA microinjection and have been used in the experiments described in this thesis.

Oocytes at stages V are 1000 to 1200 µm in diameter, and their hemispheres are well separated. Some blood vessels can be seen on the oocyte surface. The vitelline membrane reaches its maximal thickness (Dumont 1972). The maturation of oocytes is completed in stage VI, and oocytes are then categorized as being post-vitellogenetic, as the formation of yolk (vitellogenesis) is completed. These oocytes, which have increased in size to 1200 to 1300 µm are ready to ovulate naturally. Stage VI oocytes can be reliably recognized by their

unpigmented equatorial band of 200 µm in width. Figure 5 is a schematic overview of the structures of a stage VI oocyte.
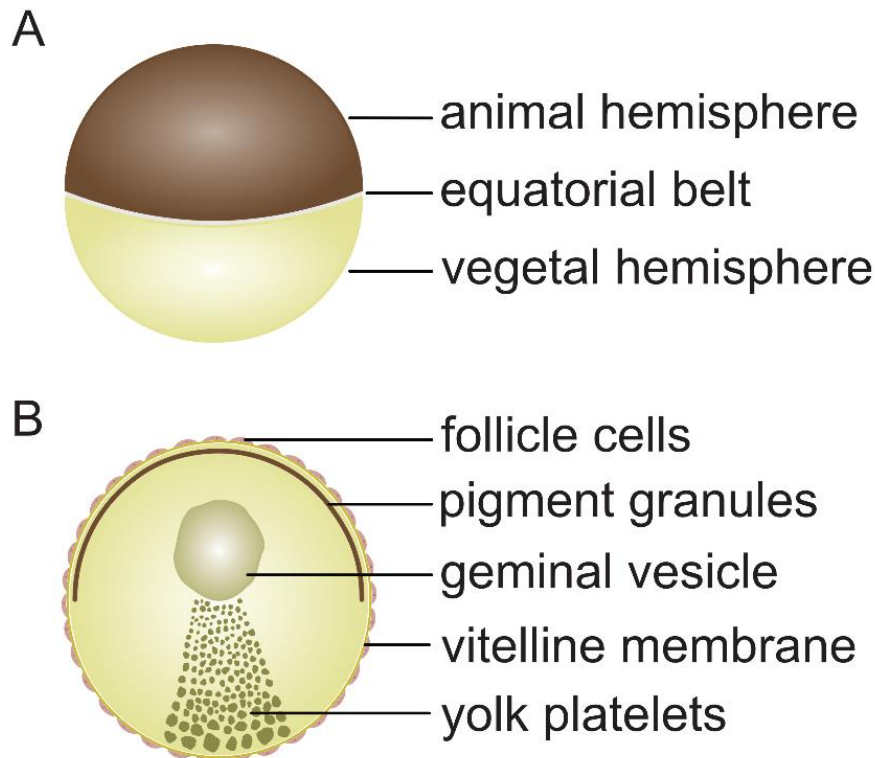

Figure 5 (A) Schematic structure of a stage VI *Xenopus laevis* oocyte. A mature oocyte has a smooth, completely round surface and a clear distinction between the darker pigmented animal hemisphere and the lighter vegetal hemisphere. The two hemispheres are separated by an unpigmented equatorial belt. The size of a stage VI oocyte is 1200 to 1300 µm in diameter. **(B) Schematic cross section of a stage VI *Xenopus laevis* oocyte.** After surgical removal of the oocytes, the cells are still surrounded by an adhesive follicle cell layer. These nutritive cells can be removed in enzymatic digestion. The vitelline membrane can be mechanically eliminated by forceps. The germinal vesicle is localized closer to the animal hemisphere, while yolk platelets of different sizes are more concentrated at the vegetal hemisphere of the cell.

3Rs in scientific research

Although *Xenopus laevis* has been a favorite animal research model for the last few decades, the use of animals in research remains a controversial subject in the media and amongst employees of scientific and medical institutions worldwide.

In 1959, Russel and Burch introduced a concept for animal welfare in their book "The Principles of Humane Experimental Technique" (Russel and Burch 1959). They proposed a new science not only to improve the treatment of research animals but to ensure the quality of scientific and medical research and testing (Tannenbaum and Bennett 2015). Based on their concepts, the 3Rs today are understood as:

1. Replacement
2. Reduction
3. Refinement

Replacement refers to methods that avoid or replace the use of animals in scientific and medical research. This can be achieved by the full replacement of animals with human

volunteers, by in vitro systems (e.g., tissues and cells), or by in silico computer or mathematical models. Replacement also includes the partial replacement of some animal species based on the assumption that they might not be capable of experiencing pain or suffering, such as Drosophila or social amoebae (Bozzaro 2013). Reduction refers to methods that aim to minimize the number of animals used in an experiment. This has to be consistent with the scientific aim and validity of the study. Furthermore, reduction includes the gathering of the maximum information gained from one animal and the reuse of research animals to reduce the utilization of additional animals. The number of animals and their possible suffering certainly needs to be carefully weighed before experiments are conducted, and experiments need to be discussed in the context of the application of animal experiments. The third "R" refinement includes methods that minimized the pain, suffering, and distress that may be experienced by an experimental animal. It often refers to the modification of housing and handling, the expression of species-specific behaviors, and the training of researchers and animal caretakers.

The protection of animals used for scientific purposes has been implemented via directive 2010/63/EU in European legislation (European Parliament 2010) and has been transposed into national law with an amendment of the German Animal Welfare Act (Tierschutzgesetz) and regulations concerning the welfare of vertebrates used for experiments or other scientific purposes (Verordnung zum Schutz von zu Versuchszwecken oder zu anderen wissenschaftlichen Zwecken verwendeten Tieren) in 2013 (Federal Ministry of Justice 2013, 2021).

3. Aims and objectives of this thesis

The identification and characterization of claudins and claudin-claudin *cis*- and *trans*-interactions are of fundamental importance for an understanding of the physiological properties of barrier function and the mechanisms involved in health and disease. Therefore, the work described in this thesis followed distinct objectives.

1. Establishment and validation of a new model for the analysis of claudins by heterologous expression in *Xenopus laevis* oocytes

In 2019, approximately 2 million vertebrates and cephalopods were used for scientific research in Germany (Federal Ministry of Food and Agriculture 2019), approximately 47 % of them being utilized for basic research including the research topic of barriology. To establish a basic research model with many fewer experimental animals compared with transgenic mouse models and to avoid the use of primary cell lines, the work described in the first part of the thesis focused on the expression of claudins in *Xenopus laevis* oocytes. In this study, human claudin-1 to claudin-3 were cloned into suitable vectors and transcribed into injectable cRNA. The oocytes processed the injected heterologous material into the encoded proteins and embedded the claudins into their plasma membrane. Immunoblots, immunohistochemical stainings, and freeze fracture microscopy were employed for the verification of the correct integration.

2. Application of the expression model for the analysis of blood-brain barrier-specific claudin-5 interactions

In the second part of the thesis, details are given concerning experiments that focused on the expression of a blood-brain barrier-specific combination of claudins. Claudin-3 and claudin-5 were co-expressed within one cell, and the interactions of these claudins were analyzed. The majority of experiments included paired oocyte assays in which two oocytes were devitellinized and clustered in pairs. Thereby, the oocytes formed circular contact areas or "oocyte junctions" in which homo- and heterophilic *trans*-interactions could be observed and characterized. Additionally, as a novel approach, the force of the connection was assessed in a hydrostatic pressure impulse (HPI) assay. This allowed the valuation of the fraction that the single claudins contributed to the junction between the oocytes.

3. Examination of elementary interactions of heterologously expressed claudins with the oocyte scaffolding protein tjp1

The third aspect of the current research was the investigation of the interaction of heterologously expressed claudins and the oocyte scaffolding protein tjp1. Unfertilized oocytes expressing human claudin-1 to -5 were scanned for endogenous tjp1 expression by protein and mRNA analyses. Immunoblots and immunohistochemical stainings were carried out for the visualization of claudin-tjp1 interactions. Additionally, mRNA quantification with real-time PCR was employed to analyze a possible regulating effect of claudin expression on *tjp1* mRNA expression levels.

4. *Xenopus* oocytes as a heterologous expression system for analysis of tight junction proteins

Authors: Constanze Vitzthum, Laura Stein, Nora Brunner, Ria Knittel, Petra Fallier-Becker, Salah Amasheh

5. Blood-Brain Barrier Protein Claudin-5 Expressed in Paired *Xenopus laevis* Oocytes Mediates Cell-Cell Interaction

Authors:Nora Brunner, Laura Stein, Valeria Cornelius, Ria Knittel, Petra Fallier-Becker, Salah Amasheh

Blood-Brain Barrier Protein Claudin-5 Expressed in Paired *Xenopus laevis* Oocytes Mediates Cell-Cell Interaction

Nora Brunner[1], Laura Stein[1], Valeria Cornelius[1], Ria Knittel[2], Petra Fallier-Becker[2] and Salah Amasheh[1]*

[1] Department of Veterinary Medicine, Institute of Veterinary Physiology, Freie Universität Berlin, Berlin, Germany, [2] Institute of Pathology and Neuropathology, University Hospital of Tuebingen, Eberhard Karls University of Tuebingen, Tuebingen, Germany

Claudin-5 determines the sealing properties of blood-brain barrier tight junctions and its function is impaired in neurodegenerative and neuroinflammatory disorders. Focusing on the contribution of claudin-5 to the *trans*-interaction within the tight junction seal, we used *Xenopus laevis* oocytes as an expression system. Cells were clustered and challenged in a novel approach for the analysis of claudin interaction. We evaluated the strengthening effect of claudin-5 to cell-cell-connection in comparison to claudin-3. Application of a hydrostatic pressure impulse on clustered control oocyte pairs revealed a reduction of contact areas. In contrast, combinations with both oocytes expressing claudins maintained an enhanced connection between the cells (cldn5–cldn5, cldn3–cldn3). Strength of interaction was increased by both claudin-3 and claudin-5. This novel approach allowed an analysis of single claudins contributing to tight junction integrity, characterizing homophilic and hetrophilic *trans*-interaction of claudins. To test a new screening approach for barrier effectors, exemplarily, this 2-cell model of oocytes was used to analyze the effect of the absorption enhancer sodium caprate on the oocyte pairs.

Keywords: tight junction, claudins, blood-brain-barrier, sodium caprate, *Xenopus laevis* oocyte

INTRODUCTION

The tight junction protein family is crucial for cell physiology as lack or impairment is associated with diseases and dysfunction of many organs and tissues, as shown e.g., in the inner ear (Wilcox et al., 2001; Florian et al., 2003), kidney (Konrad et al., 2006; Günzel et al., 2009), gastrointestinal tract (Resnick et al., 2005; Amasheh et al., 2009), epidermis (Furuse et al., 2002; Tebbe et al., 2002), and brain capillaries (Nitta et al., 2003; Wolburg et al., 2003). Claudins represent a transmembrane protein family comprising at least 27 members (Mineta et al., 2011). In addition to their four transmembrane helix domains, they contain two extracellular loops (ECL1 and ECL2), a short N-terminus and a C-terminus (Suzuki et al., 2014). Specific claudin expression patterns determine and reflect the selective permeability of epithelia, and the ability of claudin proteins to interact in *cis* (within the same membrane) and in *trans* (between the membranes of the neighboring

cell) allows the formation of barrier forming and pore forming tight junction strands (Van Itallie and Anderson, 2006).

Claudin-5 is strongly expressed in capillary endothelia and dominates the tight junction (TJ) of the blood-brain barrier (BBB) as the expression is >100 times higher compared to any other claudin (Ohtsuki et al., 2007). Moreover, it is expressed in a variety of epithelial tissues including lung (Soini, 2011), exocrine tissues (Comper et al., 2009), intestinal (Garcia-Hernandez et al., 2017), and urinary tract (Koda et al., 2011). However, claudin-5 causes a stronger barrier in brain capillaries than in other tissues (Reinhold and Rittner, 2017) and its function is impaired in neurodegenerative and neuroinflammatory disorders (Greene et al., 2019). Hence, claudin-5 is crucial for maintaining the BBB. But the BBB is not only protective, it also limits the therapeutic options as drugs are hindered to permeate this barrier.

Nitta et al. (2003) reported, that the BBB is more permeable to molecules of 800 Da in size in claudin-5 deficient mice compared to wild type mice (Nitta et al., 2003). This was in accordance with transfection experiments demonstrating a sealing effect of claudin-5 in Caco-2 cell monolayers (Amasheh et al., 2005).

Another major barrier-forming claudin is claudin-3, which has been reported to selectively seal the barrier against the passage of ions of either charge and uncharged solutes (Milatz et al., 2010). It is also expressed in the endothelial tight junction of brain capillaries and its functional loss is observed in phases of microvessel inflammation, glioblastoma and choroid plexus of patients with multiple sclerosis (Engelhardt et al., 2001; Wolburg et al., 2003).

Barrier properties can be dynamically modified, as e.g., incubation with sodium caprate was demonstrated to rapidly and reversibly decrease transepithelial electrical resistance in the human intestinal cell line HT-29/B6 (Krug et al., 2013). Sodium caprate transiently opens claudin-5 containing barriers at tight junctions of epithelial and endothelial cells (Del Vecchio et al., 2012).

This indicates, that claudin-5 is a promising target for drug delivery enhancement in the BBB.

In this study, we aimed to employ the heterologous expression system of *Xenopus laevis* oocytes (Vitzthum et al., 2019) for the analysis of claudin-5 and claudin-3 interaction and pertubation. Due to the lack of endogenous cell-cell-contacts, this single cell expression system enables the analysis of specific claudins without interference of other tight junction proteins.

MATERIALS AND METHODS

Harvest of Oocytes and cRNA Microinjection

Oocytes were collected from adult female African claw frogs by surgical laparotomy. For anasthesia, 0.2% MS222 (ethyl 3-aminobenzoate methanesulfonate, Sigma-Aldrich, Taufkirchen, Germany) was used as a bath solution for 5–10 min at 20°C. Once surgical anasthesia was reached, skin and abdominal muscle incisions were made and ovarian mass was exteriorized and ovarial tissue removed. The isolation of oocytes was conducted by enzymatic digestion at room temperature for

90 min in 1.5 mg/ml collagenase Fisher BioReagents BP2649-1 (Fisher Scientific, Schwerte, Germany) dissolved in oocyte Ringer solution (ORi) as described by Vitzthum et al. (2019). Follicular cells were removed by incubation in Ca^{2+}-free ORi containing (in mM): NaCl (90), KCl (1), EGTA (triethylene glycol diamine tetraacetic acid) (1), 5 HEPES (5); pH 7.4 for 10 min on a mechanical shaker with 50 rpm. Oocytes of stages V and VI (>1000 μm) were injected (Nanoliter 2010, World Precision Instruments, Sarasota, FL, United States) with 1 ng cRNA encoding human claudin-5, claudin-3 or RNase-free water as controls. Injection volume was 50.6 nl per oocyte. After injection, oocytes were incubated at 16°C in ORi 3 days for protein expression.

Isolation of Membrane Fractions and Immunoblotting

Ten injected oocytes were pooled for western blot analysis and resuspended in 500 μl homogenization buffer containing (in mM) $MgCl_2$ (5), NaH_2PO_4 (5), EDTA (ethylenediaminetetraacetic acid) (1), sucrose (80), and Tris (Tris(hydroxymethyl)aminomethane) (20); pH 7.4. Oocyte extracts were centrifuged twice at 200 rpm for 10 min at 4°C to discard cell debris. The supernatant was centrifuged at 13,000 rpm for 30 min at 4°C to pellet the cell membrane as described by Leduc-Nadeau et al. (2007). Pellets were resuspended in 80 μl homogenization buffer. Protein quantification was done colorimetrically using Pierce 600 nm Protein Assay Kit (Thermo Fisher Scientific, Hennigsdorf, Germany) according to the manufacturer instruction in a 96 well plate. The plate reader (PerkinElmer EnSpire Multimode Plate Reader, Waltham, MA, United States) was adjusted to 562 nm and Bovine Serum Albumin Standard (Thermo Fisher Scientific, Hennigsdorf, Germany) ranging from 125 to 2000 μg/ml was employed for evaluation. Prior to immunoblotting, samples were mixed with 4× Laemmli buffer (Bio-Rad Laboratories, Munich, Germany), loaded onto a 10% SDS polyacrylamide gel and electrophoresed. For protein transfer, PVDF membranes were used and blocked in 5% non-fat dry milk in Tris-buffered saline for 120 min. Proteins were detected by immunoblotting using primary antibodies raised against claudin-3 or claudin-5 (invitrogen #35-2500, #34-1700, #34-1600, Life Technologies, Carlsbad, CA, United States).

Peroxidase-conjugated goat anti-rabbit and anti-mouse antibodies (#7074, #7076 Cell Signaling Technology, Danvers, MA, United States) were used to bind to the primary antibodies and therefore incubated for a minimum of 45 min at room temperature. For detection, Clarity Western ECL Blotting Substrate (#1705061, Bio-Rad Laboratories GmbH, Munich, Germany) was used and signals were visualized by a ChemiDoc MP system (Bio-Rad Laboratories).

Immunohistochemistry

Injected oocytes were fixed in 4% PFA (16% paraformaldehyde, E15700, Science Service, Munich, Germany) for 4 h at room

temperature followed by dehydration gradient from 70% ethanol to xylol (Carl Roth, Karlsruhe, Germany) within 48 h. Samples were embedded in paraffin and cross-sectioned (5 μm) by using a Leica RM 2245 microtome (Leica Microsystems Heidelberg, Germany). Shortly before immunohistochemical treatment, paraffin was removed via xylol to ethanol gradient. Non-specific binding sites were blocked using 5% goat serum in phosphate-buffered saline and incubated with the same primary antibodies as for immunoblotting. Samples were incubated with the secondary antibodies Alexa Fluor-488 goat anti-rabbit and Alexa Fluor-594 goat anti-mouse (Life Technologies, Carlsbad, CA, United States) and examined by confocal laser-scanning immunofluorescence microscopy (LSM 710, Zeiss, Oberkochen, Germany).

Freeze Fracture Electron Microscopy

Freeze fracture electron microscopy was performed as reported recently (Greene et al., 2019). For fixation, injected oocytes were incubated in glutaraldehyde (2.5% in 0.1 M cacodylate buffer) overnight at 4°C. After washing with cacodylate buffer, oocytes were prepared for freeze fracturing. Samples were cryoprotected in 30% glycerol and frozen in liquid nitrogen. After fracturing, and shadowing with platinum and carbon (BAF400D; Balzers, Liechtenstein), remaining organic material was removed by a sodium hypochlorite wash. Oocytes were analyzed in a transmission electron microscope (EM-10, Zeiss, Oberkochen, Germany) and photographed with a digital camera (Tröndle GmbH). Morphometrical analysis of the tight junction strands was performed at a magnification of 20,000×.

Paired-Oocyte Assay and Quantification of Contact Areas

Mannitol was implemented to shrink the injected oocytes and allow a mechanical removal of the vitelline membrane using forceps without damaging the plasma membrane. 5–10 oocytes were placed in a petri dish (35 mm diameter, Thermo Fisher, Henningsdorf, Germany, #153066) filled with ORi. Mannitol was added and dissolved until hypertonic shrinking of the cells was achieved (approximately 400 mOsmol/l for 10 min). After manual devitellinisation, oocytes were immediately transferred to a 24 well plate (1. 86 cm² surface area, TPP Techno Plastic Products, Trasadingen, Switzerland, # 92024) containing 2 ml of ORi. In each well, two cells were gently clustered by pushing them together with a Pasteur pipette (1 ml, Thermo Fisher, Henningsdorf, Germany, #PP88SB) and a bulbous probe.

Oocyte pairs of claudin-5-expressing (cldn5 − cldn5), claudin-3-expressing (cldn3 − cldn3), claudin-3 and claudin-5 coexpressing (cldn3,5 − cldn3,5) and control oocytes (control − control) were kept together for up to 48 h in ORi at 16°C.

Bright field microscopy was employed for quantification of contact area of clustered oocytes after 1, 24, and 48 h. Images of the naïve oocyte pairs in 24 well culture dishes were taken at these time points using a Leica DMI6000 B Microscope (Leica Microsystems, Wetzlar, Germany). Diameter of contact area was measured using the micron scale (LAS-AF 3.2.0). Contact
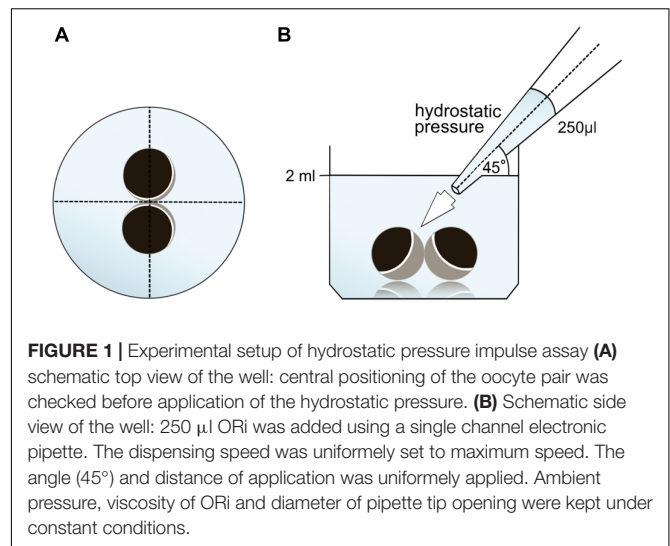

FIGURE 1 | Experimental setup of hydrostatic pressure impulse assay **(A)** schematic top view of the well: central positioning of the oocyte pair was checked before application of the hydrostatic pressure. **(B)** Schematic side view of the well: 250 μl ORi was added using a single channel electronic pipette. The dispensing speed was uniformly set to maximum speed. The angle (45°) and distance of application was uniformly applied. Ambient pressure, viscosity of ORi and diameter of pipette tip opening were kept under constant conditions.

areas are regarded to be circular and thus the contact area was calculated by using the circle equation $A = \pi \bullet r^2$.

Hydrostatic Pressure Impulse Assay

Vitelline membranes were mechanically removed as described before and oocytes clustered analagous to the paired oocyte assay. Additionally, mixed oocyte pairs (control–cldn5 and control–cldn3) were tested in the hydrostatic pressure impulse (HPI) assay. After 24 h of stabilization, a defined hydrostatic impulse was created using a single channel electronic pipette (EE-300R, Eppendorf Research Pro, software version 2.06.00, Hamburg, Germany).

Oocytes were kept in 24 well plates containing 2 ml ORi and central positioning was checked before application of the pipetting volume 250 μl ORi. The dispensing speed was uniformly set to maximum speed, equating a dispensing speed of 0.9 s. Furthermore, the angle (45°) and distance of application (~1.3 cm) was uniformly applied. Ambient pressure, viscosity of the ORi and diameter of pipette tip opening were kept under constant conditions. Bright field microscopy was employed for quantification of contact areas 30 min after the hydrostatic pressure was applied and compared to contact areas before application. The experimental setup is described in **Figure 1**.

Caprate Incubation

For caprate incubation, sodium caprate (#C4151, Sigma Aldrich, Taufkirchen, Germany) in final concentrations of 50, 100, and 500 μM, or ORi as reference group, was added to the oocytes 24 h after pairing. Oocytes were kept in 24 well plates containing 2 ml ORi and caprate solution was dissolved in a defined addition volume of 250 μl ORi per well. Width of contact area was quantified at 30, 60, and 120 min after addition.

Statistical Analysis

Statistical analysis was performed with JMP Pro 14.0.0 (NC, United States). Data are presented as medians and displayed as

FIGURE 2 | Detection of heterologously expressed claudins in *Xenopus laevis* oocytes. **(A)** Immunoblot analysis of tight junction protein claudin-5 in *X. laevis* oocytes of three animals (d1–d3). Cell membrane lysates were subjected to SDS-PAGE followed by immunoblot onto PVDF membranes. The membranes were incubated with primary antibodies and secondary peroxidase-conjugated antibodies ($n = 3$). **(B)** Immunofluorescent staining revealed specific claudin-5 signals (green) in oocyte membranes of all cRNA-injected oocytes, whereas in water-injected controls, no claudin-specific signals were detected in confocal microscopy. Representative images of oocytes derived from three animals. Scale bars: 50 μm. **(C)** Immunofluorescent staining of claudin-5 and claudin-3 expressing oocytes revealed specific claudin-3 signals (green) und claudin-5 signals (red) in oocyte membranes of cRNA-injected oocytes, whereas in water-injected controls, no claudin-specific signals were detected. Colocalization of expressed claudin proteins within the oocyte plasma membrane is revealed by double immunofluorescent staining (yellow). Scale bar: 10 μm.

percentual change based on the clustered combination at the first examination points. **Figures 4**, **5** are presented as Box plots, depicting the first quartile (25-percent), the median (50-percent) and the second quartile (75-percent). The whiskers are drawn down to the 10th percentile and up to the 90th percentile. Normal distribution was checked by using Shapiro–Wilk-test.

Kruskal–Wallis test was used for multiple comparison, followed by a Dunn-Bonferroni correction. *p*-values are given as continous numbers.

RESULTS

Expression of Claudin-5 and Integration Into *X. laevis* Oocyte Plasma Membrane

To test the successful expression and integration of the tight junction protein claudin-5 into the oocyte plasma membrane, 3 days after injection of claudin-5 cRNA, membrane fractions were analyzed by immunoblotting. All samples from three individual animals (d1–d3) revealed claudin-5 specific signals at 23 kDa, whereas RNAse-free water-injected oocytes showed no specific signal for claudin-5 expression (**Figure 2A**).

For visualization of the expressed proteins within the plasma membrane, immunohistochemical stainings were performed and

analyzed by confocal laser scanning microscopy (**Figure 2B**). Specific signals were detected and evenly distributed throughout the plasma membrane of claudin-5 expressing oocytes. In accordance with immunoblots, no specific signals were detected in control oocyte plasma membranes.

Thus, after injection of cRNA, claudin-5 was successfully expressed and integrated in the plasma membrane of *X. laevis* oocytes.

Co-expression of claudin-3 and claudin-5 in oocyte pairs revealed specific signals for claudin-5 (red) and claudin-3 (green) in both cells (**Figure 2C**). Oocyte plasma membranes showed a fusion of the neighboring cells provided by direct cldn3,5–cldn3,5 interaction (yellow).

Patches of Tight-Junction Strands Are Visible in Claudin-5 Expressing Oocytes

Oocyte plasma membranes were analyzed and visualization of tight-junction strands was successful (**Figure 3**). Freeze fracture electron microscopy showed patches of strand morphology in the plasma membranes of claudin-5 injected oocytes, and strand organization of claudin-5 expressing oocytes was highly organized and of angular shape (**Figure 3A**). Tight junction strands were primarily detected in the in the protoplasmic (P-) face of the membrane. Claudin-3 injected oocytes showed rounded highly organized tight

junction strands as reported previously (Vitzthum et al., 2019; **Figure 3B**). Freeze fracture electron microscopy of claudin-3 and claudin-5 coexpressing oocytes revealed fibrils that both bear properties of claudin-3 and claudin-5. Fibril strand architecture of coexpressing oocytes appeared both rounded and complex as claudin-3 expressing oocytes, but also discontinous and more angled as shown for claudin-5 expressing cells (**Figure 3C**). Control oocytes had a typical smooth surface (**Figure 3D**).

Paired Oocyte Assay for Analysis of Claudin *Trans*-Interaction

All clustered combinations showed a time-dependent increase in contact area over the measured period of time (**Figure 4** and **Table 1**).

The contact area of water-injected control oocytes increased to 129% after 24 h and 150% after 48 h. Clustered pairs of oocytes expressing claudin-3 also showed an increase of contact areas to 147% (24 h) and 162% (48 h). Clustered pairs of oocytes coexpressing claudin-3 and claudin-5 showed contact areas of 168% (24 h) and 209% (48 h). Clustered pairs of oocytes expressing claudin-5 alone showed contact areas of 120% (24 h) and 127% (48 h). Therefore contact areas in all tested combinations were comparable.
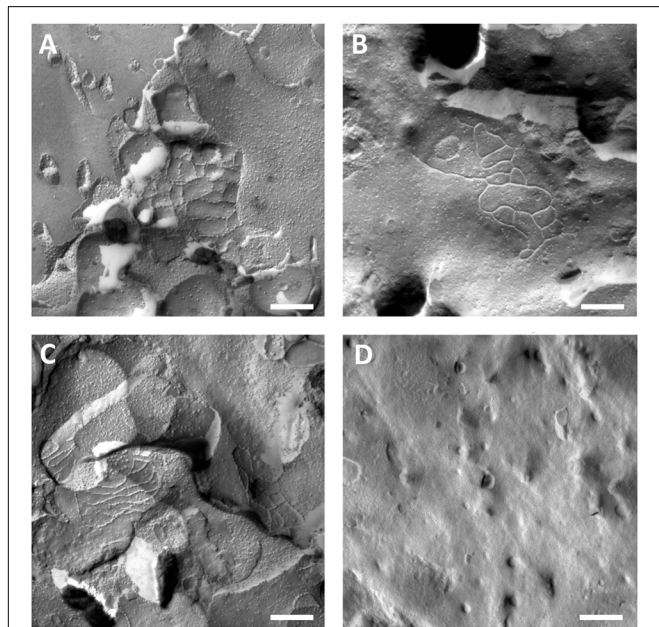

FIGURE 3 | Freeze fracture electron microscopy. **(A)** Freeze fracture electron microscopy reveals tight junction protein cldn-5 as a meshwork of angular discontinous fibrils in rows in *Xenopus laevis* oocytes. **(B)** Freeze fracture electron microscopy reveals tight junction protein cldn-3 as a meshwork of rounded fibrils in *X. laevis* oocytes. **(C)** Freeze fracture electron microscopy of claudin-3 and claudin-5 coexpressing oocytes reveal fibrils that both bear properties of claudin-3 and claudin-5. **(D)** Water injected control oocytes have a smooth surface. Representative images of oocytes derived from three animals. Scale bar: 250 nm.

Hydrostatic Pressure Impulse Assay Reveals Claudin-Specific Junction of Oocyte Pairs

In a separate approach, oocytes expressing claudin-3 or claudin-5 or coexpressing both claudins were clustered after mechanical devitellinization. Oocytes were challenged by employing a HPI and contact areas were measured and calculated 30 min after challenge and compared to initial areas after the 24 h stabilization period (**Figure 5** and **Table 2**). After hydrostatic pressure challenge, the contact area of water-injected control oocytes decreased to 89%. Clustered pairs of oocytes expressing claudin-5, claudin-3 or coexpressing claudin-3 and claudin-5 retained larger contact areas (97%, $p = 0.0235$; 96%, $p = 0.003$; 98%, $p = 0.0253$). The contact areas of mixed water-injected control oocytes and claudin-expressing oocytes (control–cldn5 and control–cldn3) did not significantly differ from control oocytes (93%, $p = 0.2900$; 83%, $p = 0.4455$).

Incubation With Caprate

In a pilot incubation experiment, oocytes were injected and paired in combinations either expressing claudin-5 (cldn5–cldn5) or injected with RNAse free water as controls (control–control). Pairs were incubated with final sodium caprate concentrations of 50, 100, or 500 µM. The incubation of oocyte pairs with ORi served as a reference group. Oocytes were clustered and after 24 h of stabilization, incubation started and contact widths were measured 30, 60, and 120 min after addition (**Supplementary Figure S1**).

The addition of ORi resulted in an initial decrease of contact areas both in claudin-expressing and water-injected oocyte pairs that is dispersed 60 or 120 min after addition. This is outlined by the parabolic shape of the connection line between the median contact areas over time (red curves in **Supplementary Figure S1**). However, incubation with 100 and 500 µM sodium caprate increased contact areas slightly (100 µM) or strongly (500 µM) 30 min after caprate addition from 5.1×10^5 to 5.2×10^5 µm^2 and 4.3×10^5 to 4.9×10^5 µ m^2.

DISCUSSION

In the present study, we employed the classic model for transporters and human disease modeling (Tammaro et al., 2009; Nenni et al., 2019), the *X. laevis* oocytes, for an in-depth analysis of claudin-5 interaction and functional contribution to the junction seal. To this end, a novel approach, introducing a HPI for challenging interaction within the contact area of clustered *Xenopus* oocytes, was established.

Claudins Contribute to Stronger Adhesion Properties

In accordance with previous results from Vitzthum et al. (2019), single claudins expressed in oocytes did not lead to an increase of interaction contact areas compared to control oocytes. However, immunoblot and immunohistochemical visualization proved the successful expression and integration into *X. laevis* oocyte plasma
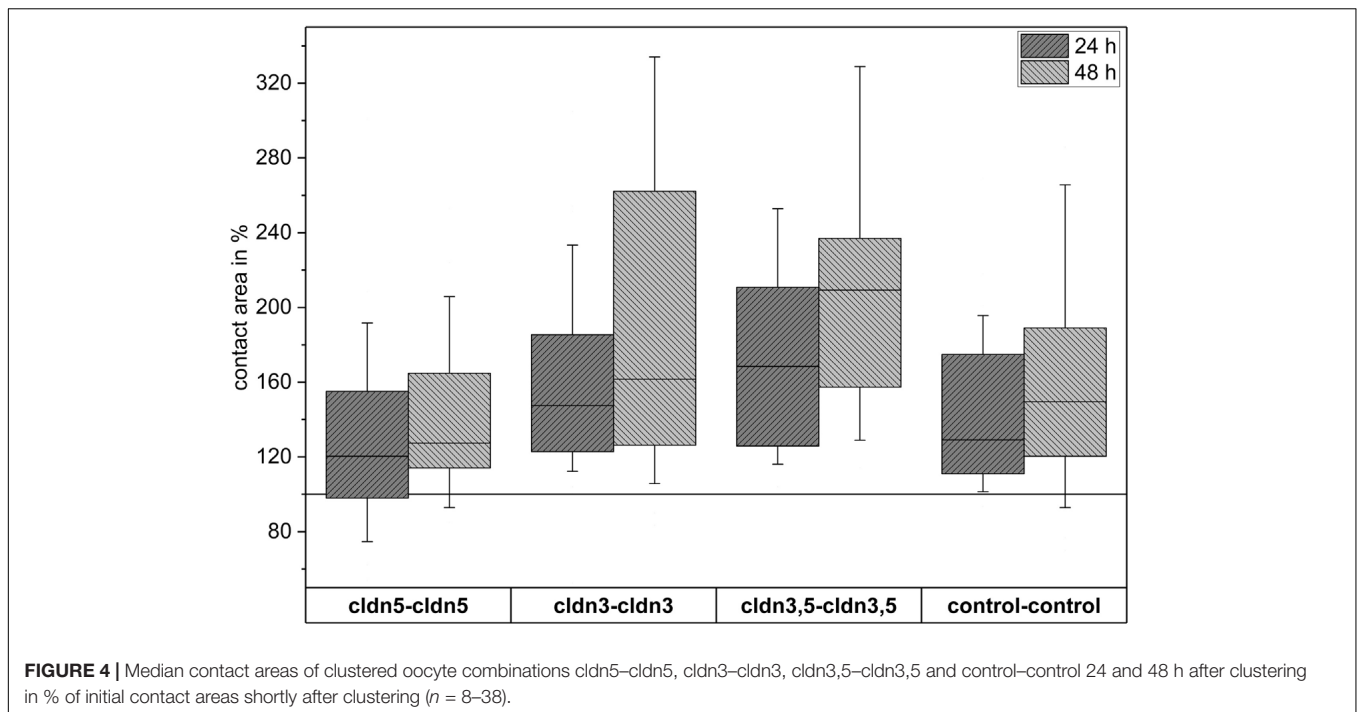
FIGURE 4 | Median contact areas of clustered oocyte combinations cldn5–cldn5, cldn3–cldn3, cldn3,5–cldn3,5 and control–control 24 and 48 h after clustering in % of initial contact areas shortly after clustering (n = 8–38).

TABLE 1 | Oocyte contact areas within 48 h after clustering.

Clustered combination	Time point	Median contact area in %	n
cldn5-cldn5	1 h	100	33
	24 h	120	33
	48 h	127	33
cldn3-cldn3	1 h	100	29
	24 h	147	29
	48 h	162	29
cldn3,5-cldn3,5	1 h	100	8
	24 h	168	8
	48 h	209	8
control-control	1 h	100	38
	24 h	129	38
	48 h	150	38

membrane. Furthermore, the use of confocal laser scanning microscopy allowed a precise localization of the expressed claudins in the plasma membrane as the pinhole blocked out-of-focus fluorescence. A quantification of immunohistochemical signals was not pursued, as the affinity of antibodies for binding their targets differs.
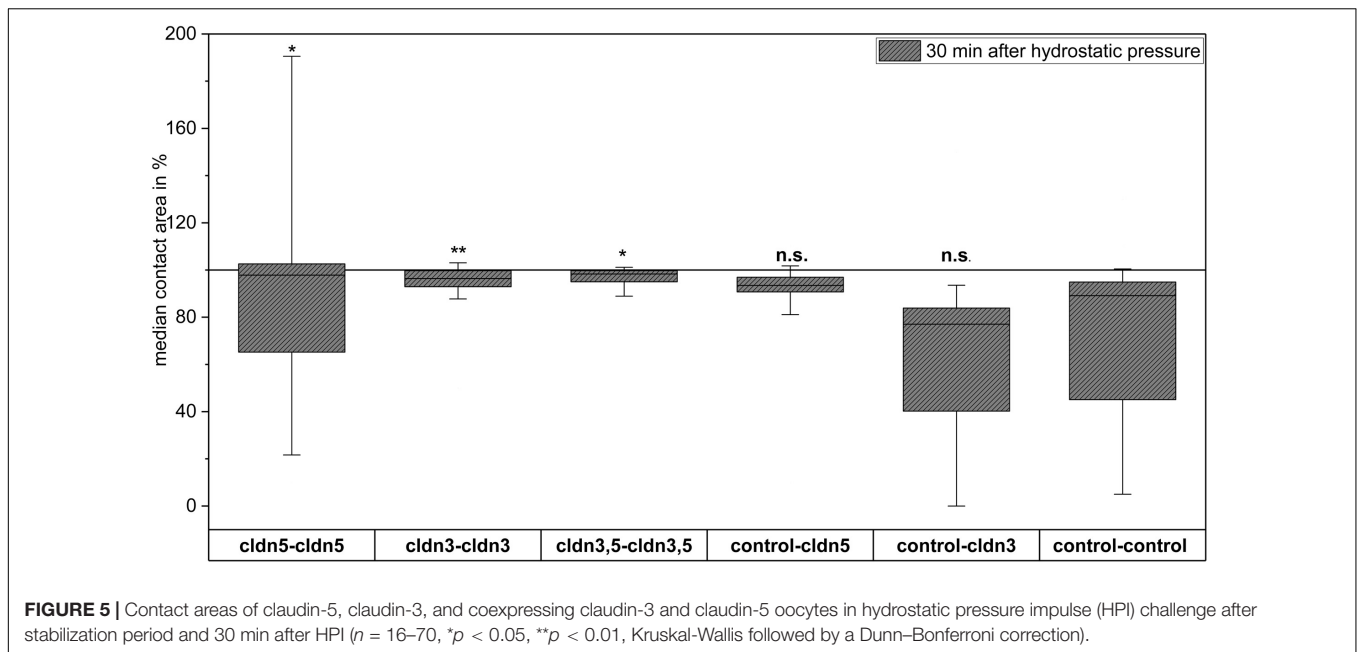
Vedula et al. (2009) used a micropipette aspiration technique to investigate aspects of claudin-claudin interaction using L-fibroblasts transfected with GFP-tagged occludin, cldn-1, and cldn-2. The separation force needed to detach two cells from each other was larger in cldn-1 and cldn-2 transfected cells (∼2.8 and 2.3 nN, respectively). Though this approach might appear also promising for the claudin-claudin- interaction analysis of expressing oocytes, preliminary tests revealed that a detachment

of clustered oocytes is not possible without disruption of the oocyte plasma membranes.

Therefore, as a novel approach, the force of the connections was measured by a HPI. Although the HPI does not provide a quantification of the separation force in absolute values (e.g., in newton's), it allowes a quick and cost-effective analysis of the claudin interaction without disturbance of other tight junction proteins (e.g., occludin, tricellulin, JAM-A). Claudins contribute to the junction of oocyte pairs as they show a larger contact area compared to water-injected oocytes after HPI. This indicates strong homophilic *trans*-interaction between the claudin-expressing cells.

Strand fibril architecture is specific for single claudins (Colegio et al., 2002). In freeze fracture electron microscopy, claudin-3 was reported to assemble a more rounded strand meshwork in loop shapes in *Xenopus* oocytes (Vitzthum et al., 2019; **Figure 3B**) while in our study, claudin-5 formed a meshwork more angular and ordered in rows. The images revealed, that the tight junction protein claudin-5 forms a meshwork of fibrils in discontinuous, angular shaped rows in *X. laevis* oocytes. This is in accordance with claudin-5 strands known to occur as chains of particles associated to the P-Phase (Piontek et al., 2011). In our experiments, geometrical shape of the fibrils seemed to have no effect on the oocytes adhesion properties. In accordance with that, paracellular resistance was reported to be unrelated to fibril number and fibril-forming properties (Colegio et al., 2002). Furthermore, claudin-3 and claudin-5 are shown to have a similar capability for homophilic *trans*-interaction in HEK293 cells (Piontek et al., 2011).

This model of *X. laevis* oocytes, expressing single tight junction proteins, allows an observation of the effect of

FIGURE 5 | Contact areas of claudin-5, claudin-3, and coexpressing claudin-3 and claudin-5 oocytes in hydrostatic pressure impulse (HPI) challenge after stabilization period and 30 min after HPI ($n = 16–70$, *$p < 0.05$, **$p < 0.01$, Kruskal-Wallis followed by a Dunn–Bonferroni correction).

TABLE 2 | Hydrostatic pressure impulse assay.

Clustered combination	Median contact area in %	n
cldn5-cldn5	97	45
cldn3-cldn3	96	44
cldn3,5-cldn3,5	98	16
control-cldn5	93	17
control-cldn3	83	19
control-control	89	70

substances like sodium caprate on the formation of contact areas between clustered oocytes. It may therefore provide a useful tool for a time and cost-efficient screening for substances affecting the tight junction barrier.

Sodium caprate concentrations of 100 and 500 μM may convey a protective effect on claudin-5 expressing oocytes, resulting in increasing contact areas after 30 min of incubation.

Krug et al. (2013) demonstrated, that incubation with sodium caprate led to a rapid and reversible decrease of transepithelial resistance in human intestinal cell line HT-29/B6. Furthermore, confocal laser-scanning microscopy revealed a marked reduction of claudin-5 in HT-29/B6 cells treated with the medium chain fatty acid laurate (Dittmann et al., 2014). The first extracellular loop of claudins (ECL1) is important for the barrier properties of the tight junction, while the second extracellular loop (ECL2) is involved in strand formation of *trans*-interaction (Piontek et al., 2008; Rossa et al., 2014; Greene et al., 2019). Claudin-5 binders targeting ECL1 or ECL2 of claudin-5 may induce intracellular uptake of the tight junction protein, thereby thwarting the claudin-5 *trans*-interactions in the tight junction seal between adjacent cells and loosening the paracellular space (Hashimoto et al., 2017).

Thus, we hypothesized that incubation with sodium caprate would led to a decrease in contact area of clustered claudin-5 expressing *X. laevis* oocytes. Unexpectedly, increasing concentrations of sodium caprate (100 and 500 μM) led to increasing contact areas of clustered oocytes expressing claudin-5 indicating a protective effect of sodium caprate on the tight junction seal. Furthermore, sodium caprate is described to induce contraction of the actomyosin perijunctional ring, widening the paracellular space (Lindmark et al., 1998; Maher et al., 2009). This effect is based on the phosphorylation of the regulatory light chain of myosin via a phospholipase C activation which leads to a cleavage of phosphatidylinositol 4,5-bisphosphate (PIP2) into inositol triphosphate (IP3) and diacylglycerol (Tomita et al., 1995). The tight junction complex linked by the scaffolding protein ZO-1 to the actin cytoskeleton is then redistributed from the tight junction to the cytoplasm (Lindmark et al., 1998; Turner, 2000). The cytoarchitecture of the *X. laevis* oocyte is crucial for cytoplasmic regionalization during oogenesis (Wylie et al., 1985). Though, prior to fertilization, tjp-1 gene expression, the gene encoding for ZO-1 is only expressed 1.9 TPM in oocyte stages V–VI (Session et al., 2016). A reduced interaction of the claudins with the cytoskeletal scaffold may therefore explain the unexpected result of the caprate incubation. Is the scope of future studies to verify the mechanistic basis of the finding.

However, a variant effect of sodium caprate on the paracellular permeability was described in literature before. In Peyer's Patch tissue taken from the intestine of adult pigs, a similar strengthening effect was detected. Claudin-5 was significantly increased after incubation with 5 mM caprate. In this study caprate led to a significantly higher transepithelial electrical resistance (TEER) in the follicle associated epithelium (Radloff et al., 2019).

CONCLUSION

In conclusion, heterologous expression of the tight junction protein claudin-5 in *X. laevis* oocytes allows new insights into the contribution of single claudins to cell-cell interaction and adhesions properties of adjacent cells. Thus, use of the *X. laevis* tight junction model for claudin-5 allows analysis of BBB components in a single-cell model.

DATA AVAILABILITY STATEMENT

The datasets generated for this study are available on request to the corresponding author.

ETHICS STATEMENT

The animal treatments were in accordance with the guidelines of German legislation, with approval by the animal welfare officer for the Freie Universität Berlin and under the governance of the Berlin Veterinary Health Inspectorate (Landesamt für Gesundheit und Soziales Berlin, permit G0025/16).

AUTHOR CONTRIBUTIONS

All authors have read and approved the manuscript. NB and SA designed, planned, and supervised the experiments and wrote the manuscript. NB, LS, VC, RK, and PF-B performed the experiments and data analysis.

SUPPLEMENTARY MATERIAL

The Supplementary Material for this article can be found online at: https://www.frontiersin.org/articles/10.3389/fphys.2020.00857/full#supplementary-material

FIGURE S1 | Contact areas of claudin-5 expressing oocyte pairs in μm^2 during incubation with sodium caprate in different concentrations ($n = 6-8$, respectively) and water-injected oocytes as controls ($n = 5-7$, respectively).

REFERENCES

Amasheh, S., Dullat, S., Fromm, M., Schulzke, J. D., Buhr, H. J., and Kroesen, A. J. (2009). Inflamed pouch mucosa possesses altered tight junctions indicating recurrence of inflammatory bowel disease. *Int. J. Colorect. Dis.* 24, 1149–1156. doi: 10.1007/s00384-009-0737-8

Amasheh, S., Schmidt, T., Mahn, M., Florian, P., Mankertz, J., Tavalali, S., et al. (2005). Contribution of claudin-5 to barrier properties in tight junctions of epithelial cells. *Cell Tissue Res.* 321, 89–96. doi: 10.1007/s00441-005-1101-0

Colegio, O. R., Van Itallie, C., Rahner, C., and Anderson, J. M. (2002). The role of claudin extracellular domains in tight junction fibril architecture and paracellular charge selectivity. *Mol Biol Cell.* 13:286.

Comper, F., Antonello, D., Beghelli, S., Gobbo, S., Montagna, L., Pederzoli, P., et al. (2009). Expression pattern of claudins 5 and 7 distinguishes solid-pseudopapillary from pancreatoblastoma, acinar cell and endocrine tumors of the pancreas. *Am. J. Surg. Pathol.* 33, 768–774. doi: 10.1097/pas.0b013e3181957bc4

Del Vecchio, G., Tscheik, C., Tenz, K., Helms, H. C., Winkler, L., Blasig, R., et al. (2012). Sodium caprate transiently opens claudin-5-containing barriers at tight junctions of epithelial and endothelial cells. *Mol. Pharm.* 9, 2523–2533. doi: 10.1021/mp3001414

Dittmann, I., Amasheh, M., Krug, S. M., Markov, A. G., Fromm, M., and Amasheh, S. (2014). Laurate permeates the paracellular pathway for small molecules in the intestinal epithelial cell model HT-29/B6 via opening the tight junctions by reversible relocation of claudin-5. *Pharm. Res. Dordr.* 31, 2539–2548. doi: 10.1007/s11095-014-1350-2

Engelhardt, B., Wolburg-Buchholz, K., and Wolburg, H. (2001). Involvement of the choroid plexus in central nervous system inflammation. *Microsc. Res. Techniq.* 52, 112–129. doi: 10.1002/1097-0029(20010101)52:1<112::aid-jemt13>3.0.co;2-5

Florian, P., Amasheh, S., Lessidrensky, M., Todt, I., Bloedow, A., Ernst, A., et al. (2003). Claudins in the tight junctions of stria vascularis marginal cells. *Biochem. Biophys. Res. Co.* 304, 5–10. doi: 10.1016/s0006-291x(03)00498-4

Furuse, M., Hata, M., Furuse, K., Yoshida, Y., Haratake, A., Sugitani, Y., et al. (2002). Claudin-based tight junctions are crucial for the mammalian epidermal barrier: a lesson from claudin-1-deficient mice. *J. Cell Biol.* 156, 1099–1111. doi: 10.1083/jcb.200110122

Garcia-Hernandez, V., Quiros, M., and Nusrat, A. (2017). Intestinal epithelial claudins: expression and regulation in homeostasis and inflammation. *Ann. N.Y. Acad. Sci.* 1397, 66–79. doi: 10.1111/nyas.13360

Greene, C., Hanley, N., and Campbell, M. (2019). Claudin-5: gatekeeper of neurological function. *Fluids Barr. CNS* 16:4321.

Günzel, D., Amasheh, S., Pfaffenbach, S., Richter, J. F., Kausalya, P. J., Hunziker, W., et al. (2009). Claudin-16 affects transcellular Cl- secretion in MDCK cells. *J .Physiol. Lond.* 587, 3777–3793. doi: 10.1113/jphysiol.2009.173401

Hashimoto, Y., Shirakura, K., Okada, Y., Takeda, H., Endo, K., Tamura, M., et al. (2017). Claudin-5-binders enhance permeation of solutes across the blood-brain barrier in a mammalian model. *J. Pharmacol. Exp. Ther.* 363, 275–283. doi: 10.1124/jpet.117.243014

Koda, R., Zhao, L. N., Yaoita, E., Yoshida, Y., Tsukita, S., Tamura, A., et al. (2011). Novel expression of claudin-5 in glomerular podocytes. *Cell Tissue Res.* 343, 637–648. doi: 10.1007/s00441-010-1117-y

Konrad, M., Schaller, A., Seelow, D., Pandey, A. V., Waldegger, S., Lesslauer, A., et al. (2006). Mutations in the tight-junction gene claudin 19 (CLDN19) are associated with renal magnesium wasting, renal failure, and severe ocular involvement. *Am. J. Hum. Genet.* 79, 949–957. doi: 10.1086/508617

Krug, S. M., Amasheh, M., Dittmann, I., Christoffel, I., Fromm, M., and Amasheh, S. (2013). Sodium caprate as an enhancer of macromolecule permeation across tricellular tight junctions of intestinal cells. *Biomaterials* 34, 275–282. doi: 10.1016/j.biomaterials.2012.09.051

Leduc-Nadeau, A., Lahjouji, K., Bissonnette, P., Lapointe, J. Y., and Bichet, D. G. (2007). Elaboration of a novel technique for purification of plasma membranes from *Xenopus laevis* oocytes. *Am. J. Physiol. Cell.* 292, C1132–C1136.

Lindmark, T., Kimura, Y., and Artursson, P. (1998). Absorption enhancement through intracellular regulation of tight junction permeability by medium chain fatty acids in Caco-2 cells. *J. Pharmacol. Exp. Ther.* 284, 362–369.

Maher, S., Leonard, T. W., Jacobsen, J., and Brayden, D. J. (2009). Safety and efficacy of sodium caprate in promoting oral drug absorption: from in vitro to the clinic. *Adv. Drug Deliver. Rev.* 61, 1427–1449. doi: 10.1016/j.addr.2009.09.006

Milatz, S., Krug, S. M., Rosenthal, R., Gunzel, D., Muller, D., Schulzke, J. D., et al. (2010). Claudin-3 acts as a sealing component of the tight junction for ions of either charge and uncharged solutes. *Biochim. Biophys. Acta* 1798, 2048–2057. doi: 10.1016/j.bbamem.2010.07.014

Mineta, K., Yamamoto, Y., Yamazaki, Y., Tanaka, H., Tada, Y., Saito, K., et al. (2011). Predicted expansion of the claudin multigene family. *FEBS Lett.* 585, 606–612. doi: 10.1016/j.febslet.2011.01.028

Nenni, M. J., Fisher, M. E., James-Zorn, C., Pells, T. J., Ponferrada, V., Chu, S., et al. (2019). Xenbase: facilitating the use of *Xenopus* to model Human disease. *Front. Physiol.* 10:154. doi: 10.3389/fphys.2019.00154

Nitta, T., Hata, M., Gotoh, S., Seo, Y., Sasaki, H., Hashimoto, N., et al. (2003). Size-selective loosening of the blood-brain barrier in claudin-5-deficient mice. *J. Cell Biol.* 161, 653–660. doi: 10.1083/jcb.200302070

Ohtsuki, S., Sato, S., Yamaguchi, H., Kamoi, M., Asashima, T., and Terasaki, T. (2007). Exogenous expression of claudin-5 induces barrier properties in cultured rat brain capillary endothelial cells. *J. Cell Physiol.* 210, 81–86. doi: 10.1002/jcp.20823

Piontek, J., Fritzsche, S., Cording, J., Richter, S., Hartwig, J., Walter, M., et al. (2011). Elucidating the principles of the molecular organization of heteropolymeric tight junction strands. *Cell Mol. Life Sci.* 68, 3903–3918. doi: 10.1007/s00018-011-0680-z

Piontek, J., Winkler, L., Wolburg, H., Muller, S. L., Zuleger, N., Piehl, C., et al. (2008). Formation of tight junction: determinants of homophilic interaction between classic claudins. *FASEB J.* 22, 146–158. doi: 10.1096/fj.07-8319com

Radloff, J., Cornelius, V., Markov, A. G., and Amasheh, S. (2019). Caprate modulates intestinal barrier function in porcine Peyer's patch follicle-associated epithelium. *Int. J. Mol. Sci.* 20:1418. doi: 10.3390/ijms20061418

Reinhold, A. K., and Rittner, H. L. (2017). Barrier function in the peripheral and central nervous system-a review. *Pflug. Arch. Eur. J. Phys.* 469, 123–134. doi: 10.1007/s00424-016-1920-8

Resnick, M. B., Gavilanez, M., Newton, E., Konkin, T., Bhattacharya, B., Britt, D. E., et al. (2005). Claudin expression in gastric adenocarcinomas: a tissue microarray study with prognostic correlation. *Hum. Pathol.* 36, 886–892. doi: 10.1016/j.humpath.2005.05.019

Rossa, J., Ploeger, C., Vorreiter, F., Saleh, T., Protze, J., Gunzel, D., et al. (2014). Claudin-3 and Claudin-5 protein folding and assembly into the tight junction are controlled by non-conserved residues in the transmembrane 3 (TM3) and extracellular loop 2 (ECL2) segments. *J. Biol. Chem.* 289, 7641–7653. doi: 10.1074/jbc.m113.531012

Session, A. M., Uno, Y., Kwon, T., Hapman, J. A. C., Toyoda, A., Takahashi, S., et al. (2016). Genome evolution in the allotetraploid frog *Xenopus laevis*. *Nature* 538, 336–343.

Soini, Y. (2011). Claudins in lung diseases. *Resp. Res.* 12:70.

Suzuki, H., Nishizawa, T., Tani, K., Yamazaki, Y., Tamura, A., Ishitani, R., et al. (2014). Crystal structure of a claudin provides insight into the architecture of tight junctions. *Science* 344, 304–307. doi: 10.1126/science.1248571

Tammaro, P., Shimomura, K., and Proks, P. (2009). "*Xenopus Oocytes* as a heterologous expression system for studying ion channels with the patch-clamp technique," in *Potassium Channels: Methods and Protocols*, ed. J. D. Lippiat (Totowa, NJ: Humana Press), 127–139.

Tebbe, B., Mankertz, J., Schwarz, C., Amasheh, S., Fromm, M., Assaf, C., et al. (2002). Tight junction proteins: a novel class of integral membrane proteins - expression in human epidermis and in HaCaT keratinocytes. *Arch Dermatol. Res.* 294, 14–18. doi: 10.1007/s00403-001-0290-y

Tomita, M., Hayashi, M., and Awazu, S. (1995). Absorption-enhancing mechanism of sodium caprate and decanoylcarnitine in Caco-2 cells. *J. Pharmacol. Exp. Ther.* 272, 739–743.

Turner, J. R. (2000). 'Putting the squeeze' on the tight junction: understanding cytoskeletal regulation. *Semin. Cell Dev. Biol.* 11, 301–308. doi: 10.1006/scdb.2000.0180

Van Itallie, C. M., and Anderson, J. M. (2006). Claudins and epithelial paracellular transport. *Annu. Rev. Physiol.* 68, 403–429. doi: 10.1146/annurev.physiol.68.040104.131404

Vedula, S. R. K., Lim, T. S., Kausalya, P. J., Lane, E. B., Rajagopal, G., Hunziker, W., et al. (2009). Quantifying forces mediated by integral tight junction proteins in Cell-cell adhesion. *Exper. Mech.* 49, 3–9. doi: 10.1007/s11340-007-9113-1

Vitzthum, C., Stein, L., Brunner, N., Knittel, R., Fallier-Becker, P., and Amasheh, S. (2019). *Xenopus oocytes* as a heterologous expression system for analysis of tight junction proteins. *FASEB J.* 33, 5312–5319. doi: 10.1096/fj.201801451rr

Wilcox, E. R., Burton, Q. L., Naz, S., Riazuddin, S., Smith, T. N., Ploplis, B., et al. (2001). Mutations in the gene encoding tight junction claudin-14 cause autosomal recessive deafness DFNB29. *Cell* 104, 165–172. doi: 10.1016/s0092-8674(01)00200-8

Wolburg, H., Wolburg-Buchholz, K., Kraus, J., Rascher-Eggstein, G., Liebner, S., Hamm, S., et al. (2003). Localization of claudin-3 in tight junctions of the blood-brain barrier is selectively lost during experimental autoimmune encephalomyelitis and human *Glioblastoma multiforme*. *Acta Neuropathol.* 105, 586–592. doi: 10.1007/s00401-003-0688-z

Wylie, C. C., Brown, D., Godsave, S. F., Quarmby, J., and Heasman, J. (1985). The cytoskeleton of *Xenopus oocytes* and its role in development. *J. Embryol. Exp. Morph.* 89, 1–15.

Conflict of Interest: The authors declare that the research was conducted in the absence of any commercial or financial relationships that could be construed as a potential conflict of interest.

6. Cellular Distribution Pattern of tjp1 (ZO-1) in *Xenopus laevis* Oocytes Heterologously Expressing Claudins

Authors: Nora Brunner, Laura Stein, Salah Amasheh

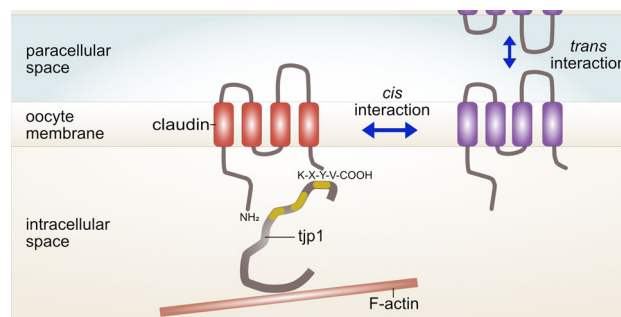# Cellular Distribution Pattern of tjp1 (ZO-1) in *Xenopus laevis* Oocytes Heterologously Expressing Claudins

Nora Brunner[1] · Laura Stein[1] · Salah Amasheh[1]

© The Author(s) 2022

Abstract

Epithelial barriers constitute a fundamental requirement in every organism, as they allow the separation of different environments and set boundaries against noxious and other adverse effectors. In many inflammatory and degenerative diseases, epithelial barrier function is impaired because of a disturbance of the paracellular seal. Recently, the *Xenopus laevis* oocyte has been established as a heterologous expression model for the analysis of transmembrane tight junction protein interactions and is currently considered to be a suitable screening model for barrier effectors. A prerequisite for this application is a physiological anchoring of claudins to the cytoskeleton via the major scaffolding protein tjp1 (tight junction protein 1, ZO-1). We have analyzed the oocyte model with regard to the interaction of heterologously expressed claudins and tjp1. Our experiments have revealed endogenous tjp1 expression in protein and mRNA analyses of unfertilized *Xenopus laevis* oocytes expressing human claudin 1 (CLDN1) to claudin 5 (CLDN5). The amphibian cell model can therefore be used for the analysis of claudin interactions.

Graphical Abstract

Abbreviations

TJ	Tight junction
CLDN	Claudin
tjp1, ZO-1	Tight junction protein 1

✉ Salah Amasheh
salah.amasheh@fu-berlin.de

1 Institute of Veterinary Physiology, Freie Universität Berlin, Oertzenweg 19b, 14163 Berlin, Germany

Introduction

The epithelium acts as a biological, chemical, and physical barrier against multiple threats and challenges and provides a structural border between organ and tissue compartments (Powell 1981). The zonula occludens (tight junction, TJ), which is a complex intercellular junction, controls the permeability and transport of substances across the epithelium and is therefore indispensable for the physiology of the organism (Zihni et al. 2016). The tetraspan TJ protein family of claudins is the main determinant of organ- and tissue-specific TJs. Thus, detailed knowledge about claudin–claudin

interactions is fundamental for the exertion of a suitable pharmacological influence on the barrier, because the paracellular seal is mainly provided by claudin–claudin protein interactions (Will et al. 2008).

The establishment of an alternative amphibian model system for barrier research has recently been described by our group (Vitzthum et al. 2019), which has shown that oocytes of the African claw frog *Xenopus laevis* can be employed for the analysis of claudin–claudin interactions. Recently, we have been able to expand this heterologous expression system to the blood–brain barrier protein CLDN5 and to extend the analytical approach by using hydrostatic pressure impulses for the further characterization of claudin *trans*-interactions (Brunner et al. 2020). Our current study focuses on fundamental aspects involved in the application of *Xenopus* oocytes for barrier research in the context of the cytoskeleton of the oocyte. Simultaneously with the establishment of the oocyte as a cell model for ion channel activity and transport mechanism, the cytoskeletal organization of the oocyte has been unveiled (Carotenuto and Tussellino 2018). As a result, a wide range of techniques had been established which allow a manipulation, disruption, and rigidization of the oocyte membrane. Some of the pharmacological strategies, e.g., the block of actin polymerization by cytochalasin D (Galizia et al. 2012, 2013) or the disruption of cytoplasmic structures by the emptied-out *Xenopus* oocyte technique (EOO) to test potential drug effects on the intracellular binding sites of the oocyte membrane (Ozu et al. 2005, 2011) may become relevant in the clinical implementation of claudin-expressing *Xenopus* oocytes, as well.

The major link between cytoskeletal actin filaments and tetraspan TJ proteins is provided by tjp1 (Furuse et al. 1994). Tjp1 is a cytoplasmic protein that contains PDZ-binding sites for barrier proteins including claudins (Furuse et al. 1998; Itoh et al. 1999), occludin (Furuse et al. 1994; Fanning et al. 1998), and tricellulin (Ikenouchi et al. 2005; Riazuddin et al. 2006). Further functions include binding to gene-regulating transcription factors, e.g., ZONAB (Balda and Matter 2000; Balda et al. 2003). Various alternative RNA splicing isoforms have been described for tjp1, namely a longer isoform with 80 extra amino acids (α^+) and a shorter isoform lacking this alpha domain (α^-) (Willott et al. 1992). Although tjp1 depletion has been shown to be lethal in mouse embryos (Katsuno et al. 2008), other authors have observed that claudins lacking the PDZ motif still localize to the TJ and can dynamically break and re-anneal into TJ strands (Ruffer and Gerke 2004; Van Itallie et al. 2017). Moreover, tjp1 plays a fundamental role in the kinetics of TJ assembly (Fanning and Anderson 2009) and has a stabilizing effect on the solute barrier through coupling to the cytoskeletal ring of the cells (Van Itallie et al. 2009). But also a manipulation through sense and antisense Shroom

oligonucleotide injection as shown for xShroom1 has an impact on membrane protein function and maintenance mediated through the effects on amiloride-sensitive Na$^+$ currents in *Xenopus* oocytes (Zuckerman et al. 1999; Assef et al. 2011; Palma et al. 2016). Many of these regulatory proteins do share similarities in domains with PDZ. In our current study, we present a first assessment of the localization of the heterologously expressed claudins and PDZ-containing tjp1, which is of major interest for the employment of the amphibian cell model in membrane barriology.

Xenopus laevis is a widely used model organism for developmental biology and translational research (Nenni et al. 2019), and thus, its genomic evolution and embryonic development have previously been described in detail (Bowes et al. 2008; Segerdell et al. 2008; Session et al. 2016). When *Xenopus* oocytes have been employed for the heterologous expression of proteins, unfertilized oocytes of stages V and VI have been used with a gene expression for *tjp1* S and for *tjp1* L of 0.9 transcripts per one million mapped reads (TPM) and of 1.9 TPM, respectively (Session et al. 2016). The relative protein expression for oocytes at stage VI is described as being 0.096, which represents the decimal fraction at this stage of total protein agglomerated over all profiled stages (Peshkin et al. 2019). In embryonic development, zygotic transcription starts from the 4000-cell stage onward (Fesenko et al. 2000), but TJs and associated structures can be observed from the (fertilized) 2-cell stage onward and are translated from maternal stores of mRNA (Cardellini et al. 1996; Heasman 2006).

An investigation of the influence of endogenous tjp1 expression on claudin-expressing oocytes and an evaluation of the functionality of the protein–scaffold interaction are essential requirements for further application of *Xenopus* oocytes in the context of barrier research. In this study, we have screened *Xenopus* laevis oocytes for their endogenous expression and localization of tjp1 protein in context with heterologous claudin expression. Additionally, we have analyzed possible claudin-specific regulatory effects on *tjp1* gene expression.

Materials and Methods

Animals

Oocytes were obtained from mature female African claw frogs. Animal treatments were conducted with approval by the animal welfare officer for the Freie Universität Berlin and under the governance of the Berlin Veterinary Health Inspectorate (Landesamt für Gesundheit und Soziales Berlin, permit O 0022/21).

Anesthetics and Surgical Procedure

To achieve surgical anesthesia of the frogs, they were transferred into a bath solution of buffered 2 g/L MS222 (ethyl 3-aminobenzoate methanesulfonate, Sigma-Aldrich, Taufkirchen, Germany, pH 7.5) for 5–10 min at 20 °C. Righting and corneal reflexes were used for the assessment of surgical anesthetic depth. Skin and abdominal muscle incisions were made to access the *Xenopus* ovaries.

cRNA Preparation

Relevant nucleotide coding consensus sequences were used for the synthesis of the human cRNA of CLDN1 to CLDN5 (ShineGene Bio-Technologies Inc., Shanghai, China; Thermo Fischer Scientific, Henningsdorf, Germany). Claudin sequences were cloned into suitable high copy ampicillin-resistant pGEM for transformation in competent DH10b *Escherichia coli*. A commercial T7 RNA-polymerase-based approach (T7 RiboMAX RNA Production System and Ribo m^{7}G Cap Analog, Promega, Walldorf, Germany) was used according to the manufacturer's instructions to generate cRNAs for injection into the amphibian germ cells.

Oocyte Isolation and cRNA Injection

Follicular cell layers were removed by enzymatic digestion at room temperature for 90 min in 1.5 mg/ml collagenase (NB4 Standard Grade, Nordmark Pharma, Germany) dissolved in oocyte Ringer solution (ORi). Cells were then separated by incubation in Ca^{2+}-free ORi (Vitzthum et al. 2019) for 10 min on a mechanical shaker at 50 rpm. Oocyte stages V and VI were injected (Nanoliter 2010, World Precision Instruments, Sarasota, USA) with 50.6 nl of 10 ng/μl, 20 ng/μl, or 40 ng/μl cRNA encoding for human CLDN1 to CLDN5 or with RNase-free water as controls. Based on the total cRNA amounts, this gave three experimental groups: 0.5, 1, and 2 ng cRNA/oocyte. Injected oocytes were incubated for 3 days at 16 °C in ORi for protein expression.

Isolation of Membrane Fractions and Immunoblotting

For Western blot analysis, ten injected oocytes were blended and resuspended in 500 μl oocyte homogenization buffer containing (in mM) 5 $MgCl_2$, 5 NaH_2PO_4, 1 EDTA, 80 sucrose, and 20 Tris, pH 7.4 in accordance with the plasma membrane buffer established by Leduc-Nadeau et al. (Leduc-Nadeau et al. 2007). Oocyte suspensions were centrifuged twice at 200 rpm for 10 min at 4 °C, and the supernatant was centrifuged at 13,000 rpm for 30 min at 4 °C. The pelletized cell membrane fractions were resuspended in homogenization buffer. Membrane samples were then quantified with

Protein Bioassay according to the manufacturer's instruction in a 96-well plate (#500-0119 RC DC Protein Assay, Bio-Rad, Munich, Germany). Bovine Serum Albumin Standard (ThermoFischer Scientific, Henningsdorf, Germany) served as the protein standard. Before the loading of the gels, samples were mixed with 4× Laemmli buffer (Bio-Rad Laboratories, Munich, Germany). Samples were loaded onto a stain-free acrylamide gel (TGX Stain-Free FastCast Acrylamide Kit, 10% #1610183, Bio-Rad Laboratories, Munich, Germany) and electrophoresed. The proteins were transferred to PVDF membranes, and the binding of nonspecific proteins was blocked with 5% nonfat dry milk in Tris-buffered saline for 60 min. We detected the proteins of interest by incubation of the membranes with primary antibodies raised against the TJ proteins CLDN1 to CLDN5 and tjp1 (#51-9000, #51-61600, #35-2500, #32-9400, #34-1700, Life Technologies, Carlsbad, USA, and LS-C145545-100, Biozol, Eching, Germany) overnight at 4 °C. Peroxidase-conjugated secondary antibodies (#7074, #7076 Cell Signaling Technology, Danvers, MA, USA) were incubated with the membranes for 45 min at room temperature and detected using Clarity Western ECL Blotting Substrate and Chemi-Doc MP (#1705061, Bio-Rad Laboratories GmbH, Munich, Germany).

Immunofluorescence Cytochemistry

Using our established protocols, oocytes were paired for the analysis of claudin *trans*-interactions (Brunner et al. 2020). Briefly, vitelline membranes were removed, and claudin-expressing oocytes were clustered to induce adhering contact areas. Oocyte pairs were incubated in ORi at 16 °C for 24 h. Oocytes were fixed in 4% PFA (16% paraformaldehyde, E15700, Science Service, Munich, Germany) for 4 h at room temperature followed by dehydration in an alcohol gradient to xylol. Samples were embedded in paraffin, cross-sectioned (5 μm), and mounted onto microscope slides.

Primary antibodies were the same as those for immunoblotting, and secondary antibodies were conjugated with photostable Alexa Fluor 488 and Alexa Fluor 594 dyes (Life Technologies, Carlsbad, USA). Slides were examined by confocal laser-scanning immunofluorescence microscopy (Zeiss LSM 710).

RNA Isolation and cDNA Synthesis

The Nucleospin RNA (Macherey & Nagel, Dueren, Germany) commercial kit was used for RNA extraction from 10 oocytes per sample. NanoPhotometer P330 (Implen GmbH, Munich, Germany) was employed to determine the levels of possible contamination. An RNA absorption ratio of light at 260/280 nm > 2 was considered to indicate that the samples were free of protein contamination. A 260/230 nm

absorption ratio of 1.7–2 was considered to indicate that the samples were free of buffer salt contamination.

cDNA was synthesized using iScript (Bio-Rad, Munich, Germany) according to the manufacturer's instructions. A–RT sample (without reverse transcriptase) was used as a negative running control. For reverse transcription, a Biorad iCycler iQTM (Biorad, USA) was used with the protocol given in Table 1.

Qualitative and Quantitative Real-Time PCR

For PCR analysis, *Xenopus laevis odc1* (ornithine decarboxylase 1), *gapdh* (glyceraldehyde-3-phosphate dehydrogenase), and *h4c4* (H4 clustered histone 4) were used as housekeeping genes, and *tjp1* as the gene of interest. Primers (Table 2) were purchased from Eurofins Genomics (Eurofins, Ebersberg, Germany). For qualitative PCR, cDNA samples from claudin-injected oocytes were pooled and transcribed using *Taq* PCR master mix (Qiagen, #201443, Düsseldorf, Germany) according to the instructions of the manufacturer. Following gene amplification (Table 3), PCR products were loaded onto a 2% agarose gel in TBE buffer. Additionally, quantitative PCR was performed using iQTM SYBR Green Supermix Kit (Biorad, USA) with three replicates per reaction and three technical replicates. Double-distilled H_2O and –RT samples served as negative controls. As primer efficiency ranged between 1.93 and 2.03, gene expression was normalized relative to the housekeeping genes and to the control group by using the Delta–Delta CT method.

Statistical Analysis

Statistical analysis was performed with JMP Pro 15.0.0 (NC, USA). The normal distribution was checked using the

Table 1 Reverse transcription protocol

	Time (min)	Temperature (°C)
Priming	5	25
Reverse transcription	30	42
Inactivation of cDNA	5	85

Table 3 PCR protocols for *tjp1* gene expression analysis

	Qualitative PCR		Quantitative PCR	
	Time	Temperature	Time	Temperature
Initial denaturation and polymerase activation	3 min	94 °C	3 min	95 °C
Denaturation	30 s	94 °C	12 s	95 °C
Annealing and extension 40 cycles	1 min	57 °C	1 min	60 °C

Shapiro–Wilk test, and Delta CT values were analyzed by one-way analysis of variance (ANOVA).
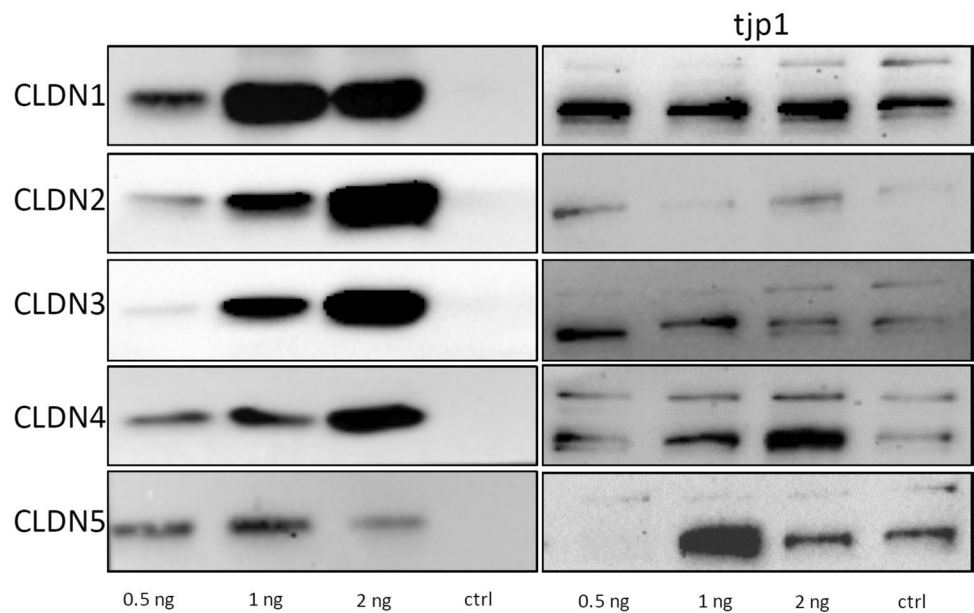
Results

Heterologous Expression of TJ Proteins in *Xenopus* oocytes

The successful expression and integration of claudins into the *Xenopus laevis* plasma membrane was verified by Western blot analysis. After 3 days of expression, membrane fractions of 10 oocytes having had injections of 0.5 ng/oocyte, 1 ng/oocyte, or 2 ng/oocyte claudin cRNA were loaded onto a stain-free acrylamide gel. All membranes revealed claudin-specific signals at the predicted protein mass in accordance with the injected cRNAs (20–27 kDa). RNAse-free water-injected oocytes were treated identically and showed no signal for the endogenous expression of claudins (Fig. 1). Samples were also incubated with tjp1 antibody to check the endogenous tjp1 expression in the claudin-injected cells. All tested oocytes showed tjp1 isoform-specific signals at 187 kDa and 195 kDa.

Oocytes Show Specific Signals of tjp1 in the Submembranous Space

After removal of vitelline membranes, claudin-expressing and water-injected control oocytes were clustered into pairs. Both control and claudin-injected oocytes showed specific immunohistochemical signals after incubation with tjp1 antibodies. The signal was mainly located in the submembranous space of the cells and appeared as a submembranous

Table 2 Primers for qPCR

	Amplicon length (bp)	Sense sequence	Antisense sequence
odc1	221	GCCATTGTGAAGACTCTCTCCATTC	TTCGGGTGATTCCTTGCC
gapdh	201	CTCTCGCAAAGGTCATCAA	CGTTCAGCTCAGGGATAAC
h4c4	103	GACGCTGTCACCTACACCGAG	CGCCGAAGCCGTAGAGAGTG
tjp1	205	GGACAGAAGTTTATCACCAAGA	CTTAAGCACCACGTCTCC

Fig. 1 Immunoblot analysis of tight junction (TJ) proteins in *X. laevis* oocytes Cell membrane lysates applied to 10% stain-free acrylamide gel and transferred onto PVDF membranes. All claudin-injected oocytes membranes revealed claudin-specific signals at the predicted protein mass in accordance with the injected cRNAs (20–27 kDa). RNAse-free water-injected oocytes were treated identically and showed no signal for endogenous expression of claudins. However, specific signals for both tjp1 isoforms α^+ (195 kDa) and α^- (187 kDa) in claudin-expressing oocytes and water-injected controls confirmed endogenous tjp1 protein expression

belt immediately underneath the oocyte plasma membrane (Fig. 2). This accumulation of signals was particularly distinct in the CLDN1-, CLDN2-, and CLDN5-expressing cells and in naïve oocytes. In CLDN2- and CLDN3-expressing cells, claudin and tjp1 signals were selectively colocalized at the plasma membrane and resulted in a yellow signal (arrows).

Claudin Injection Does Not Engage Endogenous tjp1 mRNA Expression

Tjp1 was consistently detectable by qualitative PCR (Fig. 3). We therefore performed quantitative real-time PCR to investigate the effect of claudin injection on *tjp1* mRNA levels. Delta CT values were analyzed for all three concentrations by one-way analysis of variance (ANOVA) to determine the effect of claudin injection and water-injected controls, $F(5, 48) = 0.2367$, $p \geq 0.9$). All claudin-injected oocytes showed a negligible impact of the claudin injection on *tjp1* expression compared with water-injected control oocytes, resulting in a mild n-fold upregulating trend of 1.28–2.10 for *tjp1* expression in claudin-expressing cells (not significant; Table 4 and Fig. 4).
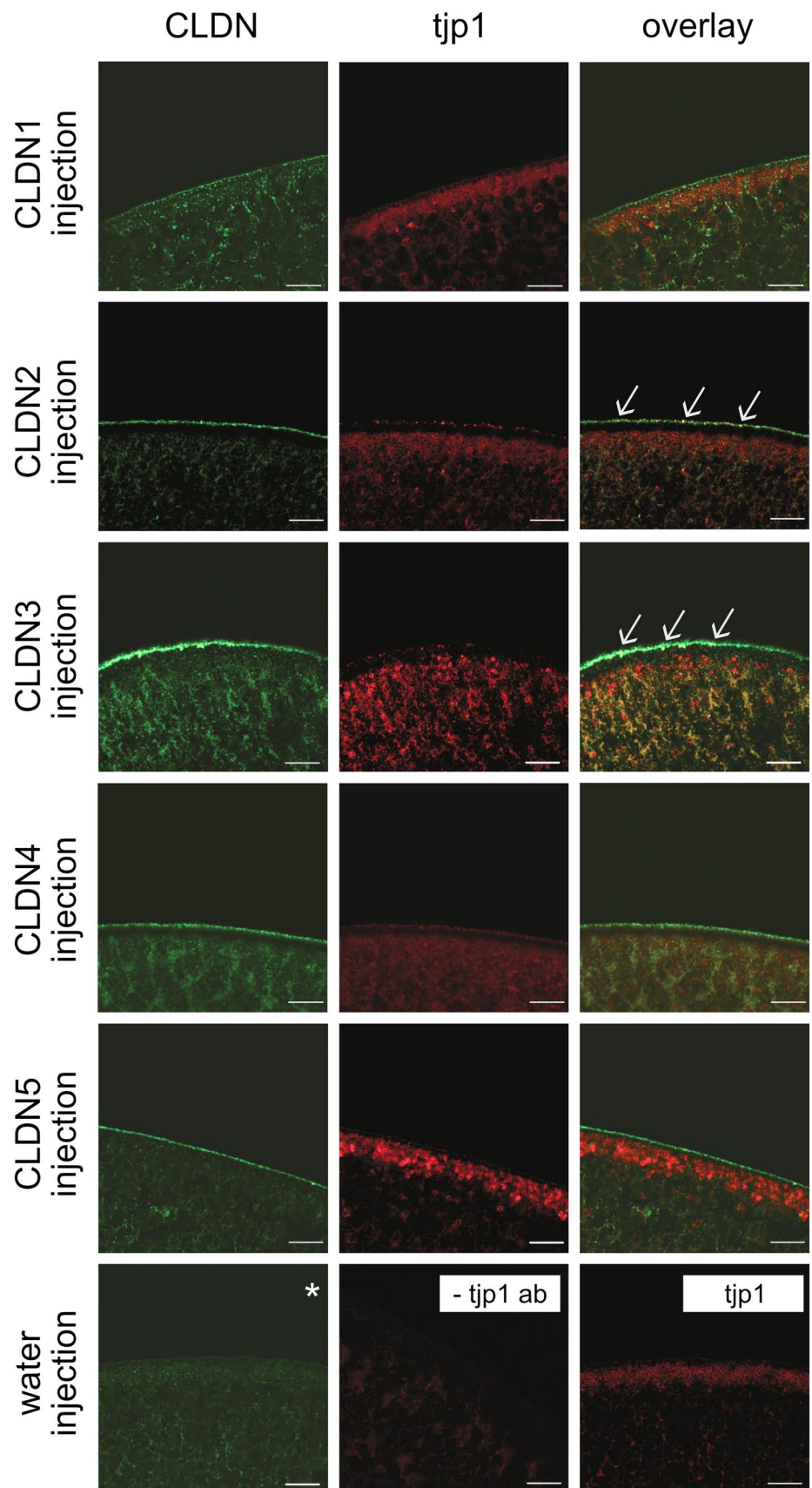
Discussion

In our present study, we have further characterized the established heterologous expression system of *Xenopus* oocytes for the analysis of barrier proteins (Vitzthum et al. 2019). As an interplay between the cytoskeletal scaffold and the expressed barrier proteins provides the foundation of physiological barrier formation (Rodgers et al. 2013), the

investigation of interactions between these proteins in *Xenopus* oocytes appears mandatory for further applications of the model system.

We employed immunoblotting and immunohistochemical staining in order to gain a comprehensive understanding of the expression, localization, and interaction of heterologously expressed claudins with tjp1 in oocytes at developmental stages V and VI. *Xenopus* oocytes at stage V–VI express small amounts of transcripts of claudin mRNA, ranging from approximately 0.06 up to 44.7 TPM (Session et al. 2016), and so, endogenous claudin protein expression might be expected in immunoblots. But the protein expression of claudins is described as a mere fraction, e.g., 0.001 for cldn3 (decimal fraction at stage VI of total protein agglomerated over all profiled stages), and the anti-human CLDN antibodies allowed a clear distinction to be made between injected and thus overexpressing oocytes and naïve germ cells. Nevertheless, we were able to verify endogenous tjp1 protein expression and to localize the protein to the submembranous space of naïve and claudin-expressing oocytes. In accordance with the literature in which both isoforms of tjp1 have been reported to be present in the *Xenopus* embryo from the first cleavage onwards (Fesenko et al. 2000), we were able to detect α^+ and α^- tjp1 in oocytes at stages V and VI.

Furthermore, our quantitative PCR analyses revealed that claudin expression did not significantly affect *tjp1* mRNA expression levels. Previously, tjp1 has been shown to have a modeling effect on cell–cell contacts by regulating nuclear processes (Gottardi et al. 1996). In addition, claudins have been described as transcriptional regulators (Hagen 2017) that not only affect other transcription factors, e.g., ZONAB (Ikari et al. 2014), but also have the ability to interact with

Fig. 2 Immunohistochemical staining of TJ proteins in *X. laevis* oocytes All claudin-injected oocytes revealed claudin-specific signals at their cell membranes in accordance with the injected CLDN cRNAs (green). RNAse-free water-injected oocytes were treated identically and showed no signal for the endogenous expression of claudins (* representative image of water-injected oocyte screened for endogenous CLDN3 expression). Additionally, immunofluorescent staining in claudin- and water-injected oocytes revealed specific tjp1 signals (red) in oocytes, whereas in no primary antibody controls, no specific signals were detected by confocal microscopy. Tjp1 signals were concentrated in the submembranous space and appeared as a belt-like structure. In CLDN2- and CLDN3-expressing oocytes, claudin and tjp1 signals were selectively colocalized at the plasma membrane and resulted in a yellow signal (arrows). Scale bars: 20 mm
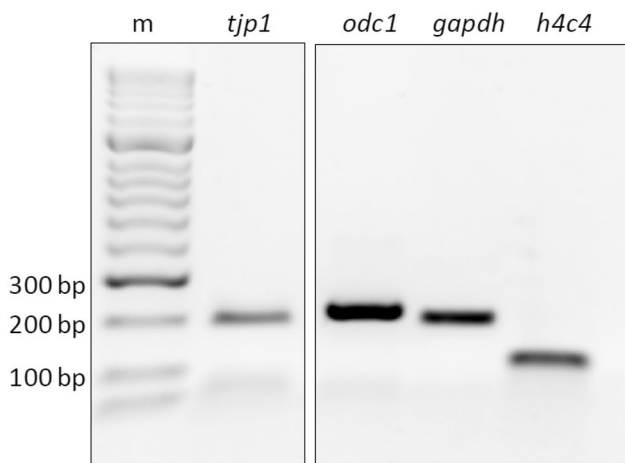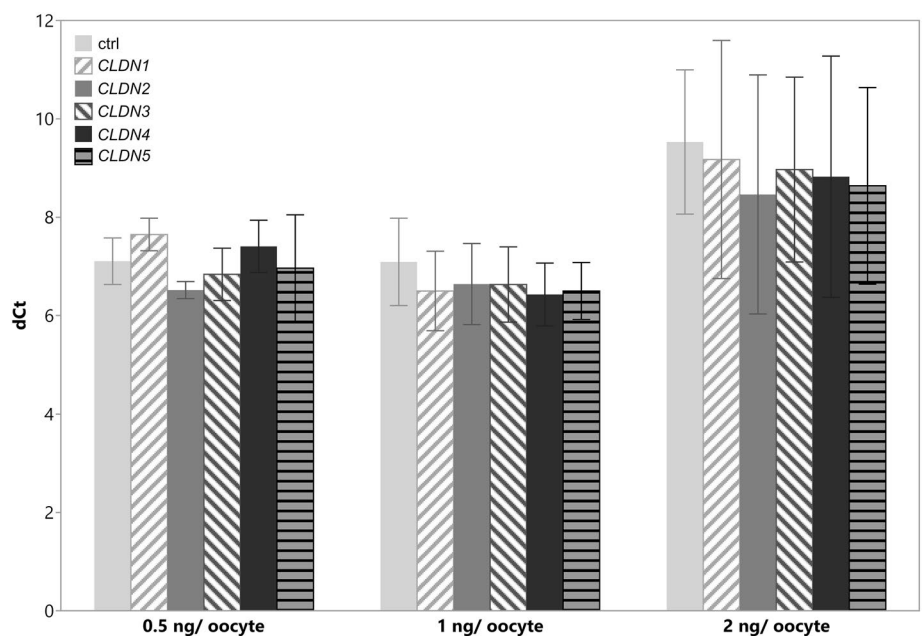
Fig. 3 Qualitative PCR of *tjp1* and housekeeping genes *odc1*, *gapdh*, and *h4c4* PCR products were loaded onto a 2% agarose gel in TBE buffer. Pooled samples of claudin-injected oocytes showed gene products in accordance with the predicted amplicon size (Table 2) of the housekeeping genes and the gene of interest

the scaffold. Schlingmann et al. have demonstrated that the binding of CLDN5 to tjp1 in alveolar epithelial cells results in paracellular leakage and the rearrangement of TJs by inhibiting the interaction of CLDN19 with the scaffold (Schlingmann et al. 2016). Moreover, a reduction in tjp1 to CLDN4 binding has been shown to lead to lower CLDN4 expression (Hamada et al. 2013). In our study, heterologous claudin expression did not affect *tjp1* gene expression in the oocytes, and claudin–scaffold interactions were reflected by only a partial colocalization of the two binding partners (CLDN and tjp1) at the same intracellular location, as shown by confocal laser-scanning analyses. Unlike the localization in epithelial cells and cell culture experiments in which tjp1 and claudins largely colocalize in the apical part of the cells, the clear distinction between the membranous claudins and the submembranous scaffolding protein tjp1 becomes more apparent, because of the large size of the germ cell of up to 1300 μm. Nevertheless, the limited counts of colocalization indicate that claudins and tjp1 are only intermittently associated corresponding to the dynamic coupling of claudin strands with the cytoskeleton (Van Itallie et al. 2017).

Table 4 Delta Ct and *n*-fold *tjp1* expression

	Delta Ct ± SEM			*n*-fold (control = 1)		
	0.5 ng/oocyte	1 ng/oocyte	2 ng/oocyte	0.5 ng/oocyte	1 ng/oocyte	2 ng/oocyte
Control	7.105 ± 0.223	7.090 ± 0.419	9.530 ± 0.692			
CLDN1	7.647 ± 0.156	6.499 ± 0.382	9.174 ± 1.142	1.28	1.51	1.28
CLDN2	6.517 ± 0.082	6.640 ± 0.389	8.462 ± 1.146	2.10	1.37	2.10
CLDN3	6.838 ± 0.251	6.629 ± 0.361	8.970 ± 0.886	1.47	1.38	1.47
CLDN4	7.406 ± 0.250	6.428 ± 0.301	8.825 ± 1.157	1.63	1.58	1.63
CLDN5	6.964 ± 0.511	6.499 ± 0.273	8.639 ± 0.693	1.85	1.51	1.85

Fig. 4 Quantitative real-time PCR of *tjp1* in claudin-expressing *X. laevis* oocytes PCR delta Ct values in control oocytes were indistinctive from claudin-expressing oocytes at all three tested concentrations of 0.5, 1, and 2 ng cRNA/ oocyte, ANOVA: $p \geq 0.9$

In the literature, actin filaments of oocyte stage VI have been observed to surround the germinal vesicle and also extend from the cortex into the subcortical cytoplasm. After this stage, a dynamic change of actin distribution has only been described after the meiotic arrest of prophase I is terminated and fertilization occurs (Roeder and Gard 1994; Christensen et al. 1984). Furthermore, independent of the interaction with tjp1 or actin, claudin strands are capable to break and re-anneal (Van Itallie et al. 2017), although the accumulation of the tjp1 signal in the submembranous space is described as an indicator of the formation of the subjunctional cytoplasmic plaque of the TJ (D'Atri and Citi 2002). The accumulation of tjp1 in a submembranous belt in oocytes resembles the concentration of tjp1 in the junctional complex region in polarized epithelial cell lines (Umeda et al. 2006), and thus, the formation of the submembranous belt in *Xenopus* oocytes might mirror this process of organization. We conclude that, in this experimental setting, physiological binding is unhampered. The reason that the submembranous signal is more apparent in CLDN1-, CLDN2-, and CLDN5-expressing cells compared with CLDN3- and CLDN4-expressing cells remains unclear and needs to be examined in more detail in future studies. An overexpression of CLDN3 and CLDN4 has been described to enhance tumorigenesis of human ovarian surface epithelial (HOSE) cells. The more diffuse pattern of tjp1 in the oocytes might therefore result from tjp1 interacting with not only claudins, but also numerous other cytosolic and nuclear proteins, e.g., pten and zonab, which play a role in the regulation of germ cell function (Heinzelmann-Schwarz et al. 2004; Agarwal et al. 2005). Additionally, Nomme et al. have identified factors of claudin specificity and affinity of binding to cytoplasmic scaffolding proteins, such as tjp1. They analyzed the binding of claudins to the tjp1 PDZ1 domain and discovered that the binding can be influenced by the presence or absence of a tyrosine residue at P_{-6} and that the affinity is reduced if the tyrosine is modified by phosphorylation (Nomme et al. 2015). However, these findings can not depict a full molecular explanation for the structural distinct cellular localization of tjp1 in the *Xenopus* oocytes, because CLDN1 and CLDN4 do not share this tyrosine residue at P_{-6}. Moreover, a potential difference might arise because of a disparate distribution of yolk platelets along the animal–vegetal axis of the oocytes (Danilchik and Gerhart 1987), rather than because of differences with regard to claudin family members.

Although *Xenopus laevis* is widely used for the investigation of transport mechanisms, signaling pathways, and human hereditary genetic diseases (Miller and Zhou 2000; Blum et al. 2009; Blum and Ott 2018), the use of *Xenopus* oocytes for barrier research is a novel approach. Two studies have recently been conducted on the mechanistic suitability of the oocytes for barriology by our group (Vitzthum et al. 2019; Brunner et al. 2020). The current study contributes to this specific field of barrier research and encourages the application of the model. Despite the information that a single or two-cell (paired oocyte) model can contribute to a multifunctional and multicellular barrier system being limited, it nevertheless allows an in-depth examination of claudin interaction in a restricted and therefore verifiable, reproducible, and cost-efficient model system.

In our experimental setup, the effects of claudin expression on the cytoskeletal scaffold are demonstrated for tjp1. In a further step toward a better understanding of tjp1-CLDN colocalization, Förster resonance energy transfer (FRET) technology or coimmunoprecipitation (coIP) could be conducted in follow-up studies to gain a sterical perception of the involved mechanism and give proof of an interaction between the binding partners. In particular, the detection of small quantities of endogenous tjp1 in *Xenopus* oocytes might be improved as it was shown for cystic fibrosis transmembrane regulator (CFTR) protein localization by Kreda et al. (Kreda and Gentzsch 2011). Additionally, a coinjection of CLDNs and tjp1 cRNA leading to a tjp1 overexpression may lead to further insights into the tjp1-CLDN interaction and might also allow a manipulation of CLDN function through the utilization of tjp1 orthologs and mutants. This might further allow clinical implications, toward an understanding and therapeutic options including the role of the actin cytoskeletal scaffold in barrier-related diseases, e.g., IBD (Kuo et al. 2021).

Although tjp1 plays an important role with regard to TJ assembly, structure, and regulation, the development of a functional barrier is dependent on a variety of factors, such as MARVEL domain proteins (Raleigh et al. 2010), junctional adhesion molecules, and cingulin (D'Atri et al. 2002; Zihni et al. 2016; Vasileva et al. 2020). Indeed, tjp1 can be regarded as a key point of TJ scaffolding, as reduced tjp1 expression correlates with increased TJ permeability and ineffective epithelial healing processes (Kuo et al. 2021). Thus, our present examination of tjp1-CLDN interactions provides a timely evaluation of the accessibility of the amphibian cell model for barrier research.

Data Availability In accordance with the rules of good scientific practice, all data are archived and available on request.

Declarations

Conflict of Interest The authors declare that the research was conducted in the absence of any commercial or financial relationships that could be construed as a potential conflict of interest.

Open Access This article is licensed under a Creative Commons Attribution 4.0 International License, which permits use, sharing, adaptation, distribution and reproduction in any medium or format, as long as you give appropriate credit to the original author(s) and the source, provide a link to the Creative Commons licence, and indicate if changes were made. The images or other third party material in this article are included in the article's Creative Commons licence, unless indicated otherwise in a credit line to the material. If material is not included in the article's Creative Commons licence and your intended use is not permitted by statutory regulation or exceeds the permitted use, you will need to obtain permission directly from the copyright holder. To view a copy of this licence, visit http://creativecommons.org/licenses/by/4.0/.

References

Agarwal R, D'Souza T, Morin PJ (2005) Claudin-3 and claudin-4 expression in ovarian epithelial cells enhances invasion and is associated with increased matrix metalloproteinase-2 activity. Cancer Res 65(16):7378–7385. https://doi.org/10.1158/0008-5472.Can-05-1036

Assef YA, Ozu M, Marino GI, Galizia L, Kotsias BA (2011) ENaC channels in oocytes from *Xenopus laevis* and their regulation by xShroom1 protein. Cell Physiol Biochem 28:259–266. https://doi.org/10.1159/000331738

Balda MS, Matter K (2000) The tight junction protein ZO-1 and an interacting transcription factor regulate ErbB-2 expression. EMBO J 19(9):2024–2033. https://doi.org/10.1093/emboj/19.9.2024

Balda MS, Garrett MD, Matter K (2003) The ZO-1-associated Y-box factor ZONAB regulates epithelial cell proliferation and cell density. J Cell Biol 160(3):423–432. https://doi.org/10.1083/jcb.200210020

Blum M, Ott T (2018) *Xenopus*: an undervalued model organism to study and model human genetic disease. Cells Tissues Organs 205(5–6):303–313. https://doi.org/10.1159/000490898

Blum M, Beyer T, Weber T, Vick P, Andre P, Bitzer E, Schweickert A (2009) *Xenopus*, an ideal model system to study vertebrate left-right asymmetry. Dev Dyn 238(6):1215–1225. https://doi.org/10.1002/dvdy.21855

Bowes JB, Snyder KA, Segerdell E, Gibb R, Jarabek C, Noumen E, Pollet N, Vize PD (2008) Xenbase: a *Xenopus* biology and genomics resource. Nucleic Acids Res 36:D761–D767. https://doi.org/10.1093/nar/gkm826

Brunner N, Stein L, Cornelius V, Knittel R, Fallier-Becker P, Amasheh S (2020) Blood-brain barrier protein claudin-5 expressed in paired *Xenopus laevis* oocytes mediates cell-cell interaction. Front Physiol. https://doi.org/10.3389/fphys.2020.00857

Cardellini P, Davanzo G, Citi S (1996) Tight junctions in early amphibian development: detection of junctional cingulin from the 2-cell stage and its localization at the boundary of distinct membrane domains in dividing blastomeres in low calcium. Dev Dyn 207(1):104–113. https://doi.org/10.1002/(SICI)1097-0177(199609)

Carotenuto R, Tussellino M (2018) Xenopus laevis oocyte as a model for the study of the cytoskeleton. CR Biol 341(4):219–227. https://doi.org/10.1016/j.crvi.2018.04.001

Christensen K, Sauterer R, Merriam R (1984) Role of soluble myosin in cortical contractions of *Xenopus* eggs. Nature 310:150–151. https://doi.org/10.1038/310150a0

Danilchik MV, Gerhart JC (1987) Differention of the animal-vegetal axis in *Xenopus laevis* oocytes: I. Polarized intracellular translocation of platelets establishes the yolk gradient. Dev Biol 122(1):101–112. https://doi.org/10.1016/0012-1606(87)90336-8

D'Atri F, Citi S (2002) Molecular complexity of vertebrate tight junctions (review). Mol Membr Biol 19(2):103–112. https://doi.org/10.1080/09687680210129236

D'Atri F, Nadalutti F, Citi S (2002) Evidence for a functional interaction between cingulin and ZO-1 in cultured cells. J Biol Chem 277(31):27757–27764. https://doi.org/10.1074/jbc.M203717200

Fanning AS, Anderson JM (2009) Zonula occludens-1 and -2 are cytosolic scaffolds that regulate the assembly of cellular junctions. Mol Struct Funct Tight Junct 1165:113–120. https://doi.org/10.1111/j.1749-6632.2009.04440.x

Fanning AS, Jameson BJ, Jesaitis LA, Anderson JM (1998) The tight junction protein ZO-1 establishes a link between the transmembrane protein occludin and the actin cytoskeleton. J Biol Chem 273(45):29745–29753. https://doi.org/10.1074/jbc.273.45.29745

Fesenko I, Kurth T, Sheth B, Fleming TP, Citi S, Hausen P (2000) Tight junction biogenesis in the early *Xenopus* embryo. Mech Dev 96(1):51–65. https://doi.org/10.1016/S0925-4773(00)00368-3

Furuse M, Itoh M, Hirase T, Nagafuchi A, Yonemura S, Tsukita S, Tsukita S (1994) Direct association of occludin with Zo-1 and its possible involvement in the localization of occludin at tight junctions. J Cell Biol 127(6):1617–1626. https://doi.org/10.1083/jcb.127.6.1617

Furuse M, Fujita K, Hiiragi T, Fujimoto K, Tsukita S (1998) Claudin-1 and -2: novel integral membrane proteins localizing at tight junctions with no sequence similarity to occludin. J Cell Biol 141(7):1539–1550. https://doi.org/10.1083/jcb.141.7.1539

Galizia L, Pizzoni A, Fernandez J, Rivarola V, Capurro C, Ford P (2012) Functional interaction between AQP2 and TRPV4 in renal cells. J Cell Biochem 113:580–589. https://doi.org/10.1002/jcb.23382

Galizia L, Marino GI, Ojea A, Kotsias BA (2013) Hypotonic regulation of mouse epithelial sodium channel in *Xenopus laevis* oocytes. J Membr Biol 246:949–958. https://doi.org/10.1007/s00232-013-9598-8

Gottardi CJ, Arpin M, Fanning AS, Louvard D (1996) The junction-associated protein, zonula occludens-1, localizes to the nucleus before the maturation and during the remodeling of cell-cell contacts. Proc Natl Acad Sci USA 93(20):10779–10784. https://doi.org/10.1073/pnas.93.20.10779

Hagen SJ (2017) Non-canonical functions of claudin proteins: beyond the regulation of cell-cell adhesions. Tissue Barriers. https://doi.org/10.1080/21688370.2017.1327839

Hamada K, Kakigawa N, Sekine S, Shitara Y, Horie T (2013) Disruption of ZO-1/claudin-4 interaction in relation to inflammatory responses in methotrexate-induced intestinal mucositis. Cancer Chemother Pharmacol 72(4):757–765. https://doi.org/10.1007/s00280-013-2238-2

Heasman J (2006) Patterning the early *Xenopus* embryo. Development 133(7):1205–1217. https://doi.org/10.1242/dev.02304

Heinzelmann-Schwarz VA, Gardiner-Garden M, Henshall SM, Scurry J, Scolyer RA, Davies MJ, Heinzelmann M, Kalish LH, Bali A, Kench JG, Edwards LS, Vanden Bergh PM, Hacker NF, Sutherland RL, O'Brien PM (2004) Overexpression of the cell adhesion molecules DDR1, claudin 3, and Ep-CAM in metaplastic ovarian epithelium and ovarian cancer. Clin Cancer Res 10(13):4427–4436. https://doi.org/10.1158/1078-0432.Ccr-04-0073

Ikari A, Watanabe R, Sato T, Taga S, Shimobaba S, Yamaguchi M, Yamazaki Y, Endo S, Matsunaga T, Sugatani J (2014) Nuclear distribution of claudin-2 increases cell proliferation in human lung adenocarcinoma cells. Biochim BiophysActa 1843(9):2079–2088. https://doi.org/10.1016/j.bbamcr.2014.05.017

Ikenouchi J, Furuse M, Furuse K, Sasaki H, Tsukita S, Tsukita S (2005) Tricellulin constitutes a novel barrier at tricellular contacts of epithelial cells. J Cell Biol 171(6):939–945. https://doi.org/10.1083/jcb.200510043

Itoh M, Furuse M, Morita K, Kubota K, Saitou M, Tsukita S (1999) Direct binding of three tight junction-associated MAGUKs, ZO-1, ZO-2 and ZO-3, with the COOH termini of claudins. J Cell Biol 147(6):1351–1363. https://doi.org/10.1083/jcb.147.6.1351

Katsuno T, Umeda K, Matsui T, Hata M, Tamura A, Itoh M, Takeuchi K, Fujimori T, Nabeshima Y, Noda T, Tsukita S, Tsukita S (2008) Deficiency of zonula occludens-1 causes embryonic lethal phenotype associated with defected yolk sac angiogenesis and apoptosis of embryonic cells. Mol Biol Cell 19(6):2465–2475. https://doi.org/10.1091/mbc.E07-12-1215

Kreda SM, Gentzsch M (2011) Imaging CFTR protein localization in cultured cells and tissues. Methods Mol Biol 742:15–33. https://doi.org/10.1007/978-1-61779-120-8_2

Kuo W-T, Zuo L, Odenwald MA, Madha S, Singh G, Gurniak CB, Abraham C, Turner JR (2021) The tight junction protein ZO-1 is dispensable for barrier function but critical for effective mucosal repair. Gastroenterology 161(6):1924–1939. https://doi.org/10.1053/j.gastro.2021.08.047

Leduc-Nadeau A, Lahjouji K, Bissonnette P, Lapointe JY, Bichet DG (2007) Elaboration of a novel technique for purification of plasma membranes from Xenopus laevis oocytes. Am J Physiol Cell Physiol 292(3):C1132–C1136. https://doi.org/10.1152/ajpcell.00136.2006

Miller AJ, Zhou JJ (2000) Xenopus oocytes as an expression system for plant transporters. Biochim Biophys Acta 1465(1–2):343–358. https://doi.org/10.1016/S0005-2736(00)00148-6

Nenni MJ, Fisher ME, James-Zorn C, Pells TJ, Ponferrada V, Chu S, Fortriede JD, Burns KA, Wang Y, Lotay VS, Wang DZ, Segerdell E, Chaturvedi P, Karimi K, Vize PD, Zorn AM (2019) Xenbase: facilitating the use of Xenopus to model human disease. Front Physiol 10:1664. https://doi.org/10.3389/fphys.2019.00154

Nomme J, Antanasijevic A, Caffrey M, Van Itallie CM, Anderson JM, Fanning AS, Lavie A (2015) Structural basis of a key factor regulating the affinity between the zonula occludens first PDZ domain and claudins. J Biol Chem 290(27):16595–16606. https://doi.org/10.1074/jbc.M115.646695

Ozu M, Dorr R, Parisi M (2005) New method to measure water permeability in emptied-out Xenopus oocytes controlling conditions on both sides of the membrane. J Biochem Biophys Methods 63:187–200. https://doi.org/10.1016/j.jbbm.2005.04.007

Ozu M, Dorr RA, Teresa Politi M, Parisi M, Toriano R (2011) Water flux through human aquaporin 1: inhibition by intracellular furosemide and maximal response with high osmotic gradients. Eur Biophys J 40:737–746. https://doi.org/10.1007/s00249-011-0687-2

Palma AG, Galizia L, Kotsias BA, Marino GI (2016) CFTR channel in oocytes from Xenopus laevis and its regulation by xShroom1 protein. Pflug Arch Eur J Physiol 468:871–880. https://doi.org/10.1007/s00424-016-1800-2

Peshkin L, Lukyanov A, Kalocsay M, Gage RM, Wang D, Pells TJ, Karimi K, Vize PD, Wühr M, Kirschner MW (2019) The protein repertoire in early vertebrate embryogenesis. bioRxiv. https://doi.org/10.1101/571174

Powell DW (1981) Barrier function of epithelia. Am J Physiol 241(4):G275–G288. https://doi.org/10.1152/ajpgi.1981.241.4.G275

Raleigh DR, Marchiando AM, Zhang Y, Shen L, Sasaki H, Wang YM, Long MY, Turner JR (2010) Tight junction-associated MARVEL proteins MarvelD3, tricellulin, and occludin have distinct but overlapping functions. Mol Biol Cell 21(7):1200–1213. https://doi.org/10.1091/mbc.E09-08-0734

Riazuddin S, Ahmed ZM, Fanning AS, Lagziel A, Kitajiri S, Ramzan K, Khan SN, Chattaraj P, Friedman PL, Anderson JM, Belyantseva IA, Forge A, Riazuddin S, Friedman TB (2006) Tricellulin is a tight-junction protein necessary for hearing. Am J Hum Genet 79(6):1040–1051. https://doi.org/10.1086/510022

Rodgers LS, Beam MT, Anderson JM, Fanning AS (2013) Epithelial barrier assembly requires coordinated activity of multiple domains of the tight junction protein ZO-1. J Cell Sci 126(Pt 7):1565–1575. https://doi.org/10.1242/jcs.113399

Roeder AD, Gard DL (1994) Confocal microscopy of F-actin distribution in Xenopus oocytes. Zygote 2(2):111–124. https://doi.org/10.1017/s0967199400001866

Ruffer C, Gerke V (2004) The C-terminal cytoplasmic tail of claudins 1 and 5 but not its PDZ-binding motif is required for apical localization at epithelial and endothelial tight junctions. Eur J Cell Biol 83(4):135–144. https://doi.org/10.1078/0171-9335-00366

Schlingmann B, Overgaard CE, Molina SA, Lynn KS, Mitchell LA, White SD, Mattheyses AL, Guidot DM, Capaldo CT, Koval M (2016) Regulation of claudin/zonula occludens-1 complexes by hetero-claudin interactions. Nat Commun. https://doi.org/10.1038/ncomms12276

Segerdell E, Bowes JB, Pollet N, Vize PD (2008) An ontology for Xenopus anatomy and development. BMC Dev Biol. https://doi.org/10.1186/1471-213x-8-92

Session AM, Uno Y, Kwon T, Hapman JAC, Toyoda A, Takahashi S, Fukui A, Hikosaka A, Suzuki A, Kondo M, van Heeringen SJ, Quigley I, Heinz S, Ogino H, Ochi H, Hellsten U, Lyons JB, Simakov O, Putnam N, Stites J, Kuroki Y, Tanaka T, Michiue T, Watanabe M, Ogdanovic OB, Lister R, Georgiou G, Paranjpe SS, Van Kruijsbergen I, Shu SQ, Carlson J, Kinoshita T, Ohta Y, Mawaributchi S, Jenkins J, Grimwood J, Schmutz J, Mitros T, Mozaffari SV, Suzuki Y, Haramoto Y, Yamamoto TS, Takagi C, Heald R, Miller K, Haudenschild C, Kitzman J, Nakayama T, Zutsu YI, Robert J, Fortriede J, Burns K, Lotay V, Karimi K, Yasuoka Y, Dichmann DS, Flajnik MF, Houston DW, Shendure J, DuPasquier L, Vize PD, Zorn AM, Ito M, Marcotte EM, Wallingford JB, Ito Y, Asashima M, Ueno N, Matsuda Y, Veenstra GJC, Fujiyama A, Harland RM, Taira M, Rokhsar DS (2016) Genome evolution in the allotetraploid frog Xenopus laevis. Nature 538(7625):336. https://doi.org/10.1038/nature19840

Umeda K, Ikenouchi J, Katahira-Tayama S, Furuse K, Sasaki H, Nakayama M, Matsui T, Tsukita S, Furuse M, Tsukita S (2006) ZO-1 and ZO-2 independently determine where claudins are polymerized in tight-junction strand formation. Cell 126(4):741–754. https://doi.org/10.1016/j.cell.2006.06.043

Van Itallie CM, Fanning AS, Bridges A, Anderson JM (2009) ZO-1 stabilizes the tight junction solute barrier through coupling to the perijunctional cytoskeleton. Mol Biol Cell 20(17):3930–3940. https://doi.org/10.1091/mbc.E09-04-0320

Van Itallie CM, Tietgens AJ, Anderson JM (2017) Visualizing the dynamic coupling of claudin strands to the actin cytoskeleton through ZO-1. Mol Biol Cell 28(4):524–534. https://doi.org/10.1091/mbc.E16-10-0698

Vasileva E, Rouaud F, Spadaro D, Huang W, Colom A, Flinois A, Shah J, Dugina V, Chaponnier C, Sluysmans S, Méan I, Jond L, Roux A, Yan J, Citi S (2020) Cingulin unfolds ZO-1 and organizes myosin-2B and γ-actin to mechanoregulate apical and tight junction membranes. bioRxiv. https://doi.org/10.1101/2020.05.14.095364

Vitzthum C, Stein L, Brunner N, Knittel R, Fallier-Becker P, Amasheh S (2019) Xenopus oocytes as a heterologous expression system for analysis of tight junction proteins. FASEB J 33(4):5312–5319. https://doi.org/10.1096/fj.201801451RR

Will C, Fromm M, Müller D (2008) Claudin tight junction proteins: novel aspects in paracellular transport. Perit Dial Int 28(6):577–584. https://doi.org/10.1177/089686080802800605

Willott E, Balda MS, Heintzelman M, Jameson B, Anderson JM (1992) Localization and differential expression of 2 isoforms of the tight junction protein Zo-1. Am J Physiol 262(5):C1119–C1124. https://doi.org/10.1152/ajpcell.1992.262.5.C1119

Zihni C, Mills C, Matter K, Balda MS (2016) Tight junctions: from simple barriers to multifunctional molecular gates. Nat Rev Mol Cell Biol 17(9):564–580. https://doi.org/10.1038/nrm.2016.80

Zuckerman JB, Chen XY, Jacobs JD, Hu BF, Kleyman TR, Smith PR (1999) Association of the epithelial sodium channel with Apx and alpha-spectrin in A6 renal epithelial cells. J Biol Chem 274:23286–23295. https://doi.org/10.1074/jbc.274.33.23286

Publisher's Note Springer Nature remains neutral with regard to jurisdictional claims in published maps and institutional affiliations.

7. Discussion

Xenopus laevis oocytes are capable of transcribing human claudin cRNA into encoding proteins

The goal of the first part of this work was to establish a basic research model for the analysis of claudin-claudin interactions. To achieve this goal, the possible expression of human claudins was examined in unfertilized stage VI oocytes of *Xenopus laevis*. Established models for TJ protein analysis traditionally rely on knockout and overexpression animal or cell models giving insights into the functional contribution of claudins to the organ- or tissue-specific function of the TJ (Seker et al. 2019). However, a limiting aspect of these models is the unclear background expression of TJ proteins. As an approach to this problem, non-epithelial cell lines, e.g., L-fibroblasts, were established for the analysis of TJ proteins in the past (Furuse et al. 1999). Nevertheless, a combined analysis of the various TJ proteins in a claudin-transfected cell line is challenging because this method requires the provision of sufficient selection pressure by several different antibiotics for each protein of interest. *Xenopus* oocytes are non-epithelial cells that naturally do not form occluding junctions with other cells. By utilizing these cells, one can bypass the endogenous background expression for the TJ proteins of interest. *Xenopus* oocytes have indeed been described to form junctions with the surrounding follicle cells, but these junctions have been identified as gap junctions and desmosomes (Browne et al. 1979; Browne and Werner 1984).

As most of the classic claudins contain a PDZ-binding motif, the transcribed claudins were hypothesized to be physiologically located to the plasma membrane of the germ cells. The widely expressed and representative claudin-1, claudin-2, and claudin-3 were utilized initially during the establishment of the model.

Claudin-1 is ubiquitously expressed and ordinarily is classified as a claudin with sealing properties. Claudin-1 overexpression increases the TEER in MDCK II cells (Furuse et al. 1998a; Inai et al. 1999). Knockout of claudin-1 is reported to lead to massive water and macromolecule loss at the epidermis and therefore can lead to the death of neonatal mice (Furuse et al. 2002). In contrast, claudin-2 is a characteristic TJ protein expressed in leaky epithelia, e.g., the proximal tubule of the kidney and the intestine (Rahner et al. 2001; Kiuchi-Saishin et al. 2002). Experiments with claudin-2 overexpression have revealed that claudin-2 acts as a cation-permeable pore and is also permeable to water (Amasheh et al. 2002; Rosenthal et al. 2010). The third protein of interest, claudin-3, is expressed in a variety of epithelia as it constitutes a sealing claudin in the respiratory, urinary, and gastrointestinal tracts. Additionally, claudin-3 is a major component of the blood-brain barrier and blood-testis barrier (Günzel and Yu 2013). Overexpression of claudin-3 in low resistance MDCK II cells increases paracellular resistance 9- to 15-fold (Milatz et al. 2010). Recent studies have highlighted that claudin-3 loss heavily impairs murine hepatic metabolism and biliary barrier function (Baier et al. 2021).

Before the oocyte culture experiments, protein encoding consensus sequences of human claudin-1 to -3 were cloned into suitable pGEM plasmid vectors, and cDNA was isolated after bacterial transformation in competent DH10b *Escherichia coli*. A T7 RNA-polymerase-based approach generated cRNAs for injection into the amphibian germ cells. Claudin-1, -2, and -3 expression was determined by Western Blot and immunohistochemical experiments. Claudin-signals were detectable reliably and permanently in injected oocytes at 3 days post-injection, whereas water-injected controls showed no endogenous claudin-specific signals (see publication chapter 4, figure 1).

Claudins co-expressed in a single oocyte are colocalized and indicate a functional heterophilic *cis*-interaction

For investigation as to whether the various claudin proteins can interact, experiments were performed combining injections of cRNA encoding for different claudins into the same oocyte.

The immunohistochemical stainings of co-injected oocytes revealed signals for the tested claudin combinations (claudin-1/claudin-2, claudin-1/claudin-3, claudin-2/claudin-3). The proteins were largely co-distributed within the oocyte plasma membrane. This potentially reflected the heterophilic *cis*-interaction of the binding partners. Some claudin combinations, particularly those co-expressing claudin-2 and claudin-3, showed a more interrupted pattern of localization. The punctate pattern of colocalization possibly occurred because of a different grade of structural organization, in accordance with the heteropolymeric TJ strand assembly HEK cell model of Piontek *et al.* (2011) who assumed that two to six claudin monomers formed claudin oligomers by *cis*-interactions. The authors utilized differences in fluorescence resonance energy transfer (FRET) efficiencies to rank the different *cis*-interactions, e.g., claudin-5/claudin-5 (homooligomer) > claudin-3/claudin-3 (homooligomer) > claudin-3/claudin-5 (heterooligomer). The higher FRET energies of claudin-5 compared with claudin-3 were consistent with oligomer size and arose because of sterically different homooligomers, e.g., a higher number of molecules ($n_{claudin-5} > n_{claudin-3}$). The authors did not observe *cis*-interactions between claudin-2 and -3. (Piontek et al. 2011).

Claudins are physiologically targeted into the oocyte plasma membrane and form heterophilic and homophilic *trans*-interactions

To access *trans*-interactions between claudins in the *Xenopus* oocyte cell model, claudin-expressing oocytes were investigated in a "paired oocyte assay". In this approach, claudin-injected oocytes or water-injected control oocytes were devitellinated, and adhering contacts were induced by pairwise clustering with a bulb-headed probe. Paired oocytes were used either for immunohistochemical stainings and freeze fracture electron microscopy or for an examination of the contact areas at the oocyte junction. After 1h, 24 h, and 48 h, contact widths were measured under bright field microscopy, and contact areas were calculated by using the circle equation:

$$A = \pi \times \left(\frac{\text{measured width}}{2}\right)^2$$

Since the clustering of the claudin-expressing oocyte pairs resulted in a strong connection between the two cells, the contact area size of the clustered cells was hypothesized to correlate with the strength of the claudin *trans*-interaction. Mechanical separation of the cells was no longer possible at 1 h after clustering without completely destroying the oocytes.

The paired oocyte assay with single claudin-expressing oocytes resulted in a time-dependent increase of contact areas in all tested control and claudin combinations. The clustering of a cell expressing claudin-1, -2, and -3 with another triple co-injected cell led to a significant increase of contact areas and supported the hypothesis that an increasing complexity of TJ strand assembly is correlated with an increase of contact areas in the paired oocyte assay (see publication chapter 4, figure 3 and 4).

Membrane freeze fracture visualizes specific strand assembly patterns for the different claudins

Freeze fracture electron microscopy was performed for the visualization of claudin TJ strand assembly in the oocyte plasma membrane. The typical claudin-specific strand morphology, as known from epithelial cell lines (Furuse 2010), was apparent. Discrete patches of complex claudin strands were detectable in triple-injected oocytes expressing a combination of claudin-1, -2, and -3. This structure was highly repetitive and highly organized being reminiscent of petal silhouettes. In contrast, the TJ patches of single-claudin-expressing oocytes demonstrated a more disorganized strand morphology. In the absence of claudin-2, a more rounded strand meshwork was dominant in claudin-1 and -3 expressing cells. This was in accordance with the literature describing strand fibril architecture specific for claudin family members (Colegio et al. 2002). Water-injected control oocytes exhibited no comparable TJ strand structures (see publication chapter 4, figure 5).

The first set of experiments thus highlights the *Xenopus laevis* oocyte as a promising expression system for the analysis of TJ protein assembly and interaction. The heterologous expression of human claudins provides new possibilities for the analysis and modeling of tissue- and organ-specific claudin combinations.

Claudin-5 as the gatekeeper of the blood-brain barrier

In the second part of the work described in this thesis, the sealing properties of claudin-5 (the dominant claudin in the blood-brain barrier were analyzed in the *Xenopus laevis* model system. The capillary endothelium at the blood-brain barrier is a tight epithelium with a claudin-5 expression >100 times higher compared with that of any other claudin (Ohtsuki et al. 2007). It restricts the blood-brain barrier to molecules smaller than 800 Da (Nitta et al. 2003). Moreover, claudin- 5 also provides sealing properties in the epithelium of the lung (Soini 2011), exocrine epithelia (Comper et al. 2009), and intestinal and urinary tracts (Koda et al. 2011). Claudin-5 downregulation is related to neurodegenerative and inflammatory disorders, and therefore, claudin-5 is referred to as the gatekeeper of neurological function (Greene et al. 2019). Claudin-5 is not only crucial for the maintenance of the blood-brain barrier, but also limits the permeability of both noxious and therapeutic substances into the brain.

Electron freeze fracture microscopy of *Xenopus* oocytes expressing claudin-5 morphologically revealed the presence of claudin-5, which formed an angular meshwork ordered in rows. The meshwork of fibrils appeared partly discontinuous. The claudin-3 in claudin-3-expressing oocytes was however assembled into a more rounded strand meshwork in loop shapes (see publication chapter 5, figure 3). This is in agreement with the literature describing claudin-5 TJ strands as assembling into chains of particles primarily associated with the E-face, whereas claudin-3 forms continuous-type strands associated with the protoplasmic P-face of the membrane (Piontek et al. 2011). Additionally, mixed P-/E-face association, as found in oocytes co-expressing claudin-3 and -5, are typically correlated with blood-brain barrier-specific tightness (Liebner et al. 2000; Wolburg et al. 2003).

In addition, claudin-3 and claudin-5 were analyzed in a paired oocyte assay. Combinations of claudin-3, claudin-5, or co-expressing claudin-3/claudin-5 cells were clustered in pairs to induce the formation of claudin *trans*-interactions. In accordance with the results from the first set of experiments that focused on oocytes expressing claudin-1, - 2, and -3, all combinations of claudin-3 and -5 showed a time-dependent increase in contact area over the measured period of 48 h. Surprisingly, the co-expression of the two sealing claudins-3 and claudin-5 did not result in a significantly larger contact area compared with the expression of the single proteins, although a tendency could be identified. Clustered pairs of oocytes co-expressing claudin-3 and claudin-5 showed increases in median contact area to 168% (24 h) and 209% (48 h), whereas oocytes expressing claudin-3 alone showed increases in median contact areas to 147% (24 h) and 162% (48 h), and the expression of claudin-5 alone resulted in increases of median contact area to 120% (24 h) and 127% (48 h) (see publication chapter 5, figure 4, table 1). These findings led to the conclusion that the measurement of contact widths of clustered oocytes and the subsequent calculation of contact areas is potentially not sufficient for an identification of the adhesion force of the claudin *trans*-interactions, exclusively.

Investigation of the quality of the *trans*-interaction: hydrostatic pressure impulse reveals claudin-specific contribution to the oocyte junction

A study of the biomechanical forces of the cell-cell connection is of importance for several reasons. First, the human organism is constantly exposed to external physical influences because of musculoskeletal movement and external environmental strains. Second, the cell-cell interaction can be altered in physiological processes and can be affected in certain human diseases that influence the mechanical properties of an epithelium. The strains on epithelial cell bonds can ultimately lead to a breakdown of the structural and functional integrity of tissues and whole organs. Additionally, within the context of biological cell responses, shear stress and mechanical forces have been described as leading to cellular responses, e.g., cell

movement, cell differentiation, and apoptosis (Dieterich et al. 2000; Fitzgerald et al. 2008; Yourek et al. 2010). Finally, the tightness of the paracellular seal of the TJ can be adjusted to physiological processes such as the absorption of macromolecules in the gastrointestinal tract or into the brain. Therefore, a characterization of the barrier properties and the involved forces is of fundamental value with regard to drug delivery and the biomedical application of potential drug candidates.

The mechanical forces in barriology have been investigated by multiple approaches with respect to the character of the force and the experimental context, e.g., the experimental model and the available experimental tools.

For the analysis of biological structures from ~ 1 nm to 500 nm such as DNA, viruses, and actin, the experimental techniques for conducting mechanical tests in single cells and single molecules mainly involve atomic force microscopy and laser tweezers that function as an optical trap. In the past few years, the influence of vibration on cell adhesion (Ito et al. 2011) and the effects of shear stress on endothelial tissue have been analyzed in flow chamber experiments and by other specialized methods (Brakemeier et al. 2003; Zhang and Neelamegham 2017). The attachment force of claudin *trans*-interactions have even been examined in cell lines. Vedula et al. (Vedula et al. 2009) applied a "step pressure technique" utilizing micropipettes for aspiration of the cells and hence measured the force needed to detach L-fibroblasts transfected with GFP-tagged occludin, claudin-1, and claudin-2. They were able to identify separation forces in a nanonewton scale (~2.8 nN for claudin-1, ~2.3 nN for claudin-2). Micropipette aspiration is suitable for use on microscale biostructures such as red blood cells and neutrophils (Lim et al. 2006). Although this approach similarly seemed to be promising for the analysis of claudin-claudin interactions in *Xenopus* oocytes, preliminary tests revealed that the detachment of clustered oocytes is not possible without the disruption of the plasma membrane of the oocyte. This is in agreement with the literature describing the application of the micropipette aspiration technique for the investigation of membrane elasticity and membrane deformation (Rand and Burton 1964; Dong et al. 1988). Furthermore, the disadvantages of the micropipette aspiration technique include the stress concentration at the pipette edge and the friction between the micropipette surface and the cell membrane. Thus, an approach without strains caused by the fixation of the cells to the equipment was attempted in the current work.

For the analysis of the claudin-interaction in *Xenopus* oocytes, a new methodical approach was therefore undertaken to analyze the strength of adhesion of the clustered oocyte pairs. The most robust results were obtained in a hydrostatic pressure impulse assay. Analogous to the paired oocyte assay, oocytes were devitellinated and clustered mechanically to form adhering contact areas. The first 24 h after clustering were set as a stabilization period. During this time, no manipulation of the pairs was performed. Next, a defined hydrostatic impulse was applied using a single channel electronic pipette. The experimental setup was standardized with the dispensing speed being consistently set to maximum speed, equating a dispensing speed of 0.9 s for a volume of 250 µl. In addition, the angle (45°) and distance of application (~1.3 cm) were unified. Oocytes were challenged by employing the liquid pressure impulse, and contact areas were measured and calculated 30 min after challenge and compared with areas measured immediately after the stabilization period. Clustered pairs of oocytes expressing claudin-5 or claudin-3 or co-expressing claudin-3/claudin-5 retained significantly larger contact areas after the liquid strain (97%, p = 0.0235; 96%, p = 0.003; 98%, p = 0.0253), whereas mixed water-injected and claudin-expressing pairs (claudin-3 – control and claudin-5 – control) and control pairs (control – control) separated at the contact regions (see publication chapter 5, figure 5).

The results from current setup suggested that both claudin-3 and claudin-5 contributed to stronger adhesion properties in *Xenopus* oocytes. Even though single claudins expressed in oocytes did not lead to an increase of contact areas compared with the control oocytes (Vitzthum et al. 2019; Brunner et al. 2020), the force of claudin *trans*-interaction was assessable with the hydrostatic pressure impulse assay. Despite the hydrostatic pressure

impulse assay not allowing quantification in absolute values, it facilitated a quick and cost-effective analysis of the claudin interaction in combination with the advantages of the *Xenopus* expression system, e.g., no disturbances because of the presence of other TJ proteins such as occludin, tricellulin, or junctional adhesion molecules.

Incubation experiments with sodium caprate

As mentioned above, the manipulation of barrier properties might become of beneficial value with regard to drug delivery and the medical application of potential drug candidates. Consequently, the *Xenopus* oocyte barrier model might function as a potential screening model for possible claudin-barrier manipulators. In the literature, the medium-chain fatty acid sodium caprate has been established to impair the epithelial barrier reversibly. It can therefore be clinically employed as an absorption enhancer for intestinal drug uptake because of the improvement of the membrane permeation of pharmaceutical agents (Lindmark et al. 1997). In the colonic epithelial cell line HT29/B6, sodium caprate leads to a reduction of barrier properties because of a reversible paracellular leak mediated by claudin-5. This has been detected by a reduced TEER in Ussing chamber experiments with the cell line and in vitro experiments of porcine jejunum (Krug et al. 2013; Radloff et al. 2017).

Thus, incubation with sodium caprate might also result in a decrease in the contact areas of clustered claudin-5-expressing *X. laevis* oocytes, as the mode of action of sodium caprate is known to lead to a contraction of the perijunctional actomyosin ring of cells and, hence, to a widening of the paracellular space (Maher et al. 2009). This effect is based on an intracellular increase of Ca^{2+} concentration attributable to phospholipase C activation, which subsequently activates myosin light chains in response to the cleavage of phosphatidylinositol 4,5-bisphosphate (PIP2) into inositol triphosphate (IP3) and diacylglycerol (DAG) (Tomita et al. 1995). Some authors have also described an increase of transcellular permeability for sodium caprate by its functioning as a tenside surfactant (Maher et al. 2009).

For the experiments described here, oocytes were injected with relevant claudin-5 cRNA and combined in a paired oocyte assay in which both cells expressed claudin-5 (claudin-5 – claudin-5). At 24 h after the stabilization period, pairs were incubated with final sodium caprate concentrations of 50, 100, or 500 mM, and contact widths were measured at 30, 60, and 120 min after the sodium caprate addition. In both control and claudin-5-expressing cells, the addition of the test substance (or culture medium) resulted in an initial decrease of contact areas that dispersed 60 or 120 min after addition. This was indicated by the parabolic shape of the connection line between the median contact areas over time and possibly reflected a strain of the claudin *trans*-interaction because of turbulence after the liquid addition.

Surprisingly, incubation with 100 mM and 500 mM sodium caprate increased contact areas at 30 min after addition with no initial decrease being detectable indicating a protective effect of sodium caprate on the oocyte junction rather than a widening of the oocyte junction (see publication chapter 5, figure S1).

A strengthening effect of sodium caprate on paracellular permeability has previously been described in the literature. In porcine Peyer's Patch tissue, claudin-5 was significantly increased after incubation with 5 mM caprate and led to a significantly higher TEER of the specialized follicle-associated epithelium (Radloff et al. 2019). In their study, the authors discussed the overall increase of claudin-5 expression that led to a compensatory effect and an increase in TEER.

Despite the first hypothesized widening of the paracellular seal because of a cytoskeletal contraction, a tearing of the TJ *trans*-interaction is only possible when the claudins are connected to the cytoskeleton and hence pulled apart by the cytoskeletal contraction. The molecular mechanisms through which cytoskeletal contraction assigns changes in the tight junction are still debated. The most prominent candidate for linking the actomyosin ring to the tight junction is tjp1, although tjp2 and/or tjp3 interactions may serve as a scaffold. Furthermore, a linkage with cingulin and actin or cingulin and myosin might elicit TJ widening

(Turner 2000). Consequently, the third set of experiments presented here focuses on the interaction of heterologously expressed claudins with the oocyte scaffolding protein tjp1.

Additional to the physiological binding of the claudins to the cell scaffolding protein tjp1, a closer understanding of the organization of the actin filaments of the oocyte has to be obtained with regard to the sodium caprate mechanism. *Xenopus laevis* oocytes are a traditional model system for embryonic development, and therefore, many studies have been conducted on the development and maturation of these germ cells. Since 1976, amphibian oocytes have been known to contain all classes of cytoskeletal elements including large amounts of actin with concentrations exceeding 4mg/ml (Clark and Merriam 1977). In immature oocytes, cytoplasmic actin filaments are accumulated beneath the vegetal side of the germinal vesicle (Yamagishi and Abe 2015). The actin filaments localize in three main cellular domains: a network of cytoplasmic cables surrounding the germinal vesicle as mentioned by Yamagishi and Abe (2015), the nucleus, and the cortex region. Actin filaments have been observed to surround the germinal vesicle and also extend from the cortex into the subcortical cytoplasm (Roeder and Gard 1994). Taking the actin filament contribution into account, the ability of the oocyte to enforce a directed drag on the oocyte junction is uncertain. No statistical analysis was performed on this set of data as the oocyte pairs showed a large variation between the pairs, and the expected differences were considered small. Hence, further experiments concerning the suitability of these oocytes for the analysis of barrier proteins needed to be conducted.

Xenopus laevis oocytes show specific signals for tjp1 in submembranous space

The oocyte model has been analyzed with regard to the interaction of heterologously expressed claudins and tjp1. The investigation of interactions between tjp1 and the expressed claudins in *Xenopus* oocytes is mandatory for further applications of the model system. In the literature, tjp1 is described as being present in the *Xenopus laevis* embryo from the first cleavage onwards (Fesenko et al. 2000). In studies on genome evolution of the allotetraploid *Xenopus laevis*, researchers have identified the gene expression of *tjp1* S and for *tjp1* L of 0.9 transcripts per one million mapped reads (TPM) and of 1.9 TPM, respectively, in unfertilized oocytes of stages V and VI (Session et al. 2016). The relative protein expression for oocytes at stage VI is described as being 0.096, which represents the decimal fraction at this stage of total protein agglomerated over all profiled stages (Peshkin et al. 2019). To date, no immunohistochemical visualization of tjp1 protein in *Xenopus laevis* oocytes are available. In the experiments described in this thesis, both α+ and α- tjp1 isoforms were first detectable in oocyte stages V and VI not only by immunoblotting, but also by immunohistochemical staining (see publication chapter 6, figure 1 and 2). Oocyte stages V and VI were injected cRNA encoding for human claudin-1, -2, -3, -4, or claudin-5 in three test groups of 0.5 ng cRNA per oocyte, 1 ng cRNA per oocyte, or 2 ng cRNA per oocyte. All membrane fractions of the sampled cells revealed claudin-specific signals at the predicted protein mass in accordance with the injected cRNAs, and all tested and control oocytes showed tjp1-isoform-specific signals at 195 kDa ($α^+$) and 187 kDa ($α^-$). The localization of the tjp1 signal was examined by immunohistochemical staining: tjp1 was mainly located in the submembranous space of the cells and appeared as a sub-membranous belt immediately underneath the oocyte plasma membrane. The accumulation of tjp1 in a submembranous belt in oocytes resembles the concentration of tjp1 in the junctional complex region in polarized epithelial cell lines (Umeda et al. 2006), and thus, the formation of the submembranous belt in *Xenopus* oocytes might mirror this process of organization. Moreover, the concentration of tjp1 in the submembraneous space is described as an indicator of the formation of the subjunctional cytoplasmic TJ plaque (D'atri and Citi 2002). In claudin-2-and claudin-3-expressing cells, signals for claudins and tjp1 have been selectively colocalized at the plasma membrane, and the limited counts of colocalization suggest that claudins and tjp1 are only intermittently associated. Researchers have stated that the dynamic behavior of claudin strand assembly, breaking, and rejoining is independent of the interaction with tjp1 or actin. Claudins and tjp1 are only intermittently associated reflecting a dynamic coupling of claudin strands with the cytoskeleton (Van Itallie et al. 2017). This is in accordance with the immunohistochemical tjp1 staining of the oocytes, and hence, the physiological binding is hypothesized to be

unhampered in the model system. The immunohistochemical of signals for tjp1 in the form of a submembranous belt was particularly distinct in claudin-1-, -2-, and -5-expressing cells and in naïve oocytes in comparison with claudin-2- and claudin-4-expressing cells. In human ovarian surface epithelial (HOSE) cells, an overexpression of claudin-3 and claudin-4 has been described to enhance tumorigenesis. The more diffuse pattern of tjp1 in the oocytes might therefore result from tjp1 interacting also with numerous other cytosolic and nuclear proteins, e.g., PTEN and ZONAB, which play a role in the regulation of ovarial cell function (Heinzelmann-Schwarz et al. 2004; Agarwal et al. 2005) Additionally, Nomme et al. (2015) have identified factors of claudin affinity and specifity of binding to cytoplasmic scaffolding proteins, such as tjp1. The authors examined the binding of claudins to the tjp1 PDZ domain and discovered that the binding can be influenced by the presence or absence of a tyrosine residue at P_{-6}, and that the affinity is reduced if the tyrosine is modified by phosphorylation (Nomme et al. 2015). However, these findings cannot depict the full molecular explanation for the structural distinct cellular localization of tjp1 in the *Xenopus* oocytes, because CLDN1 and CLDN4 do not share this tyrosine residue at P-6. Moreover, a potential difference might arise because of a disparate distribution of yolk platelets along the animal-vegetal axis of the oocytes (Danilchik et al. 1987), rather than because of differences with regard to claudin family members.

Claudin injection does not engage endogenous *tjp1* mRNA expression

The use of *Xenopus* oocytes as a heterologous expression system naturally involves the introduction of external cRNA into the cell, a manipulation that might interact with the endogenous gene products of the oocyte. Claudins have been described to act as transcriptional regulators and to affect other transcription factors, e.g.,ZONAB (Ikari et al. 2014; Hagen 2017). Experimental findings suggest that the ability of claudins to interact with the scaffold influences epithelial properties: In alveolar epithelial cells, the binding of claudin-5 to tjp1 results in a paracellular leak and rearrangement of TJs by an inhibition of the interaction of other claudin family members (e.g., claudin-19) with the scaffold (Schlingmann et al. 2016). Furthermore, a reduced tjp1 binding to claudin-4 has been shown to lead to a reduction in claudin-4 expression (Hamada et al. 2013). In this regard, *tjp1* mRNA levels in claudin-expressing oocytes were examined in the three cRNA injection groups of 0.5 ng per oocyte, 1 ng per oocyte, and 2 ng per oocyte. Because *tjp1* was consistently detectable in qualitative PCR, quantitative real-time PCR was performed to investigate the effect of claudin injection on *tjp1* mRNA levels (see publication chapter 6, figure 3 and 4). All tested claudin-injected oocytes showed a negligible impact on *tjp1* expression compared with water-injected controls, resulting in a non-significant n-fold up-regulative trend of 1.28 - 2.10 in claudin-expressing cells. With regard to the developmental stage of the germ cells, immature *Xenopus* oocytes are arrested in prophase I of the meiotic division. Maternal stores of mRNA and, hence, larger amounts of *tjp1*, can only be transcribed at the induction of maturation, with a maximum transcription of 20.88 per one million mapped reads in NF stage 9 (Session et al. 2016). The mechanism that prevents the translation of larger amounts of maternal mRNA remains unknown, but the suggestion of a lowering of cyclic adenosine monophosphate (cAMP) and protein kinase A (PKA) is controversial (Nader et al. 2016). The capacity for translation in stage VI oocytes might be limited by some component of the translational apparatus other than mRNA, e.g., the rough endoplasmic reticulum (Richter and Smith 1981). Researchers have observed that, whereas exogenous cRNA is transcribed, protein synthesis from endogenous mRNA decreases. In the past, injections of 60 ng cRNA per oocyte have led to a decrease of endogenous protein synthesis by 31% in stage VI oocytes with the net result being no change in total protein synthesis (Taylor et al. 1985). With regard to the maximum injection of 2 ng claudin cRNA per oocyte in these experiments, this mechanism is hypothesized to have a negligible impact on the endogenous *tjp1* expression. The results of the quantitative real-time PCR indicate that claudin injection has no adverse effect on endogenous *tjp1* expression.

Xenopus oocytes provide several advantages for the implementation of the 3R concept in barriology research

The scientifically most important quality of the *Xenopus* oocytes is their ability to efficiently translate injected exogenous mRNA into proteins. Additionally, the African clawed frog provides other advantages with regard to animal welfare and the implementation of the 3R concept in scientific research.

Xenopus laevis is easily kept and bred in captivity and is available from commercial suppliers at low costs (Wu and Gerhart 1991). In accordance with the concept of 3Rs, the minimum number of animals required for an experiment must be found without compromising the scientific integrity of the study. One method of reduction is the reuse of animals in multiple independent experiments (Kovalcsik et al. 2006). For the experiments described in this thesis, the animals were not purchased from a commercial breeder but rather were acquired from animal surpluses from cooperating work groups. For reasons of standardization, only *Xenopus laevis* females of the same age and physical constitution were used in order to obtain comparable results. Second, individual animals were reused to reduce the total number of animals required. When reusing individuals for the surgical harvesting of oocytes, several requirements had to be fulfilled without exception:

1. Multiple surgeries on a single animal should not result in a significant extra burden on the individual compared with an increase in the total used animals. In an ethical assessment, the procedural steps for the animals were analyzed and critically discussed.
2. Sufficient time was allowed between two surgical procedures for full convalescence of the individual. A minimum of three months between surgeries enabled full recovery and healing of the incision site, and oocyte collection was alternated between left and right ovaries to maximize the interval for the individual animal.
3. The total number of laparotomies was limited and depended on the condition of the animal, the quality of oocytes, and the total number of surgeries during the lifespan of the animal. The maximum number of surgeries was in accordance with the guidelines of German legislation, with approval by the animal welfare officer for the Freie Universität Berlin and under the governance of the Berlin Veterinary Health Inspectorate (permit G0025/16 and O 0022/21).

In general, oocytes can be harvested non-seasonally in large quantities, and the cells can be easily prepared because of their large size. From an environmental point of view, oocytes are often laid in water bodies with potentially substandard conditions. As a result, they are comparatively sturdy and resistant to temperature and water quality fluctuations. The egg yolk particles and maternal stores of mRNA provide substrates for growth and the efficient translation of proteins, independent of nutrient uptake.

Additional to the goal of animal reduction, methods were refined in the procedural steps of oocyte harvesting and the handling of the animals:

1. Minimal invasive operation technique: Ovarian tissue was removed through a small skin and abdominal muscle incision of approximately 10 mm in length, and the wound was subsequently closed with a delicate re-absorbable suture (Vicryl 4-0, P-3, Ethicon V494). The closure of the two layers (muscle layer and skin) was carried out to minimize post-surgical complications. Surgeries under adequate anesthesia were performed by trained personnel. Laparotomies were performed aseptically, and sterilized instruments were always used.
2. Use of anesthetics: For surgical anesthesia, frogs were carefully transferred into a bath containing a solution of buffered 2 gram per liter MS222 (ethyl 3-aminobenzoate methanesulfonate, pH 7.5) for 5-10 min at 20° C. Righting and corneal reflexes were used for the assessment of surgical anesthetic depth.
3. Use of analgesics: Laronde-Robert et al. (2012) advocate immersion of frogs in a bath of 2 g / L MS222 for 20 minutes is appropriate for surgical procedures of less than 60

minutes. For surgical anesthetic evaluation and pain indication, an acetic acid test and withdrawal and corneal reflexes were used in this study (Lalonde-Robert et al. 2012). Analgesics that are commonly used in other species or for other applications have been reported to have limited efficacy in *Xenopus laevis* following surgery for oocyte harvesting. In a study from 2018, neither the application of butorphanol (0.05 mg / kg and 1 mg / kg) nor fentanyl (0.05 mg / kg, 0.25 mg / kg and 0.5 mg / kg) resulted in a significant reduction of pain signals during surgery under MS222. Because of cardiovascular side effects, the authors did not find any practical benefits for the use of these substances (Strobel et al. 2018). In an investigation from 2011, the administration of flunixin meglumine (25 mg / kg via the dorsal lymph sac) resulted in significant analgesia in *Xenopus laevis*, but the authors expressed concerns in terms of pharmaceutical drug safety as the histopathology of one animal indicated bilateral kidney congestion (Coble et al. 2011). As a consequence of these findings, no additional analgesics were administered after MS222 immersion of the frogs in the experiments here. This approach is supported by the observations that MS222 blocks the activity of both sensory and motor nerves compatible with the mechanistic action of effective anesthetics (Ramlochansingh et al. 2014). Hence, to date, MS222 is regarded as an effective single-drug anesthetic for surgical interventions in anamniotes.

4. Handling refinements: Animals were handled with finely woven nets, and gloves were used to protect the delicate skin of the amphibians. The use of a net reduces damage to the mucous layer of the frog and is considered less traumatic than physical handling (Green 2010).

5. Environmental enrichment: In 2014, Michaels et al. reviewed the importance of environmental enrichment for advancing amphibian welfare and described that the provision of shelter allows the animals to exhibit a range of species-specific behaviors and reduces negative effects of captivity (Michaels et al. 2014). The animals used for the work detailed in this thesis were allocated shelter providing cover in the form of easy-to-clean aquaristic clay tubes and caves.

Conclusion

The results presented in this thesis indicate that *Xenopus laevis* oocytes constitute a suitable one-cell or two-cell (paired oocyte) model for the analysis of TJ proteins, namely the claudins. They highlight the advantages of the use of the amphibian germ cells for the heterologous expression of human claudins. Novel methods have been introduced for the functional characterization of claudin *trans*-interactions.

Human claudins have been successfully expressed and characterized, and protocols for the barrier model have been established. The paired oocyte assays serve as a novel approach for analyzing the claudin *trans*-interaction and have been refined by the establishment of a hydrostatic pressure impulse assay. This method also represents a new tool for approaching the quality of *trans*-interaction in the oocyte junction of paired oocytes.

Although the use of amphibians as a model system might appear, at first glance, to have little translational relevance, the proteins of interest have been constructed from human data sources. The described results highlight the potential for the use of this model in human physiology and for the understanding of epithelial barrier properties in health and disease.

8. Summary

Summary of the Ph.D. Thesis:

***Xenopus laevis* oocyte cell model for barrier research of tight junction proteins**

Tight junctions (TJs) ring the lateral membrane of polarized epithelial cells and thus establish a border at the apical plasma membrane allowing the epithelium to perform its main function, namely to serve as a selectively permeable barrier. TJs are mainly formed by small (20- 27kDa) transmembrane claudins that span the cellular membrane four times, with the N-terminus and C-terminus being located in the cytoplasm of the cells. The barrier properties of the epithelium are mainly attributed to the claudin protein family (Markov et al. 2015). Various claudin family members can associate into functional groups of sealing or barrier-forming and pore- or channel-forming claudins, but this classification is in part fluent, as claudins can fulfill a range of functions (Günzel and Yu 2013).

The work in this thesis focused on three aspects of a new barrier model:

1. **Establishment and validation of a new model for the analysis of claudins by heterologous expression in *Xenopus laevis* oocytes**

The functional characterization of claudins and claudin-claudin interactions is of fundamental importance for understanding the physiological properties of barrier function and relevant mechanisms in health and disease. The intention of the research detailed here was to establish a barrier research model as an alternative for transgenic mouse models or primary cell lines. The heterologous expression of claudins was therefore examined in *X. laevis* oocytes. Claudin-1, claudin-2, and claudin-3 were used for the establishment of the model system. When co-expressed in a single oocyte, the claudins colocalized, with indications of functional heterophilic *cis*-interactions. Not only were the injected claudins physiologically targeted into the oocyte plasma membrane and formed heterophilic and homophilic *trans*-interactions, but membrane freeze fracture images also revealed claudin-specific strand assembly patterns for the examined claudins in the oocyte membranes. Moreover, *Xenopus* oocytes were found to provide many advantages for the implementation of the 3Rs in barriology research.

2. **Application of the expression model for the analysis of blood-brain barrier-specific claudin-5 interaction**

Following the verification of the general suitability of the germ cells for the analysis of claudin *cis*- and *trans*-interactions, the expression model was applied to the analysis of blood-brain barrier-specific claudin-5 interactions. In addition to the establishment of a paired oocyte assay in which oocyte contact areas were evaluated, the connection forces of the oocyte junctions were measured by a hydrostatic pressure impulse (HPI) assay. This novel approach allowed for an evaluation of the fraction that the single claudins contribute to the junction of the oocytes and revealed the strength of *trans*-interaction.

3. **Examination of elementary interactions of heterologously expressed claudins with the oocyte scaffolding protein tjp1**

In the third set of experiments, interactions were examined between tjp1 and heterologously expressed claudins in *Xenopus* oocytes. The functional interplay between the scaffolding proteins of the cell and the heterologously expressed claudins is mandatory for further applications of the model system. Immunoblots and immunohistochemical staining confirmed and visualized this functional interplay between the two binding partners, as *X. laevis* oocytes showed a specific signal for tjp1 in the sub-membranous space without influence of claudin cRNA injection on endogenous *tjp1* mRNA expression.

Zusammenfassung der Dissertation:

Xenopus laevis-Oozyten als Barrieremodell zur Untersuchung von Tight Junction-Proteinen

Die Tight Junction umschließt die laterale Zellmembran polarisierter Epithelien und bildet durch Zell-Zell-Verbindungen eine Kompartimentierung, die es dem Epithel erlaubt, eine selektive Barriere aufzubauen. Diese Zell-Zellverbindungen werden hauptsächlich durch 20-27 kDa große transmembrane Claudine gebildet. Claudine besitzen vier transmembrane Domänen, während der C- und N-Terminus im Intrazellularraum liegen. Die permeabilitätsbestimmenden Eigenschaften der Barriere werden insbesondere durch diese Proteinfamilie bestimmt (Markov et al. 2010). Funktionell konnten grundlegende Unterschiede zwischen den Claudinen dargestellt werden, daher können sie in abdichtende und porenbildende Claudine klassifiziert werden. Untersuchungen einzelner Proteine stellte aber auch eine nicht eindeutige Funktion einiger Claudin-Familienmitglieder fest (Günzel and Yu 2013).

Im Rahmen dieser Dissertation zur Etablierung eines oozytären Barrieremodells wurden drei grundlegende Aspekte untersucht:

1. **Etablierung des Barrieremodells und Feststellung der Eignung der *Xenopus laevis*-Oozyten als Modell zur Analyse von Claudinen**

Die funktionelle Charakterisierung der Claudine, sowie der Claudin-Claudin-Interaktionen, ist von großer Bedeutung zum Verständnis physiologischer Eigenschaften der Barriere im gesunden und erkrankten Organismus. Mit dem Ziel, ein Barrieremodell unter geringem Tierverbrauch im Vergleich zu transgenen Mausmodellen oder primären Zellkulturmodellen zu entwickeln, wurden in dieser Dissertation Claudine in *Xenopus laevis*-Oozyten heterolog exprimiert. Zur Etablierung des Oozytenmodells wurden exemplarisch zunächst Claudin-1, Claudin-2 und Claudin-3 genutzt. Wird die entsprechende Claudin-cRNA in die Keimzellen eingebracht, werden die Claudine in der Zelle exprimiert. Ein physiologischer Einbau der heterolog exprimierten Proteine findet regulär statt und auch eine Ausbildung von hetero- und homophilen *trans*- und *cis*-Interaktionen konnte beobachtet werden. In Gefrierbruchaufnahmen der Claudin-injizierten Oozyten konnte eine Claudin-spezifische Strangausbildung dargestellt werden.

2. **Anwendung des Barrieremodells zur Analyse Blut-Hirn-Schranken-spezifischer Claudine und deren Interaktion**

Nach der generellen Etablierung des Modells wurden Blut-Hirn-Schranken-spezifische Claudine exprimiert und deren *trans*-Interaktionen untersucht. Zusätzlich zum Einsatz des gepaarten Oozytenassays wurden die methodischen Ansätze erweitert, eine Messung der Qualität der Oozytenkontaktfläche wurde im Rahmen des Hydrostatic Pressure Impulse Assays (HPI) vorgenommen. Dieser Versuchsaufbau erlaubte eine Einordnung der Anteile, mit denen das jeweilige Claudin zur Kontaktflächenverbindung der gepaarten Oozyten beiträgt, sowie eine Einschätzung der Claudin-*trans*-Interaktionsstärke. Der HPI zeigte eine claudin-spezifische Beteiligung der Proteine an der Kontaktflächenverbindung der gepaarten Zellen.

3. **Untersuchung der endogenen tjp1-Interaktion mit den heterolog exprimierten Claudinen**

Im dritten Teil der Dissertationsexperimente wurden Untersuchungen zur Interaktion zwischen dem endogenen Adapterprotein tjp1 und den heterolog exprimierten Claudinen durchgeführt. Das funktionelle Zusammenspiel der TJ-Proteine ist eine zwingende Voraussetzung für den regelgerechten Einbau der Claudine in der Oozytenzellmembran und damit den weiteren

Einsatz des Modells zur Charakterisierung weiterer Claudinkombinationen. In Western Blot-Experimenten und immunhistochemischen Färbungen konnte eine Colokalisation der beiden Bindungspartner erstmals visualisiert werden. Dabei zeigten die Oozyten tjp1-spezifische Signale in Form einer gürtelförmigen Anreicherung im submembranösen Raum, ohne dass injizierte Claudin-cRNAs Einfluss auf die endogenen *tjp1*-mRNA-Expressionslevel nahmen.

References

Adams CL, Nelson WJ (1998):
Cytomechanics of cadherin-mediated cell-cell adhesion.
Current Opinion in Cell Biology, 10, 5, 572-577. doi: 10.1016/S0955-0674(98)80031-8

Amasheh S, Meiri N, Gitter AH, Schoneberg T, Mankertz J, Schulzke JD, Fromm M (2002):
Claudin-2 expression induces cation-selective channels in tight junctions of epithelial cells.
Journal of Cell Science, 115, 24, 4969-4976. doi: 10.1242/jcs.00165

Amasheh S, Milatz S, Krug SM, Markov AG, Günzel D, Amasheh M, Fromm M (2009):
Tight junction proteins as channel formers and barrier builders.
Ann N Y Acad Sci, 1165, 211-219. doi: 10.1111/j.1749-6632.2009.04439.x

Amasheh S, Fromm M, Günzel D (2011):
Claudins of intestine and nephron - a correlation of molecular tight junction structure and barrier function.
Acta Physiol (Oxf), 201, 133-140. doi: 10.1111/j.1748-1716.2010.02148.x

Anderson JM, Van Itallie CM (2009):
Physiology and function of the tight junction.
Cold Spring Harb Perspect Biol, 1, a002584. doi: 10.1101/cshperspect.a002584

Baier FA, Sánchez-Taltavull D, Yarahmadov T, Castellà C G, Jebbawi F, Keogh A, Tombolini R, Odriozola A, Dias MC, Deutsch U, Furuse M, Engelhardt B, Zuber B, Odermatt A, Candinas D, Stroka D (2021):
Loss of Claudin-3 Impairs Hepatic Metabolism, Biliary Barrier Function, and Cell Proliferation in the Murine Liver.
CMGH Cell. Mol. Gastroenterol. Hepatol., 12, 2, 745-767. doi: 10.1016/j.jcmgh.2021.04.003

Balda MS, Matter K (1998):
Tight junctions.
Journal of Cell Science, 111, 5, 541-547. doi: 10.1242/jcs.111.5.541

Balda MS, Flores-Maldonado C, Cereijido M, Matter K (2000a):
Multiple domains of occludin are involved in the regulation of paracellular permeability.
J Cell Biochem, 78, 85-96.

Balda MS, Matter K (2000b):
The tight junction protein ZO-1 and an interacting transcription factor regulate ErbB-2 expression.
Embo Journal, 19, 9, 2024-2033. doi: 10.1093/emboj/19.9.2024

Banerjee S, Sousa AD, Bhat MA (2006):
Organization and function of septate junctions: an evolutionary perspective.
Cell Biochem Biophys, 46, 1, 65-77. doi: 10.1385/cbb:46:1:65

Bazzoni G, Martinez-Estrada OM, Mueller F, Nelboeck P, Schmid G, Bartfai T, Dejana E, Brockhaus M (2000):
Homophilic interaction of junctional adhesion molecule.
J Biol Chem, 275, 40, 30970-30976. doi: 10.1074/jbc.M003946200

Bazzoni G (2003):
The JAM family of junctional adhesion molecules.
Current Opinion in Cell Biology, 15, 5, 525-530. doi: 10.1016/S0955-0674(03)00104-2

Beyer EC, Berthoud VM (2017):
Gap junction structure: unraveled, but not fully revealed.
F1000Research, 6, 568-568. doi: 10.12688/f1000research.10490.1

Blum M, Ott T (2018):
Xenopus: An Undervalued Model Organism to Study and Model Human Genetic Disease.
Cells Tissues Organs, 205, 5-6, 303-313. doi: 10.1159/000490898

Borradori L, Sonnenberg A (1999):
Structure and Function of Hemidesmosomes: More Than Simple Adhesion Complexes.
Journal of Investigative Dermatology, 112, 4, 411-418. doi: 10.1046/j.1523-1747.1999.00546.x

Bozzaro S (2013):
The model organism Dictyostelium discoideum.
Methods Mol Biol, 983, 17-37. doi: 10.1007/978-1-62703-302-2_2

Brakemeier S, Kersten A, Eichler I, Grgic I, Zakrzewicz A, Hopp H, Köhler R, Hoyer J (2003):
Shear stress-induced up-regulation of the intermediate-conductance Ca2+-activated K+ channel in human endothelium.
Cardiovascular Research, 60, 3, 488-496. doi: 10.1016/j.cardiores.2003.09.010

Brink PR (1998):
Gap junctions in vascular smooth muscle.
Acta physiologica Scandinavica, 164, 4, 349-356. doi: 10.1046/j.1365-201x.1998.00439.x

Browne CL, Wiley HS, Dumont JN (1979):
Oocyte-follicle cell gap junctions in *Xenopus laevis* and the effects of gonadotropin on their permeability.
Science, 203, 4376, 182-183. doi: 10.1126/science.569364

Browne CL, Werner W (1984):
Intercellular junctions between the follicle cells and oocytes of *Xenopus laevis*.
J Exp Zool, 230, 1, 105-113. doi: 10.1002/jez.1402300114

Bruce A, Johnson A, Lewis J, Raff M, Roberts K, Walter P (2002):
Molecular Biology of the Cell.
4th Edition, New York: Garland Science. ISBN: 0815332181

Brunner N, Stein L, Cornelius V, Knittel R, Fallier-Becker P, Amasheh S (2020):
Blood-Brain Barrier Protein Claudin-5 Expressed in Paired *Xenopus laevis* Oocytes Mediates Cell-Cell Interaction.
Frontiers in Physiology, 11, 857. doi: 10.3389/fphys.2020.00857

Carotenuto R, Tussellino M (2018):
Xenopus laevis oocyte as a model for the study of the cytoskeleton.
Comptes Rendus Biologies, 341, 4, 219-227. doi: 10.1016/j.crvi.2018.04.001

Carson JL (2014):
Fundamental technical elements of freeze-fracture/freeze-etch in biological electron microscopy.
J Vis Exp, 91, 51694. doi:10.3791/51694

Citi S, Sabanay H, Jakes R, Geiger B, Kendrick-Jones J (1988):
Cingulin, a new peripheral component of tight junctions.
Nature, 333, 6170, 272-276. doi: 10.1038/333272a0

Clark TG, Merriam RW (1977):
Diffusible and bound actin nuclei of *Xenopus laevis* oocytes.
Cell, 12, 4, 883-891. doi: 10.1016/0092-8674(77)90152-0

Claude P, Goodenough DA (1973):
Fracture faces of zonulae occludentes from "tight" and "leaky" epithelia.
J Cell Biol, 58, 2, 390-400. doi: 10.1083/jcb.58.2.390

Coble DJ, Taylor DK, Mook DM (2011):
Analgesic effects of meloxicam, morphine sulfate, flunixin meglumine, and xylazine
hydrochloride in African-clawed frogs (*Xenopus laevis*).
J Am Assoc Lab Anim Sci, 50, 3, 355-360.

Colegio OR, Van Itallie CM, Rahner C, Anderson JM (2002):
The role of claudin extracellular domains in tight junction fibril architecture and paracellular
charge selectivity.
Molecular Biology of the Cell, 13, 286a-286a.

Comper F, Antonello D, Beghelli S, Gobbo S, Montagna L, Pederzoli P, Chilosi M, Scarpa A
(2009):
Expression Pattern of Claudins 5 and 7 Distinguishes Solid-pseudopapillary From
Pancreatoblastoma, Acinar Cell and Endocrine Tumors of the Pancreas.
Am. J. Surg. Pathol., 33, 5, 768-774. doi: 10.1097/PAS.0b013e3181957bc4

D'Atri F, Citi S (2001):
Cingulin interacts with F-actin in vitro.
FEBS Letters, 507, 1, 21-24. doi: 10.1016/S0014-5793(01)02936-2

D'Atri F, Citi S (2002):
Molecular complexity of vertebrate tight junctions (Review).
Molecular Membrane Biology, 19, 2, 103-112. doi: 10.1080/09687680210129236

Danilchik MV, Gerhart JC (1987):
Differention of the animal-vegetal axis in *Xenopus laevis* oocytes: I. Polarized intracellular
translocation of platelets establishes the yolk gradient.
Developmental Biology, 122, 1, 101-112. doi: 10.1016/0012-1606(87)90336-8

De Robertis EM, Larraín J, Oelgeschläger M, Wessely O (2000):
The establishment of Spemann's organizer and patterning of the vertebrate embryo.
Nat Rev Genet, 1, 3, 171-181. doi: 10.1038/35042039

Delpire E, Gagnon KB, Ledford JJ, Wallace JM (2011):
Housing and husbandry of *Xenopus laevis* affect the quality of oocytes for heterologous
expression studies.
J Am Assoc Lab Anim Sci, 50, 1, 46-53.

Dieterich P, Odenthal-Schnittler M, Mrowietz C, Krämer M, Sasse L, Oberleithner H,
Schnittler HJ (2000):
Quantitative Morphodynamics of Endothelial Cells within Confluent Cultures in Response to
Fluid Shear Stress.
Biophysical Journal, 79, 3, 1285-1297. doi: 10.1016/S0006-3495(00)76382-X

Dong C, Skalak R, Sung KL, Schmid-Schönbein GW, Chien S (1988):
Passive deformation analysis of human leukocytes.
J Biomech Eng, 110, 1, 27-36. doi: 10.1115/1.3108402

Dumont JN (1972):
Oogenesis in *Xenopus laevis* (Daudin). I. Stages of oocyte development in laboratory maintained animals.
Journal of Morphology, 136, 2, 153-179. doi: 10.1002/jmor.1051360203

Ebnet K, Schulz CU, Meyer zu Brickwedde MK, Pendl GG, Vestweber D (2000):
Junctional Adhesion Molecule Interacts with the PDZ Domain-containing Proteins AF-6 and ZO-1.
Journal of Biological Chemistry, 275, 36, 27979-27988. doi: 10.1074/jbc.M002363200

European Commision (2021):
Animals used for scientific purposes.
Retrieved 02.03.2022, from
https://ec.europa.eu/environment/chemicals/lab_animals/3r/alternative_en.htm

European Parliament, Council of the European Union (2010):
Directive 2010/63/EU of the European Parliament and of the Council of 22 September 2010, Official Journal of the European Union, 33–79

Fanning AS, Jameson BJ, Jesaitis LA, Anderson JM (1998):
The tight junction protein ZO-1 establishes a link between the transmembrane protein occludin and the actin cytoskeleton.
Journal of Biological Chemistry, 273, 45, 29745-29753. doi: 10.1074/jbc.273.45.29745

Farquhar MG, Palade GE (1963):
Junctional complexes in various epithelia.
J Cell Biol, 17, 2. 375-412. doi: 10.1083/jcb.17.2.375

Fesenko I, Kurth T, Sheth B, Fleming TP, Citi S, Hausen P (2000):
Tight junction biogenesis in the early *Xenopus* embryo.
Mechanisms of Development, 96, 1, 51-65. doi: 10.1016/S0925-4773(00)00368-3

Fitzgerald TN, Shepherd BR, Asada H, Teso D, Muto A, Fancher T, Pimiento JM, Maloney SP, Dardik A (2008):
Laminar shear stress stimulates vascular smooth muscle cell apoptosis via the Akt pathway.
Journal of Cellular Physiology, 216, 2, 389-395. doi: 10.1002/jcp.21404

Federal Ministry of Food and Agriculture (2019):
Animals used under § 7 (2) of the Animal Protection Act 2019.
Retrieved 22.11.2021, 2021, from
https://www.bmel.de/DE/themen/tiere/tierschutz/versuchstierzahlen2019.

Förster C (2008):
Tight junctions and the modulation of barrier function in disease.
Histochemistry and cell biology, 130, 1, 55-70. doi: 10.1007/s00418-008-0424-9

Furuse M, Hirase T, Itoh M, Nagafuchi A, Yonemura S, Tsukita S, Tsukita S (1993):
Occludin: a novel integral membrane protein localizing at tight junctions.
J Cell Biol, 123, 6, 1777-1788. doi: 10.1083/jcb.123.6.1777

Furuse M, Fujita K, Hiiragi T, Fujimoto K, Tsukita S (1998a):
Claudin-1 and -2: Novel integral membrane proteins localizing at tight junctions with no sequence similarity to occludin.
J Cell Biol, 141, 7, 1539-1550. doi: 10.1083/jcb.141.7.1539

Furuse M, Sasaki H, Fujimoto K, Tsukita S (1998b):
A single gene product, claudin-1 or -2, reconstitutes tight junction strands and recruits occludin in fibroblasts.
J Cell Biol, 143, 2, 391-401. doi: 10.1083/jcb.143.2.391

Furuse M, Sasaki H, Tsukita S (1999):
Manner of interaction of heterogeneous claudin species within and between tight junction strands.
J Cell Biol, 147, 4, 891-903. doi: 10.1083/jcb.147.4.891

Furuse M, Hata M, Furuse K, Yoshida Y, Haratake A, Sugitani Y, Noda T, Kubo A, Tsukita S (2002):
Claudin-based tight junctions are crucial for the mammalian epidermal barrier: a lesson from claudin-1-deficient mice.
J Cell Biol, 156, 6, 1099-1111. doi: 10.1083/jcb.200110122

Furuse M (2010):
Molecular basis of the core structure of tight junctions.
Cold Spring Harb Perspect Biol, 2, 1, a002907. doi: 10.1101/cshperspect.a002907

Gong Y, Himmerkus N, Sunq A, Milatz S, Merkel C, Bleich M, Hou J (2017):
ILDR1 is important for paracellular water transport and urine concentration mechanism.
Proceedings of the National Academy of Sciences, 114, 20, 5271-5276. doi: 10.1073/pnas.1701006114

Green KJ, Gaudry CA (2000):
Are desmosomes more than tethers for intermediate filaments?
Nature Reviews Molecular Cell Biology, 1, 3, 208-216. doi: 10.1038/35043032

Green SL (2010):
The Laboratory *Xenopus sp.*
1st Edition, Boca Raton, Florida: CRC Press. ISBN: 9781420091090

Greene C, Hanley N, Campbell M (2019):
Claudin-5: gatekeeper of neurological function.
Fluids and Barriers of the Cns, 16, 4321. doi: 10.1186/s12987-019-0123-z

Guillemot L, Citi S (2006):
Cingulin regulates claudin-2 expression and cell proliferation through the small GTPase RhoA.
Mol Biol Cell, 17, 8, 3569-3577. doi: 10.1091/mbc.e06-02-0122

Günzel D, Yu ASL (2013):
Claudins and the Modulation of Tight Junction Permeability.
Physiological Reviews, 93, 2, 525-569. doi: 10.1152/physrev.00019.2012

Gurdon JB, Lane CD, Woodland HR, Marbaix G (1971):
Use of Frog Eggs and Oocytes for the Study of Messenger RNA and its Translation in Living Cells.
Nature, 233, 5316, 177-182. doi: 10.1038/233177a0

Hagen SJ (2017):
Non-canonical functions of claudin proteins: Beyond the regulation of cell-cell adhesions.
Tissue Barriers, 5, 2, e1327839. doi: 10.1080/21688370.2017.1327839

Hamada K, Kakigawa N, Sekine S, Shitara Y, Horie T (2013):

Disruption of ZO-1/claudin-4 interaction in relation to inflammatory responses in methotrexate-induced intestinal mucositis.
Cancer Chemotherapy and Pharmacology, 72, 4, 757-765. doi: 10.1007/s00280-013-2238-2

Hewitt KJ, Agarwal R, Morin PJ (2006):
The claudin gene family: expression in normal and neoplastic tissues.
BMC Cancer, 6, 1, 186. doi: 10.1186/1471-2407-6-186

Higashi T, Katsuno T, Kitajiri S, Furuse M (2015):
Deficiency of angulin-2/ILDR1, a tricellular tight junction-associated membrane protein, causes deafness with cochlear hair cell degeneration in mice.
PLoS One, 10, 3, e0120674. doi: 10.1371/journal.pone.0120674

Higashi T, Tokuda S, Kitajiri S, Masuda S, Nakamura H, Oda Y, Furuse M (2013):
Analysis of the 'angulin' proteins LSR, ILDR1 and ILDR2-tricellulin recruitment, epithelial barrier function and implication in deafness pathogenesis.
J Cell Sci, 126, 4, 966-977. doi: 10.1242/jcs.116442

Hou J, Renigunta A, Konrad M, Gomes AS, Schneeberger EE, Paul DL, Waldegger S, Goodenough DA (2008):
Claudin-16 and claudin-19 interact and form a cation-selective tight junction complex.
J Clin Invest, 118, 2, 619-628. doi: 10.1172/jci33970

Ikari A, Watanabe R, Sato T, Taga S, Shimobaba S, Yamaguchi M, Yamazaki Y, Endo S, Matsunaga T, Sugatani J (2014):
Nuclear distribution of claudin-2 increases cell proliferation in human lung adenocarcinoma cells.
Biochim Biophys Acta Mol Cell Res, 1843, 9, 2079-2088. doi: 10.1016/j.bbamcr.2014.05.017

Ikenouchi J, Furuse M, Furuse K, Sasaki H, Tsukita S, Tsukita S (2005):
Tricellulin constitutes a novel barrier at tricellular contacts of epithelial cells.
Journal of Cell Biology, 171, 6, 939-945. doi: 10.1083/jcb.200510043

Inai T, Kobayashi J, Shibata Y (1999):
Claudin-1 contributes to the epithelial barrier function in MDCK cells.
European Journal of Cell Biology, 78, 12, 849-855. doi: 10.1016/S0171-9335(99)80086-7

Irudayanathan FJ, Wang X, Wang N, Willsey SR, Seddon IA, Nangia S (2018):
Self-Assembly Simulations of Classic Claudins- Insights into the Pore Structure, Selectivity, and Higher Order Complexes.
The Journal of Physical Chemistry B, 122, 30, 7463-7474. doi: 10.1021/acs.jpcb.8b03842

Ito Y, Kimura T, Ago Y, Nam K, Hiraku K, Miyazaki K, Masuzawa T, Kishida A (2011):
Nano-vibration effect on cell adhesion and its shape.
Biomed Mater Eng, 21, 3, 149-158. doi: 10.3233/bme-2011-0664

Itoh M, Nagafuchi A, Yonemura S, Kitani-Yasuda T, Tsukita S, Tsukita S (1993):
The 220-kD protein colocalizing with cadherins in non-epithelial cells is identical to ZO-1, a tight junction-associated protein in epithelial cells: cDNA cloning and immunoelectron microscopy.
J Cell Biol, 121, 3, 491-502. doi: 10.1083/jcb.121.3.491

Itoh M, Furuse M, Morita K, Kubota K, Saitou M, Tsukita S (1999):
Direct binding of three tight junction-associated MAGUKs, ZO-1, ZO-2 and ZO-3, with the COOH termini of claudins.
J Cell Biol, 147, 6, 1351-1363. doi: 10.1083/jcb.147.6.1351

Federal Ministry of Justice (2013):
Tierschutz-Versuchstierverordnung.
BGBl. 47, 3125-3126

Federal Ministry of Justice (2021):
Tierschutzgesetz in der Fassung der Bekanntmachung vom 18. Mai 2006 (BGBl. I S. 1206, 1313), das zuletztdurch Artikel 105 des Gesetzes vom 10. August 2021 (BGBl. I S. 3436) geändert worden ist.
BGBl. 34, 1826

Kiuchi-Saishin Y, Gotoh S, Furuse M, Takasuga A, Tano Y, Tsukita S (2002):
Differential expression patterns of claudins, tight junction membrane proteins, in mouse nephron segments.
J Am Soc Nephrol, 13, 4, 875-886. doi: 10.1681/asn.V134875

Koda R, Zhao LN, Yaoita E, Yoshida Y, Tsukita S, Tamura A, Nameta M, Zhang Y, Fujinaka H, Magdeldin SXB, Narita I, Yamamoto T (2011):
Novel expression of claudin-5 in glomerular podocytes.
Cell and Tissue Research, 343, 3, 637-648. doi: 10.1007/s00441-010-1117-y

Kovalcsik R, Devlin T, Loux S, Martinek M, May J, Pickering T, Tapp R, Wilson S, Serota D (2006):
Animal reuse: balancing scientific integrity and animal welfare.
Lab Anim (NY), 35, 9, 49-53. doi: 10.1038/laban1006-49

Krause G, Winkler L, Piehl C, Blasig I, Piontek J, Müller SL (2009):
Structure and function of extracellular claudin domains.
Ann N Y Acad Sci, 1165, 34-43. doi: 10.1111/j.1749-6632.2009.04057.x

Krug SM, Amasheh M, Dittmann I, Christoffel I, Fromm M, Amasheh S (2013):
Sodium caprate as an enhancer of macromolecule permeation across tricellular tight junctions of intestinal cells.
Biomaterials, 34, 1, 275-282. doi: 10.1016/j.biomaterials.2012.09.051

Lalan M, Bagchi T, Misra A (2011):
The Cell. Challenges in Delivery of Therapeutic Genomics and Proteomics.
1st Edition, London: Elsevier, 1-43. ISBN: 9780123849649

Lalonde-Robert V, Beaudry F, Vachon P (2012):
Pharmacologic parameters of MS222 and physiologic changes in frogs (*Xenopus laevis*) after immersion at anesthetic doses.
J Am Assoc Lab Anim Sci, 51, 4, 464-468.

Landschaft D (2020):
Gaps and barriers: Gap junctions as a channel of communication between the soma and the germline.
Seminars in Cell & Developmental Biology, 97, 167-171. doi: 10.1016/j.semcdb.2019.09.002

Liang TW, DeMarco RA, Mrsny RJ, Gurney A, Gray A, Hooley J, Aaron HL, Huang A, Klassen T, Tumas DB, Fong S (2000):
Characterization of huJAM: evidence for involvement in cell-cell contact and tight junction regulation.
Am. J. Physiol., Cell Physiol., 279, 6, C1733-C1743. doi: 10.1152/ajpcell.2000.279.6.C1733

Liebner S, Fischmann A, Rascher G, Duffner F, Grote EH, Kalbacher H, Wolburg H (2000):

Claudin-1 and claudin-5 expression and tight junction morphology are altered in blood vessels of human glioblastoma multiforme.
Acta Neuropathol, 100, 3, 323-331. doi: 10.1007/s004010000180

Lim CT, Zhou EH, Li A, Vedula SRK, Fu H (2006):
Experimental techniques for single cell and single molecule biomechanics.
Materials Science and Engineering C, 26, 1278-1288.

Lim TS, Vedula SRK, Hunziker W, Lim CT (2008):
Kinetics of Adhesion Mediated by Extracellular Loops of Claudin-2 as Revealed by Single-Molecule Force Spectroscopy.
Journal of Molecular Biology, 381, 3, 681-691. doi: 10.1016/j.jmb.2008.06.009

Lindmark T, Söderholm JD, Olaison G, Alván G, Ocklind G, Artursson P (1997):
Mechanism of absorption enhancement in humans after rectal administration of ampicillin in suppositories containing sodium caprate.
Pharm Res, 14, 1, 930-935.

Liu Y, Nusrat A, Schnell FJ, Reaves TA, Walsh S, Pochet M, Parkos CA (2000):
Human junction adhesion molecule regulates tight junction resealing in epithelia.
J Cell Sci, 113, 13, 2363-2374.

Madara JL, Nash S, Moore R, Atisook K (1990):
Structure and function of the intestinal epithelial barrier in health and disease.
Monogr Pathol, 31, 306-324.

Maher S, Leonard TW, Jacobsen J, Brayden DJ (2009):
Safety and efficacy of sodium caprate in promoting oral drug absorption: from in vitro to the clinic.
Adv Drug Deliv Rev, 61, 15, 1427-1449. doi: 10.1016/j.addr.2009.09.006

Markov AG, Aschenbach JR, Amasheh S (2015):
Claudin clusters as determinants of epithelial barrier function.
IUBMB Life, 67, 1, 29-35. doi: https://doi.org/10.1002/iub.1347

Markov AG, Veshnyakova A, Fromm M, Amasheh M, Amasheh S (2010):
Segmental expression of claudin proteins correlates with tight junction barrier properties in rat intestine.
J Comp Physiol B, 180, 4, 591-598. doi: 10.1007/s00360-009-0440-7

Martìn-Padura I, Lostaglio S, Schneemann M, Williams L, Romano M, Fruscella P, Panzeri C, Stoppacciaro A, Ruco L, Villa A, Simmons D, Dejana E (1998):
Junctional adhesion molecule, a novel member of the immunoglobulin superfamily that distributes at intercellular junctions and modulates monocyte transmigration.
J Cell Biol, 142, 1, 117-127. doi: 10.1083/jcb.142.1.117

Mertz JE, Gurdon JB (1977):
Purified DNAs are transcribed after microinjection into *Xenopus* oocytes.
Proc. Natl. Acad. Sci. U.S.A., 74, 4, 1502-1506. doi: 10.1073/pnas.74.4.1502

Michaels CJ, Downie JR, Campbell-Palmer R (2014):
The importance of enrichment for advancing amphibian welfare and conservation goals: A review of a neglected topic.
Amphibian & Reptile Conservation, 8, 7-23.

Milatz S, Krug SM, Rosenthal R, Günzel D, Müller D, Schulzke JD, Amasheh S, Fromm M (2010):
Claudin-3 acts as a sealing component of the tight junction for ions of either charge and uncharged solutes.
Biochim Biophys Acta Biomembr, 1798, 11, 2048-2057. doi: 10.1016/j.bbamem.2010.07.014

Mineta K, Yamamoto Y, Yamazaki Y, Tanaka H, Tada Y, Saito K, Tamura A, Igarashi M, Endo T, Takeuchi K, Tsukita S (2011):
Predicted expansion of the claudin multigene family.
FEBS Letters, 585, 4, 606-612. doi: 10.1016/j.febslet.2011.01.028

Mitic LL, Van Itallie CM, Anderson JM (2000):
Molecular Physiology and Pathophysiology of Tight Junctions I. Tight junction structure and function: lessons from mutant animals and proteins.
Am J Physiol Gastrointest Liver Physiol, 279, 2, G250-G254. doi: 10.1152/ajpgi.2000.279.2.G250

Miyamoto T, Morita K, Takemoto D, Takeuchi K, Kitano Y, Miyakawa T, Nakayama K, Okamura Y, Sasaki H, Miyachi Y, Furuse M, Tsukita S (2005):
Tight junctions in Schwann cells of peripheral myelinated axons : a lesson from claudin-19–deficient mice.
J Cell Biol, 169, 3, 527-538. doi: 10.1083/jcb.200501154

Moellic CL, Boulkroun S, González-Nunez D, Dublineau I, Cluzeaud F, Fay M, Blot-Chabaud M, Farman N (2005):
Aldosterone and tight junctions: modulation of claudin-4 phosphorylation in renal collecting duct cells.
Am. J. Physiol., Cell Physiol., 289, 6, C1513-C1521. doi: 10.1152/ajpcell.00314.2005

Morita K, Furuse M, Fujimoto K, Tsukita S (1999):
Claudin multigene family encoding four-transmembrane domain protein components of tight junction strands.
Proc. Natl. Acad. Sci. U.S.A., 96, 2, 511-516. doi: 10.1073/pnas.96.2.511

Mowry KL (2020):
Using the *Xenopus* Oocyte Toolbox.
Cold Spring Harbor protocols, 2020, 4, 095844-095844. doi: 10.1101/pdb.top095844

Nader N, Courjaret R, Dib M, Kulkarni RP, Machaca K (2016):
Release from *Xenopus* oocyte prophase I meiotic arrest is independent of a decrease in cAMP levels or PKA activity.
Development, 143, 11, 1926-1936. doi: 10.1242/dev.136168

Nielsen MS, Axelsen LN, Sorgen PL, Verma V, Delmar M, Holstein-Rathlou NH (2012):
Gap junctions.
Compr Physiol, 2, 3, 1981-2035. doi: 10.1002/cphy.c110051

Nieuwkoop PD, Faber J (1994):
Normal table of *Xenopus laevis* (Daudin) : a systematical and chronological survey of the development from the fertilized egg till the end of metamorphosis.
1st Edition, New York : Garland Pub. ISBN: 9780815318965

Nitta T, Hata M, Gotoh S, Seo Y, Sasaki H, Hashimoto N, Furuse M, Tsukita S (2003):
Size-selective loosening of the blood-brain barrier in claudin-5-deficient mice.
J Cell Biol, 161, 3, 653-660. doi: 10.1083/jcb.200302070

Ohtsuki S, Sato S, Yamaguchi H, Kamoi M, Asashima T, Terasaki T (2007):
Exogenous expression of claudin-5 induces barrier properties in cultured rat brain capillary endothelial cells.
Journal of Cellular Physiology, 210, 1, 81-86. doi: 10.1002/jcp.20823

Olson JH, Chandler DE (1999):
Xenopus laevis egg jelly contains small proteins that are essential to fertilization.
Dev Biol, 210, 2, 401-410. doi: 10.1006/dbio.1999.9281

Patel SD, Chen CP, Bahna F, Honig B, Shapiro L (2003):
Cadherin-mediated cell–cell adhesion: sticking together as a family.
Current Opinion in Structural Biology, 13, 6, 690-698. doi: 10.1016/j.sbi.2003.10.007

Peshkin L, Lukyanov A, Kalocsay M, Gage RM, Wang D, Pells TJ, Karimi K, Vize PD, Wühr M, Kirschner MW (2019):
The protein repertoire in early vertebrate embryogenesis.
bioRxiv, 571174. doi: 10.1101/571174

Philpott A, Yew PR (2008):
The *Xenopus* cell cycle: an overview.
Mol Biotechnol, 39, 1, 9-19. doi: 10.1007/s12033-008-9033-z

Piontek J, Winkler L, Wolburg H, Müller SL, Zuleger N, Piehl C, Wiesner B, Krause G, Blasig IE (2008):
Formation of tight junction: determinants of homophilic interaction between classic claudins.
The FASEB Journal, 22, 1, 146-158. doi: 10.1096/fj.07-8319com

Piontek J, Fritzsche S, Cording J, Richter S, Hartwig J, Walter M, Yu D, Turner JR, Gehring C, Rahn HP, Wolburg H, Blasig IE (2011):
Elucidating the principles of the molecular organization of heteropolymeric tight junction strands.
Cellular and Molecular Life Sciences, 68, 23, 3903-3918. doi: 10.1007/s00018-011-0680-z

Piontek J, Krug SM, Protze J, Krause G, Fromm M (2020):
Molecular architecture and assembly of the tight junction backbone.
Biochim Biophys Acta Biomembr, 1862, 7, 183279. doi: 10.1016/j.bbamem.2020.183279

Radloff J, Cornelius V, Markov AG, Amasheh S (2019):
Caprate Modulates Intestinal Barrier Function in Porcine Peyer's Patch Follicle-Associated Epithelium.
Int J Mol Sci, 20, 6, 1418. doi: 10.3390/ijms20061418

Radloff J, Zakrzewski SS, Pieper R, Markov AG, Amasheh S (2017):
Porcine milk induces a strengthening of barrier function in porcine jejunal epithelium in vitro.
Annals of the New York Academy of Sciences, 1397, 1, 110-118. doi: 10.1111/nyas.13340

Rahner C, Mitic LL, Anderson JM (2001):
Heterogeneity in expression and subcellular localization of claudins 2, 3, 4, and 5 in the rat liver, pancreas, and gut.
Gastroenterology, 120, 2, 411-422. doi: 10.1053/gast.2001.21736

Ramlochansingh C, Branoner F, Chagnaud BP, Straka H (2014):
Efficacy of Tricaine Methanesulfonate (MS-222) as an Anesthetic Agent for Blocking Sensory-Motor Responses in *Xenopus laevis* Tadpoles.
PLOS ONE, 9, 7, e101606. doi: 10.1371/journal.pone.0101606

Rand RP, Burton AC (1964):
Mechanical Properties of the Red Cell Membrane: I. Membrane Stiffness and Intracellular Pressure.
Biophysical Journal, 4, 2, 115-135. doi: 10.1016/S0006-3495(64)86773-4

Rasar MA, Hammes SR (2006):
The physiology of the *Xenopus laevis* ovary.
Methods Mol Biol, 322, 17-30. doi: 10.1007/978-1-59745-000-3_2

Riazuddin S, Ahmed ZM, Fanning AS, Lagziel A, Kitajiri S, Ramzan K, Khan SN, Chattaraj P, Friedman PL, Anderson JM, Belyantseva IA, Forge A, Riazuddin S, Friedman TB (2006):
Tricellulin is a tight-junction protein necessary for hearing.
American Journal of Human Genetics, 79, 6, 1040-1051. doi: 10.1086/510022

Richter JD, Smith LD (1981):
Differential capacity for translation and lack of competition between mRNAs that segregate to free and membrane-bound polysomes.
Cell 27, 1, 183-191. doi: 10.1016/0092-8674(81)90372-x

Roeder AD, Gard DL (1994):
Confocal microscopy of F-actin distribution in *Xenopus* oocytes.
Zygote, 2, 2, 111-124. doi: 10.1017/s0967199400001866

Rosenthal R, Milatz S, Krug SM, Oelrich B, Schulzke JD, Amasheh S, Günzel D, Fromm M (2010):
Claudin-2, a component of the tight junction, forms a paracellular water channel.
J Cell Sci, 123, 11, 1913-1921. doi: 10.1242/jcs.060665

Russel WMS, Burch RL (1959):
The principles of humane experimental technique.
New Edition (31. 10.1992), Wheathampstead, UK: Universities Federation for Animal Welfare. ISBN: 9780900767784

Saitou M, Furuse M, Sasaki H, Schulzke JD, Fromm M, Takano H, Noda T, Tsukita S (2000):
Complex phenotype of mice lacking occludin, a component of tight junction strands.
Mol Biol Cell, 11, 12, 4131-4142. doi: 10.1091/mbc.11.12.4131

Sato K, Tokmakov AA (2020):
Toward the understanding of biology of oocyte life cycle in *Xenopus laevis*: No oocytes left behind.
Reproductive Medicine and Biology, 19, 2, 114-119. doi: 10.1002/rmb2.12314

Schlingmann B, Overgaard CE, Molina SA, Lynn KS, Mitchell LA, White SD, Mattheyses AL, Guidot DM, Capaldo CT, Koval M (2016):
Regulation of claudin/zonula occludens-1 complexes by hetero-claudin interactions.
Nature Communications, 7, 12276. doi: 10.1038/ncomms12276

Schneeberger K, Roth S, Nieuwenhuis EES, Middendorp S (2018):
Intestinal epithelial cell polarity defects in disease: lessons from microvillus inclusion disease.
Disease Models & Mechanisms, 11, 2, dmm031088. doi: 10.1242/dmm.031088

Seker M, Fernandez-Rodriguez C, Martinez-Cruz LA, Müller D (2019):
Mouse Models of Human Claudin-Associated Disorders: Benefits and Limitations.
Int J Mol Sci, 20, 21, 5504. doi: 10.3390/ijms20215504

Session AM, Uno Y, Kwon T, Hapman JAC, Toyoda A, Takahashi S, Fukui A, Hikosaka A, Suzuki A, Kondo M, van Heeringen SJ, Quigley I. Heinz S, Ogino H, Ochi H, Hellsten U, Lyons JB, Simakov O, Putnam N, Stites J, Kuroki Y, Tanaka T, Michiue T, Watanabe M, Ogdanovic OB, Lister R, Georgiou G, Paranjpe SS, Van Kruijsbergen I, Shu SQ, Carlson J, Kinoshita T, Ohta Y, Mawaribuchi S, Jenkins J, Grimwood J, Schmutz J, Mitros T, Mozaffari SV, Suzuki Y, Haramoto Y, Yamamoto TS, Takagi C, Heald R, Miller K, Haudenschild C, Kitzman J, Nakayama T, Zutsu YI, Robert J, Fortriede J, Burns K, Lotay V, Karimi K, Yasuoka Y, Dichmann DS, Flajnik MF, Houston DW, Shendure J, DuPasquier L, Vize PD, Zorn AM, Ito M, Marcotte EM, Wallingford JB, Ito Y, Asashima M, Ueno N, Matsuda Y, Veenstra GJC, Fujiyama A, Harland RM, Taira M, Rokhsar DS (2016):
Genome evolution in the allotetraploid frog *Xenopus laevis*.
Nature, 538, 7625, 336-343. doi: 10.1038/nature19840

Sohet F, Lin C, Munji RN, Lee SY, Ruderisch N, Soung A, Arnold TD, Derugin N, Vexler ZS, Yen FT, Daneman R (2015):
LSR/angulin-1 is a tricellular tight junction protein involved in blood–brain barrier formation.
Journal of Cell Biology, 208, 6, 703-711. doi: 10.1083/jcb.201410131

Soini Y (2011):
Claudins in lung diseases.
Respiratory Research, 12, 70. doi: 10.1186/1465-9921-12-70

Stevenson BR, Siliciano JD, Mooseker MS, Goodenough DA (1986):
Identification of ZO-1: a high molecular weight polypeptide associated with the tight junction (zonula occludens) in a variety of epithelia.
Journal of Cell Biology, 103, 3, 755-766. doi: 10.1083/jcb.103.3.755

Strobel S, Hagedorn A, Ott S, Kempf H, Waschulzik B, Gröger M, Kress S, Radermacher P, Potschka H, Baumgartner CM (2018):
A Comparison Of The Analgesic Effects Of Fentanyl And Butorphanol In African Clawed Frogs (*Xenopus laevis*) Under Tricaine Methanesulfonate (MS222) Anaesthesia.
SOJ Anesthesiology & Pain Management, 5, 2, 1-10. doi: 10.15226/2374-684X/5/2/00158

Sugawara T, Furuse K, Otani T, Wakayama T, Furuse M (2021):
Angulin-1 seals tricellular contacts independently of tricellulin and claudins.
Journal of Cell Biology, 220, 9, e202005062. doi: 10.1083/jcb.202005062

Sung KL, Sung LA, Crimmins M, Burakoff SJ, Chien S (1986):
Determination of junction avidity of cytolytic T cell and target cell.
Science, 234, 4782, 1405-1408. doi: 10.1126/science.3491426

Suzuki H, Nishizawa T, Tani K, Yamazaki Y, Tamura A, Ishitani R, Dohmae N, Tsukita S, Nureki O, Fujiyoshi Y (2014):
Crystal Structure of a Claudin Provides Insight into the Architecture of Tight Junctions.
Science, 344, 6181, 304-307. doi: 10.1126/science.1248571

Swisshelm K, Macek R, Kubbies M (2005):
Role of claudins in tumorigenesis.
Advanced Drug Delivery Reviews, 57, 6, 919-928. doi: 10.1016/j.addr.2005.01.006

Tannenbaum J, Bennett BT (2015):
Russell and Burch's 3Rs Then and Now: The Need for Clarity in Definition and Purpose.
Journal of the American Association for Laboratory Animal Science, 54, 2. 120-132.

Taylor MA, Johnson AD, Smith LD (1985):
Growing *Xenopus* oocytes have spare translational capacity.

Proc. Natl. Acad. Sci. U.S.A., 82, 19, 6586-6589. doi: 10.1073/pnas.82.19.6586

Tomita M, Hayashi M, Awazu S (1995):
Absorption-enhancing mechanism of sodium caprate and decanoylcarnitine in Caco-2 cells.
J Pharmacol Exp Ther, 272, 2. 739-743.

Tsukita S, Tanaka H, Tamura A (2019):
The Claudins: From Tight Junctions to Biological Systems.
Trends in Biochemical Sciences, 44, 2, 141-152. doi: 10.1016/j.tibs.2018.09.008

Turner JR (2000):
'Putting the squeeze' on the tight junction: understanding cytoskeletal regulation.
Semin Cell Dev Biol, 11, 4, 301-308. doi: 10.1006/scdb.2000.0180

Uehara T, Yamada M, Umetsu S, Nittono H, Suzuki H, Fujisawa T, Takenouchi T, Inui A, Kosaki K (2020):
Biallelic Mutations in the LSR Gene Cause a Novel Type of Infantile Intrahepatic Cholestasis.
The Journal of Pediatrics, 221, 251-254. doi: 10.1016/j.jpeds.2020.01.064

Umeda K, Ikenouchi J, Katahira-Tayama S, Furuse K, Sasaki H, Nakayama M, Matsui T, Tsukita S, Furuse M, Tsukita S (2006):
ZO-1 and ZO-2 Independently Determine Where Claudins Are Polymerized in Tight-Junction Strand Formation.
Cell, 126, 4, 741-754. doi: 10.1016/j.cell.2006.06.043

Van Itallie CM, Rahner C, Anderson JM (2001):
Regulated expression of claudin-4 decreases paracellular conductance through a selective decrease in sodium permeability.
J Clin Invest, 107, 10, 1319-1327. doi: 10.1172/jci12464

Van Itallie CM, Anderson JM (2013):
Claudin interactions in and out of the tight junction.
Tissue Barriers, 1, 3, e25247. doi: 10.4161/tisb.25247

Van Itallie CM, Tietgens AJ, Anderson JM (2017):
Visualizing the dynamic coupling of claudin strands to the actin cytoskeleton through ZO-1.
Molecular Biology of the Cell, 28, 4, 524-534. doi: 10.1091/mbc.E16-10-0698

Vedula SRK, Lim TS, Kausalya PJ, Lane EB, Rajagopal G, Hunziker W, Lim CT (2009):
Quantifying Forces Mediated by Integral Tight Junction Proteins in Cell-Cell Adhesion.
Experimental Mechanics, 49, 1, 3-9. doi: 10.1007/s11340-007-9113-1

Vermette D, Hu P, Canarie MF, Funaro M, Glover J, Pierce RW (2018):
Tight junction structure, function, and assessment in the critically ill: a systematic review.
Intensive Care Med Exp, 6, 1, 37. doi: 10.1186/s40635-018-0203-4

Vitzthum C, Stein L, Brunner N, Knittel R, Fallier-Becker P, Amasheh S (2019):
Xenopus oocytes as a heterologous expression system for analysis of tight junction proteins.
Faseb Journal, 33, 4, 5312-5319. doi: 10.1096/fj.201801451RR

Wagner CA, Friedrich B, Setiawan I, Lang F, Bröer S (2000):
The Use of *Xenopus laevis* Oocytes for the Functional Characterization of Heterologously Expressed Membrane Proteins.
Cellular Physiology and Biochemistry, 10, 1-2, 1-12. doi: 10.1159/000016341

Walko G, Castañón MJ, Wiche G (2015):

Molecular architecture and function of the hemidesmosome.
Cell and tissue research, 360, 2, 363-378. doi: 10.1007/s00441-014-2061-z

Wen HJ, Watry DD, Marcondes MCG, Fox HS (2004):
Selective decrease in paracellular conductance of tight junctions: role of the first extracellular domain of claudin-5.
Molecular and Cellular Biology, 24, 19, 8408-8417. doi: 10.1128/MCB.24.19.8408-8417.2004

Wheeler GN, Brandli AW (2009):
Simple vertebrate models for chemical genetics and drug discovery screens: lessons from zebrafish and *Xenopus*.
Dev Dyn, 238, 6, 1287-1308. doi: 10.1002/dvdy.21967

Wittchen ES, Haskins J, Stevenson BR (1999):
Protein interactions at the tight junction. Actin has multiple binding partners, and ZO-1 forms independent complexes with ZO-2 and ZO-3.
Journal of Biological Chemistry, 274, 49, 35179-35185. doi: 10.1074/jbc.274.49.35179

Wolburg H, Wolburg-Buchholz K, Kraus J, Rascher-Eggstein G, Liebner S, Hamm S, Duffner F, Grote EH, Risau W, Engelhardt B (2003):
Localization of claudin-3 in tight junctions of the blood-brain barrier is selectively lost during experimental autoimmune encephalomyelitis and human glioblastoma multiforme.
Acta Neuropathologica, 105, 6, 586-592. doi: 10.1007/s00401-003-0688-z

Worzfeld T, Schwaninger M (2016):
Apicobasal polarity of brain endothelial cells.
J Cereb Blood Flow Metab, 36, 2, 340-362. doi: 10.1177/0271678x15608644

Wu M, Gerhart J (1991):
Raising *Xenopus* in the laboratory.
Methods Cell Biol, 36, 3-18. doi: 10.1016/s0091-679x(08)60269-1

Yamagishi Y, Abe H (2015):
Reorganization of actin filaments by ADF/cofilin is involved in formation of microtubule structures during *Xenopus* oocyte maturation.
Molecular Biology of the Cell, 26, 24, 4387-4400. doi: 10.1091/mbc.E15-01-0035

Yourek G, McCormick SM, Mao JJ, Reilly GC (2010):
Shear stress induces osteogenic differentiation of human mesenchymal stem cells.
Regenerative Medicine, 5, 5, 713-724. doi: 10.2217/rme.10.60

Zhang C, Neelamegham S (2017):
Application of microfluidic devices in studies of thrombosis and hemostasis.
Platelets, 28, 5, 434-440. doi: 10.1080/09537104.2017.1319047

Zhao J, Krystofiak ES, Ballesteros A, Cui R, Van Itallie CM, Anderson JM, Fenollar-Ferrer C, Kachar B (2018):
Multiple claudin–claudin cis interfaces are required for tight junction strand formation and inherent flexibility.
Communications Biology, 1, 1, 50. doi: 10.1038/s42003-018-0051-5

Zihni C, Mills C, Matter K, Balda MS (2016):
Tight junctions: from simple barriers to multifunctional molecular gates.
Nature Reviews Molecular Cell Biology, 17, 9, 564-580. doi: 10.1038/nrm.2016.80

List of publications / Veröffentlichungen

Publications (peer reviewed)

- Stein L, <u>Brunner N</u>, Amasheh S
  Functional Analysis of Gastric Tight Junction Proteins in *Xenopus laevis* Oocytes
  Membranes. 2022 July 23; 12(8): 731. https://doi: 10.3390/membranes12080731

- <u>Brunner N</u>, Stein L, Amasheh S
  Cellular distribution pattern of tjp1 (ZO-1) in *Xenopus laevis* oocytes heterologously expressing claudins

  J Membrane Biol. 2022 June 23; https://doi.org/10.1007/s00232-022-00251-z

- Droessler L, Cornelius V, Boehm E, Stein L, <u>Brunner N</u>, Amasheh S
  Barrier Perturbation in Porcine Peyer's Patches by Tumor Necrosis Factor is Associated With a Dysregulation of Claudins

  Front Physiol. 2022 May 30; 13:889552; https://doi.org/10.3389/fphys.2022.889552

- <u>Brunner N</u>, Stein L, Cornelius V, Knittel R, Fallier-Becker P, Amasheh S
  Blood-Brain Barrier Protein Claudin-5 Expressed in Paired *Xenopus laevis* Oocytes Mediates Cell-Cell Interaction

  Front Physiol. 2020 July 21; 11:857; https://doi.org/10.3389/fphys.2020.00857

- Vitzthum C, Stein L, <u>Brunner N</u>, Knittel R, Fallier-Becker P, Amasheh S
  ***Xenopus* oocytes as a heterologous expression system for analysis of tight junction proteins**

  FASEB J. 2019 January 15; 33(4): 5312-5319; https://doi.org/10.1096/fj.201801451RR

Abstracts in proceedings & participation in conferences

- <u>Brunner N</u>, Stein L, Amasheh S
  Analysis of ZO-1 in claudin-expressing *Xenopus laevis* oocytes
  DVG Fachgruppentagung Physiologie und Biochemie 2022, Gießen 24.06.2022 - 26.06.2022

- Stein L, <u>Brunner N</u>, Amasheh S
  Exploring the function of the gastric barrier protein claudin-18 in a heterologous expression model
  75. digitale Tagung der Gesellschaft für Ernährungsphysiologie, Berlin 16.03.-18.03.2021.

- Stein L, <u>Brunner N</u>, Amasheh S
  Analysis of the pH-dependent interaction of human gastric TJ proteins expressed in *Xenopus laevis* oocytes
  4th Tight Junction Conference, Berlin 27.09.2021- 29.09.2021

- <u>Brunner N</u>, Amasheh S
  Heterologous expression of claudin-5 in *Xenopus laevis* oocytes
  98th Meeting of the German Physiological Society, Ulm 30.09.2019- 02.10.2019

- <u>Brunner N</u>, Amasheh S
  Establishing *Xenopus laevis* oocytes as a novel model system for blood brain barrier analyses
  22nd European Congress on Alternatives to Animal Testing &19th Annual Congress of EUSAAT, Linz 10.10.2019- 13.10.2019
  Altex Proceedings, Volume 8, No. 1, ISSN 2194-0479 (2019)

Funding sources / Finanzielle Unterstützung

Conflict of interest / Interessenskonflikte

There is not conflict of interest in the financial support of this work.
Im Rahmen dieser Arbeit bestehen keine Interessenskonflikte durch Zuwendungen Dritter.

Author contribution / Autorenbeitrag

1. Vitzthum C, Stein L, <u>Brunner N</u>, Knittel R, Fallier-Becker P, Amasheh S
    Xenopus oocytes as a heterologous expression system for analysis of tight junction proteins
    FASEB J. 2019 April; 33(4): 5312-5319

I have performed immunoblot experiments and paired oocyte assays for preparation of the freeze fracture experiments. I participated in study outcome, data analysis, manuscript discussion and reviewed the manuscript.

2. <u>Brunner N</u>, Stein L, Cornelius V, Knittel R, Fallier-Becker P, Amasheh S
    Blood-Brain Barrier Protein Claudin-5 Expressed in Paired *Xenopus laevis* Oocytes Mediates Cell-Cell Interaction
    Front Physiol. 2020 July 21; 11:857

I designed, planned, and supervised the experiments and wrote the manuscript. I personally performed the experiments and data analysis.

3. Droessler L, Cornelius V, Boehm E, Stein L, <u>Brunner N</u>, Amasheh S
    Barrier Perturbation in Porcine Peyer's Patches by Tumor Necrosis Factor is Associated With a Dysregulation of Claudins
    Front Physiol. 2022 May 30

I performed some of the experiments and participated in manuscript review.

4. <u>Brunner N</u>, Stein L, Amasheh S
    Cellular distribution pattern of tjp1 (ZO-1) in *Xenopus laevis* oocytes heterologously expressing claudins
    J Membrane Biol. 2022 June 23

I performed the experiments and conceptualized the study. I prepared the figures, analyzed the data, and wrote and reviewed the manuscript.

5. Stein L, <u>Brunner N</u>, Amasheh S
    Functional Analysis of Gastric Tight Junction Proteins in *Xenopus laevis* Oocytes
    Membranes. 2022 July 23

I performed some of the experiments, established some of the methodology and supervised the study. I participated in manuscript preparation.

Declaration of independence / Selbständigkeitserklärung

I hereby confirm that I have written this thesis independently. I certify that I have used only the sources and aids indicated.
Hiermit bestätige ich, dass ich die vorliegende Arbeit selbstständig angefertigt habe. Ich versichere, dass ich ausschließlich die angegebenen Quellen und Hilfen in Anspruch genommen habe.

Berlin, den 21.10.2022   Unterschrift: Nora Brunner